NBSIR 73-130 (R)

Report on Dental Research at the National Bureau of Standards

Dr. James M. Cassel, et al

Dental Research Section
National Bureau of Standards
Washington, D. C. 20234

January 1973

Semi–annual Progress Report for Period
July – December 1972

Prepared for
American Dental Association
National Institute of Dental Research
Veterans Administration
U.S. Army Medical Research & Development Command

NBSIR 73-130

REPORT ON DENTAL RESEARCH AT THE NATIONAL BUREAU OF STANDARDS

Dr. James M. Cassel, et al

Dental Research Section
National Bureau of Standards
Washington, D. C. 20234

January 1973

Semi-annual Progress Report for Period
July - December 1972

This is a progress report. The work is incomplete and is continuing. Results and conclusions are not necessarily those that will be included in the final report. For this reason, before reference to this report is made, permission should be requested from the Chief of the Dental Research Section, National Bureau of Standards, Washington, D. C. 20234

Prepared for
American Dental Association
National Institute of Dental Research
Veterans Administration
U.S. Army Medical Research & Development Command

U. S. DEPARTMENT OF COMMERCE, Frederick B. Dent, Secretary

NATIONAL BUREAU OF STANDARDS, Richard W. Roberts, Director

TABLE OF CONTENTS

NBS Report 10979	Clinical Evaluation of a Radiopaque Composite Restorative Material After Three and One-half Years.
NBS Report 10980	Clinical Evaluation of a Tooth-Restoration Coupling Agent.
NBS Report 10981	$Ca_4(PO_4)_2O$, Tetracalcium Diphosphate Monoxide; Crystal Structure and Relationships to $Ca_5(PO_4)_3OH$ and $K_3Na(SO_4)_2$.
NBS Report 10982	The Formation of Fluorapatite and Calcium Fluoride in Topical Fluoride Treatments.
NBS Report 10983	Experimental Study of the Surface and Lattice Effects on the Solubility of Hydroxyapatite.

REPORT ON DENTAL RESEARCH

AT THE

NATIONAL BUREAU OF STANDARDS

1. INTRODUCTION

Dental research at the National Bureau of Standards during the half year ending December 31, 1972, included investigations of a wide range of materials used in restorative dentistry and of hard and soft natural tissues. The research program is supported by the Council on Dental Research of the American Dental Association, the Collaborative Research Office of the National Institute of Dental Research, the Dental Research Division of the U. S. Army Medical Research and Development Command, and the Veterans Administration. Support from the National Institute of Dental Research is also provided in the form of grants to Research Associates sponsored by the American Dental Association. This support is designated NIDR (Grant) where reference to it is made. In the summaries of work in progress, sponsors of various projects are identified. However, since most of the projects are closely related both technically and administratively, reports on all projects are presented for the information of all sponsors. Detailed reports issued during the period on some phases of the research are listed and are appended to this report.

2. REPORTS ISSUED

NBS Report 10916 The Crystal Structure of V_3Rh_5.

NBS Report 10978 $Ca(H_2PO_4)_2$, A Crystal Structure Containing Unusual Hydrogen Bonding.

NBS Report 10979 Clinical Evaluation of a Radiopaque Composite Restorative Material After Three and One-half Years.

NBS Report 10980 Clinical Evaluation of a Tooth-Restoration Coupling Agent.

NBS Report 10981 $Ca_4(PO_4)_2O$, Tetracalcium Diphosphate Monoxide; Crystal Structure and Relationships to $Ca_5(PO_4)_3OH$ and $K_3Na(SO_4)_2$.

NBS Report 10982 The Formation of Fluorapatite and Calcium Fluoride in Topical Fluoride Treatments.

NBS Report 10983 Experimental Study of the Surface and Lattice Effects on the Solubility of Hydroxyapatite.

3. PAPERS PUBLISHED

Dickens, B.; Bowen, J. S.; and Brown, W. E. A Refinement of the Crystal Structure of $CaHPO_4$ (synthetic monetite). Acta Cryst. B28:797-806, March 1972.

Dickens, B. and Bowen, J. S. Refinement of the Crystal Structure of $Ca(H_2PO_4)_2 \cdot H_2O$. Acta Cryst. B27:2247-2255, Nov. 1971.

Bowen, R. L. and Argentar, H. A Stabilizing Comonomer: I. Synthesis and Confirmation of Structure. J. Dent. Res. 51:1071-1074, July-Aug. 1972.

Dickson, G. and Cassel, J. M. Dental Materials Research. Proc. 50th Anniv. Symposium, National Bureau of Standards 1969, NBS Spec. Pub. 354, July 1972.

Bowen, R. L.; Barton, J. A., Jr.; and Mullineaux, A. L. Composite Restorative Materials. In: Dental Materials Research, Proc. 50th Anniv. Symposium, National Bureau of Standards 1969, NBS Spec. Pub. 354, July 1972, p.93-100.

Brauer, G. M. Cements Containing O-ethoxybenzoic Acid (EBA). In: Dental Materials Research, Proc. 50th Anniv. Symposium, National Bureau of Standards, NBS Spec. Pub. 354, July 1972, pgs. 101-111.

Oglesby, P. L. Viscoelastic Behavior. In: Dental Materials Research, Proc. 50th Anniv. Symposium, National Bureau of Standards 1969, NBS Spec. Pub. 354, July 1972, pgs. 127-144.

Dickson, G. Ultrasonic Methods for Determination of Mechanical Properties. In: Dental Materials Research, Proc. 50th Anniv. Symposium, National Bureau of Standards 1969, NBS Special Pub. 354, 1972, pp. 161-168.

Huget, E. F.; Brauer, G. M.; Kumpula, J. W. and Civjan, S. Filled Cold-Curing Acrylic Resin as a Splinting Material. US Patent 3,675,327, July 1972.

Paffenbarger, G. C. The Role of Dental Materials in the Prevention of Dental Diseases. Int. Dent. J. 22:343-349, September 1972.

Dickens, B. and Brown, W. E. The Crystal Structure of $CaKAsO_4 \cdot 8H_2O$. Acta Cryst. B28:3056-3065, October 1972.

Loebenstein, W. V. Heats of Adsorption of Ammonia and Carbon Dioxide on Tooth Components. J. Dent. Res. 51:1529-1536, Nov.-Dec. 1972.

Bowen, R. L. and Argentar, H. A Stabilizing Comonomer: II. Stabilization and Polymerization Characteristics. J. Dent. Res. 51:1614-1618, Nov.-Dec. 1972.

4. WORK IN PROGRESS

4.1. Properties and Interactions of Tissue Structures and Restorative Materials

4.1.1 Physical, Electrical, Chemical and Mechanical Properties of Tissues

Sponsor: NIDR

4.1.1.1 Dimensional Changes in Tooth Structure

One of the properties of tooth or bone structure which must be given consideration in any restoration procedure is the capacity to expand or contract as a function of temperature. While the determination of this property for enamel is straightforward over all temperatures to which the mouth conceivably may be exposed (near 0°C to 60°C), a time dependent aspect combined with orientation effects have made the similar measurement on dentin and bone more complex. Aside from the relation to the clinical situation, these types of measurements are important because they assist in defining the nature of the natural composite systems in these respective tissues.

Measurements of the thermal expansion of bone were made over the temperature range of 10 to 70°C. Results for bovine femur are similar in many respects to those obtained for human tooth dentin. The larger specimens available from bone facilitate the study of the anisotropic characteristics of the thermal expansion. Cubiform specimens were prepared so that measurements could be made on a single specimen in the axial, circumferential and radial directions of the femur. Average results for the temperature range of 10 to 50°C are given in the table:

Direction	Coefficient X 10^{-6} per °C		
	Rapid Heating	Slow Heating	Approximate Range
Axial	7.9	7.2	± 1.0
Circumferential	2.7	1.4	± 2.0
Radial	-0.8	-1.4	± 5.0
Volume (calculated)	9.8	7.2	---

The coefficient in the axial direction is the same within experimental variation as that found in the axial direction for human

tooth root dentin during rapid temperature changes. Time dependent dimensional changes are present in bone as in dentin, but are confined primarily to the circumferential and radial directions. The time scale for these effects appears to be shorter in bone than in dentin. At the fastest rates of temperature change used in this investigation (about 4°C/min), the thermal expansion curves in the circumferential and radial directions are not linear and variations with time and previous thermal history are readily apparent. These variations are indicated by the large ranges of values on which the average coefficients shown in the table are based. Between 50 and 70°C, the coefficient in the axial direction remained essentially the same as for lower temperatures. In the other directions, the rate of time dependent shrinkage on heating generally increased above 50°C. The observed differences between human tooth dentin and bovine femur are probably in part the result of more uniformity of structural orientation in the bone specimens.

The time dependent dimensional changes observed in bovine femur support the previously suggested mechanism for such changes in dentin, namely that they result from changes in the water content of the organic component of the material. Large changes in water content (190×10^{-6} g/g per °C based on dry weight) were determined for the bovine femur, but these cannot be quantitatively related to the linear dimensional changes. The methods do not permit simultaneous measurements of dimensions and water content and are not of high enough precision to establish quantitative relationships even if simultaneous determinations could be made. However, the water content measurements do provide data for calculating the volumetric thermal expansion of the organic component of the bone. Using the data in the table, a measured value of 12.5% for the water content of the bone at 23°C, published values for the expansion of water and the mineral component of the bone and a published value of 35 to 65 for the ratio of the organic to the mineral content of dry bone, the calculated value for the volumetric thermal expansion of the organic component of the bone is 560×10^{-6}/°C. This is in agreement with the average value of 540×10^{-6} previously determined by Weir for kangaroo tail tendon collagen (NBS J. Res. 41:279, 1948).

4.1.1.2 Piezoelectric and Dynamic Mechanical Measurements of Bone, Dentin and Collagen

The construction and assembly of piezoelectric and mechanical properties measurement apparatus is being brought to completion. This apparatus is to be used in an extensive and long-term study of the properties of bone and collagen over a wide range of temperature, humidity and frequency. Several project goals are: (1) to obtain a molecular explanation for the piezoelectric effect, (2) to obtain a collection of basic characterization data, (3) to observe the effect of chemical alteration (such as fluorine substitution) in bone and collagen, and (4) to investigate the differences in the effects which occur in bone and in collagen. Two important long-range goals are the use of the piezoelectric effect as a diagnostic tool and an investigation of the role of the piezoelectric effect in caries formation and osteogenesis.

The schematic diagram of Figure 1 shows the components of the apparatus. Essentially, the system consists of a transducer driver for applying an alternating stress to the sample, a voltage detection circuit for measuring the piezoelectric voltage, a phase measuring circuit for determining the phase difference between applied stress and resultant observed piezoelectric voltage or resultant strain, and a displacement transducer to detect sample strain. Measurement of the phase angle will provide an observation of the viscoelastic effects in terms of the loss tangent tan δ.

All components of the system, except the amplifier in the bucking voltage circuit, have been constructed as purchased. The feasibility of the system has been established in an observation of the stress-strain properties of a sample of dry bovine femur. In this experiment, a 220-volt rms signal at 150 Hz was applied to a ceramic transducer driver. This resulted in an alternating stress of about 1 lb. being applied to the sample and a corresponding strain in the sample of approximately 5×10^{-3}%. Sample displacement was approximately 5×10^{-5} cm which gave an adequate signal of 50 millivolts from the displacement transducer.

Before complete experimental runs can be made, an extensive calibration of the system must be undertaken. The phase shift in

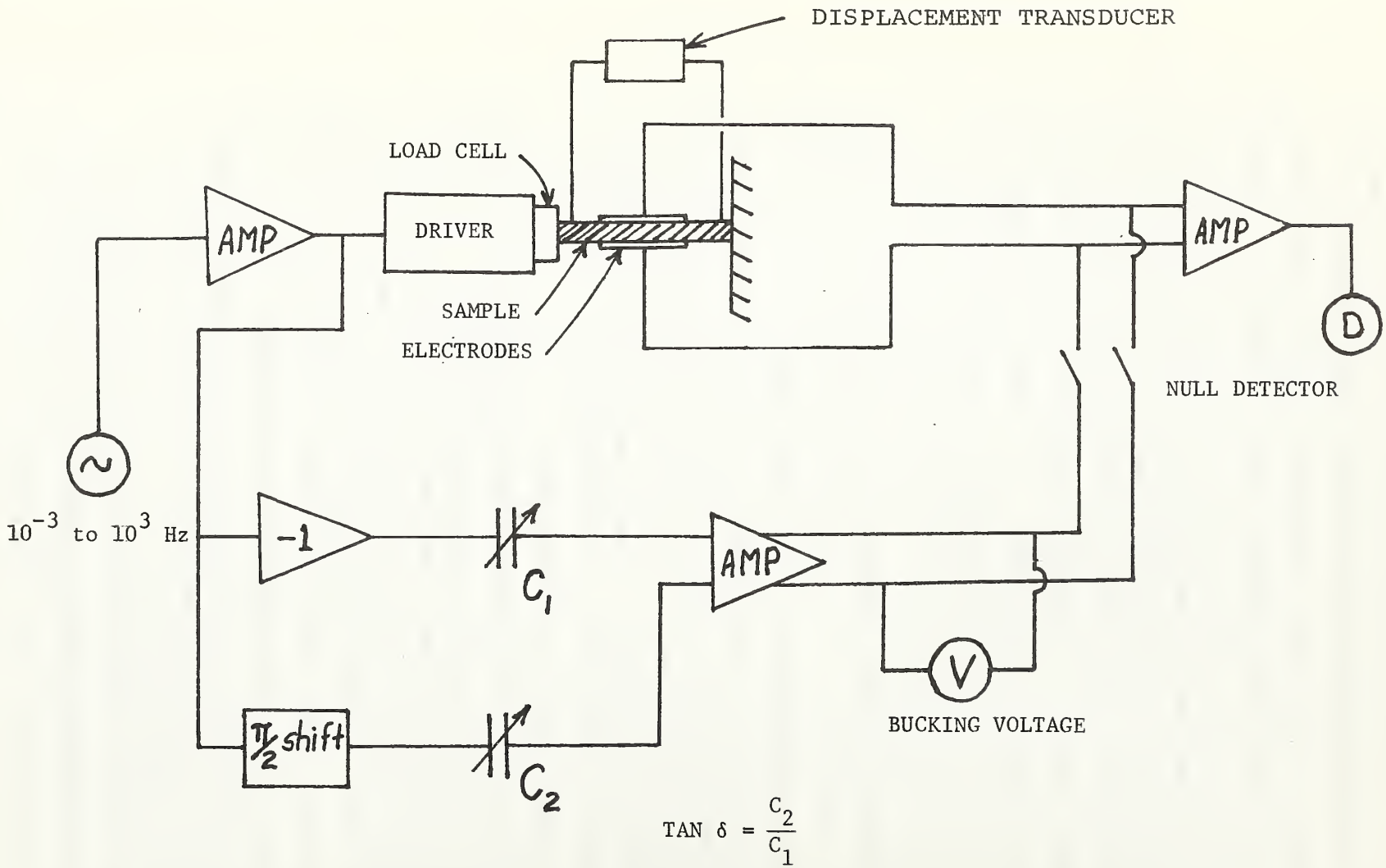

Fig. 1. Schematic Diagram of Piezoelectric Measurement Apparatus.

each amplifier must be determined and the accuracy of the -1 inverting amplifier and the $\pi/2$ phase shifter must be known. Also, the load cell and the displacement transducer must be calibrated. These calibrations will require the assembly of specific calibration circuits.

At this time, we are proceeding with the calibration of the phase shift in the amplifiers. A result from a measurement of the phase shift in the -1 amplifier is 10^{-3} radians at 1000 Hz, but only 10^{-5} radians at 10 Hz, and less than 10^{-5} radians at frequencies below 10 Hz. Since we are interested in a resolution of 10^{-3} radians, correction for the amplifier phase shift becomes significant only above 10 Hz.

For the immediate future, calibration will continue for several months and the sample holder design will be formulated.

4.1.1.3 Characteristics and Thermal Stability of Hard and Soft Tissue Collagen

Compared with collagen from other sources, the collagen derived from bovine dentin (and, presumably, human dentin) has been shown by Veis to have infinitely less capacity to absorb large quantities of water as the system is made acidic or basic. This fact has been attributed to a combination of the morphology of dentinal collagen, i.e. its thin fibers packed in a very tightly interwoven array, and an apparently greater degree of crosslinking. By comparing the interaction of collagens from different tissue sources with a variety of solvents, we are seeking to provide better understanding on a macromolecular level of these collagenous tissues and to relate this information to that being obtained on a molecular level by amino acid sequence studies in other laboratories.

It is well known that compounds which form strong hydrogen bonds can disrupt the hydrogen bonding that exists in synthetic and natural polypeptides. However, care must be exercised that the chemical agents do not degrade the peptide bonds as well. Thus, certain strong organic acids, e.g. trifluoroacetic acid, in addition to disrupting the inter or intra-molecular hydrogen bonding of peptides also can cause degradation of the polyamide backbone. It has been reported

that certain highly fluorinated alcohols and diols possess excellent hydrogen bonding capacities while causing little, if any, of the degradative side effects. For example, it is claimed that even leather, i.e. tanned collagen, may be altered (improved scuff resistance, oil and water repellency, etc.) by treatment with certain polyfluorinated gem diols (U. S. Patent 3,094,370). Since these diols and other fluorinated alcohols are such potent solvents for a wide variety of polar polymers (polyamides, polyesters, polyethers, etc.), it is of interest to determine their effect on collagen, especially dentinal collagen.

We have found that highly fluorinated alcohols such as 2,2,2-trifluoroethanol, 1,1,3-trihydrotetrafluoropropanol, hexafluoroisopropanol and the gem diol of sym-dichlorotetrafluoroacetone cause significant changes in the morphology of kangaroo tail tendon, achilles tendon, and collagen film.

For example, at room temperature 2,2,2-trifluoroethanol will cause an initial rapid lateral swelling and then subsequent longitudinal contraction (denaturation) in kangaroo tail tendon. Achilles tendon, on the other hand, exhibits only slow lateral expansion in this solvent. Bovine dentinal collagen (demineralized) exhibits very little swelling, but some curling at the edges after 24 hours at room temperature.

A more potent solvent is hexafluoroisopropanol. Kangaroo tail tendon is most affected by this agent (very rapid lateral swelling, followed by longitudinal contraction, gelation and possibly some solution degradation). Achilles tendon behaves in a similar fashion at about the same rate. Dentinal collagen does not appear to swell in hexafluoroisopropanol even after prolonged exposure (several weeks). However, this form of collagen does appear to be undergoing some change, perhaps in morphology, as witnessed by the edges of the collagen curled inward and the material becoming translucent. After removal from the solvent and washing with distilled water and air drying, the treated collagen seemed tougher than the untreated material. On immersion in water, the curling effect returned. Aqueous solutions of hexafluoroisopropanol had similar effect on all forms of collagen.

In the case of aqueous solution of the gem diol of sym-dichlorotetrafluoroacetone, pronounced rapid swelling followed by longitudinal contraction was observed with kangaroo tail tendon and achilles tendon. With dentinal collagen, not much swelling was observed, but, again, the edges of the collagen curl inward, probably indicative of strong internal stresses occurring in the structure.

As reported earlier, certain forms of collagen exhibit interesting swelling behavior when immersed in certain organic compounds (monomers, such as 2-chloroethyl methacrylate and alkyl iodides) in the presence of water. In the case of the methacrylate monomers (e.g. 2-chloroethyl methacrylate, trifluoroethyl methacrylate, ethylene dimethacrylate) only lateral swelling has been observed. Presently, it is suspected that traces of impurities of methacrylic acid and the corresponding alcohol may be contributing, if not causing, the swelling phenomenon. However, methacrylate monomers that have been washed repeatedly with water to remove these impurities still exhibit this swelling potency. An apparent decrease in pH with time suggests that some hydrolysis of the ester may be occurring. We find that only a very small amount of methacrylic acid in water $<10^{-4}$ mol/l can induce significant swelling in kangaroo tail tendon. Dentinal collagen does not appear to swell significantly under these conditions.

Achilles tendon, again, exhibits intermediate swelling behavior. In none of the above experiments was any longitudinal contraction observed.

A third potent swelling system is certain alkyl iodides in the presence of water. Particularly effective are methyl iodide, ethyl iodide and perfluoroheptyl iodide. All cause gradual but very pronounced lateral swelling in kangaroo tail tendon. No longitudinal contraction is observed. In fact, after several months the tendon appears to be converted to a film-like form of collagen. Thus far, dentinal collagen has shown only slight swelling and some tendency to curl in these solvent systems. Achilles tendon exhibits intermediate behavior in this solvent system.

A study of mineralized forms of collagen such as turkey leg tendon, and bone by differential scanning calorimetry (DSC), revealed no melt endotherms below 90°C. A sample of expanded kangaroo tail tendon that had been swollen by octafluoropentyl methacrylate-H_2O treatment and then washed and subjected to vacuum freeze drying exhibited a melt endotherm at 55°C compared with 59°C for a control specimen.

4.1.2 Grafting of Polymers to Natural Tissue

4.1.2.1 Grafting to Collagen and Soft Tissues

Sponsor: U. S. Army

The physical properties of previously synthesized steer hide collagen graft copolymers were studied. Water sorption at 50% RH was always lowered on treatment of the collagen. This even applied for products containing hydrophilic groups in the side chain. Thus, the collagen-hydroxyethyl methacrylate product had a water uptake of 7.4% compared to 19.2% for collagen powder. Water sorption was dependent on the presence of hydrophilic groups and also on the amount of copolymer incorporated in the product. Lowest water uptake of about 4% was obtained for products containing fluorinated acrylates or the higher molecular weight esters of acrylic or methacrylic acid.

The reaction products of collagen with acrylic acid, methacrylic acid, hydroxyethyl methacrylate and cyanoethyl acrylate were hydrophilic and gave a zero contact angle within 15 seconds. Exact contact angles were difficult to determine because of the porous and uneven surface of the specimens. The collagen-lauryl methacrylate and collagen-2-ethylhexyl acrylate had approximate contact angles of 85° whereas those of the fluorinated acrylates and methacrylate products had contact angle values over 90°.

A procedure was worked out to graft monomers containing basic groups such as dimethylaminoethyl methacrylate onto collagen. These could not be grafted by the procedure previously used. The aqueous solution of the monomer is acidified with 2N nitric acid prior to the addition of the monomer to the collagen. Although a considerable

amount of soluble homopolymer formed, some grafting also took place as indicated by a weight increase after extraction of homopolymer.

A paper entitled "Grafting of Acrylates and Vinyl Chains Upon Collagen with Ceric Initiator" has been accepted for publication in the Journal of Applied Polymer Science.

Work was continued on the grafting to soft tissue (ratskin). Over 30 acrylates, methacrylates or vinyl monomers reacted with ratskin. By far the largest increase in weight (163%) was obtained with the highly fluorinated pentadecaoctylfluoroacrylate. The coefficient of variation for the weight increases averaged 28%, a satisfactory reproducibility considering that the ratskins vary in surface topology and chemical composition because of their natural origin. Reaction of diallyl phosphite or tri-allyl phosphate with skin produced modified surfaces containing phosphite or phosphate groups, respectively.

Reducing the reaction time below 3 hours decreased the amount of polymer formed. However, significant weight increases occurred when the reaction time was lowered to 20 minutes. Hence, relatively short reaction times should be sufficient to modify the chemical and biological characteristics of ratskin surfaces. By using selected monomers, the ratskin surface could be made hydrophilic or hydrophobic. Mineral oil completely wets untreated ratskin. Oil repellency was incorporated in the subdermal surface on polymerization with pentadecafluorooctyl acrylate, but efforts to obtain oleophobic epidermal surfaces were not successful. This behavior toward non-polar liquids differs from that of grafted collagen powder or film and presumably results from the keratinous nature of the epidermal surface.

Modification of wetting characteristics was more easily accomplished with collagen than with ratskin. Water uptake for the treated specimens differed little from that of the controls. The uptake from 0 to 50% RH was generally in the 7 to 10% range. An exception was ratskin-pentadecafluorooctyl acrylate which had a water sorption value at 50% RH of 3.1%. These results differ from those obtained with collagen powder where grafting always lowered water sorption. The high

yields for grafting onto collagen indicate that the reaction takes place throughout the specimen, whereas the much lower weight increase with skin is a result of mainly surface grafting. Thus, it is not surprising that water sorption, which is predominantly a function of water absorption throughout the specimen, is not altered greatly for the grafted ratskins.

Growth of microorganisms is retarded or completely inhibited after reacting the skins with monomers. Mold growth was not found after one week or one month on skins treated with methyl methacrylate, glycidyl methacrylate, isodecyl acrylate, hexafluoroisopropyl acrylate or acrylonitrile. Profuse growth was observed on the ratskin controls. Some growth took place at the edges where the skins had been cut after grafting treatment and where, apparently, the tissue was not exposed to monomer. This indicates again that grafting occurred predominantly at the surfaces.

Recently, a persulfate-bisulfite redox system has been suggested for grafting side chains to chromium-tanned collagen. Using this redox system, we obtained yields of methyl methacrylate grafted to ratskin somewhat larger than those obtained in the ceric ammonium nitrate-initiated polymerization. Even larger increases in weight were obtained with butyl acrylate, especially on addition of 10% acrylic acid, both for 3-hour and for 20-minute reaction times. A methyl methacrylate-10% acrylic acid comonomer gave a 10% increase in weight for a 20-minute reaction period.

This reaction was conducted in a carbon dioxide atmosphere. Substituting CO_2 for nitrogen in the ceric ion initiated polymerization did not affect the yield. Carbon dioxide is readily available as "dry ice" and may, therefore, be preferable for practical applications.

Studies have been initiated to graft to ratskin using donor-acceptor complexes. Polymerization is limited to certain comonomer pairs having electron donor and acceptor properties, respectively. Weight increases have been obtained with methyl methacrylate-styrene comonomers. It is anticipated that the side chains in the product

have alternating styrene-methacrylate units. Future investigations will determine the feasibility of using ultraviolet radiation to initiate grafting. It has been proven conclusively that the ratskin surface is altered by the reaction with various monomers. Investigations will be initiated to determine if such surfaces improve adhesion to various substrates.

4.1.2.2 Grafting to Hard Tissue

Sponsor: NIDR

The feasibility of grafting selected monomers to hard bone tissue has been established in previous work conducted in this laboratory. The investigation now in progress has the following aims: (1) standardization of preparation of test specimen and grafting techniques; (2) determination of the scope of the ceric ammonium nitrate (CAN) initiated graft polymerization to bone using selected monomers; (3) establish the reproducibility of the results obtained by this technique; (4) determine extent of modification in surfaces; (5) investigate the use of other chemical initiator systems such as persulfate-bisulfite, polymerization with charge-transfer (donor-acceptor comonomer) complexes which may lead to stereoregular side chains and may yield more rapid grafting; (6) investigate use of ultraviolet radiation as the initiator of side chain grafting; (7) assess improvement in adhesion and resistance to environmental attack generated by the polymeric graft technique; (8) characterization of the side chain grafted to bone; and (9) application of the technique to modify hard tissue for clinical application.

Experimentally, bone marrow pulverized to powder at dry-ice temperature was used. The sieved powder was equilibrated to 50% R.H. and stored for one hour in the presence of wetting agent. The suspension was then deaerated and a 0.05 M ceric ammonium nitrate solution and monomer were added. After reaction times varying from 20 minutes to 3 hours, the bone was filtered off, dried and weighed. Homopolymer was assiduously removed by extraction with a suitable solvent, usually acetone. The extent of grafting was assessed gravimetrically by making comparison to a control experiment (initiator and monomer absent). A

small weight loss occurred in the control experiment as a result of the slight decalcification incurred in the presence of the acidic (initial pH = 2.2) ceric ammonium nitrate solution.

The higher homologues of the acrylate and methacrylate esters could be grafted onto powdered bone. Grafting to obtain products containing fluorinated acrylate or methacrylate side chains is being studied. Such products should possess a highly hydrophobic surface.

The bone-polymer product can be further modified. For instance, the glycidyl methacrylate side chain contains an oxirane ring. A variety of functional groups such as hydroxy or amino groups can be incorporated into the side chain through a ring opening process.

Generally, it was observed that the presence of mineral in the tissue restricted the yields of graft polymer (yields based on total bone powder weight) relative to that achieved with pure collagenous powder (steer hide powder). This might be expected since less collagenous surface per gram of substrate would be available, and there is also less swelling capacity in the mineralized collagen. An exception, however, was found on grafting dimethylaminoethyl methacrylate which, unless acidified prior to the addition to the reaction mixture, will not graft to a pure collagen powder surface. With bone, however, this monomer reacts readily and the mechanism of this reaction needs to be studied further.

The presence of polymer in the substrate is indicated by the infrared spectra of the products. However, the absorption spectra do not permit one to distinguish between homopolymer which was formed in the reaction in the interstices or at the surface of the bone, from truly covalently attached polymer.

We have explored in a preliminary way the possibility of using so-called mechano-chemical techniques for grafting. These techniques have been used with polyamides and substrates such as wool and cellulose. For exploratory purposes, we have used collagen rather than bone. We appear to get graft polymerization (there is no initiator or catalyst in the normal sense of these terms) when polymerization was attempted in vacuum for relatively long periods (up to several

weeks). Modification of the procedure so that reaction was under nitrogen for relatively short periods of time (one to eight hours) failed to yield any graft polymer. A more drastic swelling reaction appears to be a requirement for grafting by this procedure and, if so, the potential application to bone or dentin would appear to be very reduced.

4.1.3 Surface Characterization by Water Adsorption

Sponsor: NIDR

Surface phenomena play a critical role in development of caries, development of periodontal problems, and in the efficacy of a tooth restoration process. Surface phenomena are also basic to development of preventive dentistry techniques. It is a dichotomy that we do not understand the mechanism by which undesired plaque adhere to the tooth surface so tenaciously and that we are unable to date to develop an adhesive procedure which will effectively bond dental materials to tooth structure.

Immediately previous to initiating studies of water adsorption on natural and synthetic dental materials, we had determined the adsorptive capacity and energy of interaction with gases such as N_2, CO_2, NH_3 and CH_3NH_2 and a portion of this research was recently published (J. Dent. Res. 51:1529-36, 1972).

It has been pointed out recently by Brunauer et al (J. Colloid and Interface Science 29:485, 1969) that there are many important adsorbents that have part of their pore systems, often the major part, inaccessible to nitrogen but accessible to water vapor. Inasmuch as the work on CO_2 and NH_3 adsorption demonstrated the profound influence of polar groups on the capacity for adsorption by dentin and because water is the most abundant component of all biological systems, the water vapor project was initiated.

After careful study, a circulating closed system utilizing a peristaltic type pump to control the rate of circulation of air saturated with water vapor was selected for the measurements. A weighing tube containing the adsorbent was mounted up stream from the

pump and saturator with the effluent connected back to the pump to complete the circuit. Relative humidities between 10-97% are used. Dead volume of the system is very small compared with other systems and this, together with a minimum of dependence on diffusion, contributes appreciably to the superior performance of the apparatus. Final revisions were made on a manuscript describing the procedure and initial results and it is presently slated for publication in J. Dent. Res., March-April 1973.

A striking observation of the water adsorption characteristics of collagen-containing adsorbents, e.g. dentin, is the large hysteresis loops which persist over the entire range of humidities. A manuscript is under review by the NBS Editorial Board on the extension and experimental verification of an adsorption hysteresis theory.

Among the synthetic dental materials being studied are a poly-(methyl methacrylate), hardened silicate cement, and investment material. Surface area, hysteresis boundary curves and scanning curves are determined. Interpretation of these data appears to relate to dimensional changes as well as sizes, shapes and distribution of pores within the substrates.

Considerable effort has been spent in revision of a manuscript to be submitted to J. Colloid and Interface Science. This is entitled "Surface Area of Aggregates". In its present form, the theory is entirely free from some objectionable aspects of the original formulation. As a consequence, it has lent considerable strength to the possibility of using adsorption theory as a tool to detect the permeability toward water vapor (or other adsorbate molecules) possessed by the resinous component of an aggregate. This concept is now being tested experimentally by means of water vapor adsorption measurements. The samples consist of different known percentage compositions of the same two components in resinous aggregates, as well as the components, themselves, measured separately. Application of these results, it is hoped, will be directly translatable to "pit and fissure" type sealants.

Valve attachments have been designed and constructed to increase

the range of applicability of the water vapor adsorption apparatus. They enable the adsorption to be performed in the absence of air, when so desired. Any gas can now be used to replace air as the carrier medium. This is especially useful when room temperature oxidation of the sample might otherwise occur, giving rise to erroneous results.

4.2 Crystallographic, Solubility and Chemical Studies on Ca and/or P Minerals

4.2.1 Crystal Structure Determinations and Crystal Chemistry

Sponsor: NIDR, NIDR (Grant), ADA

This research is an integral part of a major program on the mechanism as opposed to the etiology of dental caries. Input is also provided by these studies to the development of adhesion between restorative materials and tooth structure.

We have continued to obtain structural data on substances of biological importance or relevance, including substances with deliberately introduced amounts of impurities of biological significance. Structural parameters give the averaged atomic arrangement and strong indications of the sites of impurities. Often the reason for the choice of a particular site by an impurity and the means whereby it affects the physical and chemical properties of the host substance become apparent. Along more interpretive lines, systemization of these crystal structures by geometric properties and crystal energies, development of epitaxial relationships, and elucidation of the role of hydrogen bonding will provide a better basis for understanding how hard tissues are organized.

β-$Ca_3(PO_4)_2$

β-$Ca_3(PO_4)_2$ is an important constituent of dental calculus, particularly in those areas where the drinking water contains magnesium ions. Its presence in carious lesions has also been suspected. The two main points of interest in β-$Ca_3(PO_4)_2$ are (1) the role of Mg in acting as a stabilizing impurity, which when present favors the formation of Mg-containing β-$Ca_3(PO_4)_2$ rather than $Ca_5(PO_4)_3OH$,

hydroxyapatite, and (2) the exact nature of the salt when formed at either ∿1000°C under dry conditions or body temperature in an aqueous environment. We have obtained x-ray data and structural parameters for samples of β-$Ca_3(PO_4)_2$ containing 0-14% of cations as Mg^{2+}. The analysis of the pure compound showed that the even requirement of the C-glide plane in the space group R3c is met by having four normal cations and one cation which appears as two "half" cations by being randomly distributed over two sites (i.e. the disorder, which is necessary to conform to the symmetry requirements of the space group and to the electrical neutrality requirement, is confined to one cation). It is obvious from the structural parameters that this disorder has a considerable effect on the rest of the structure.

The analyses of the Mg-containing samples showed that (1) the stabilizing effect of Mg arises because the smaller Mg ion replaces Ca in an octahedron of oxygens which is actually smaller than a typical coordination of Ca, (2) there is a small amount of additional disorder of the cation found to be disordered in pure β-$Ca_3(PO_4)_2$, and (3) extra precautions are necessary in the least squares refinements to allow for the effect of the cation disorder on the rest of the structure, i.e. to insure that the numbers obtained in the computer programs are not unduly influenced by artifact. Because of factors (2) and (3), the computational analysis is more complicated than usual, but we believe a satisfactory method of procedure in the least squares refinements has been devised. After we have applied this procedure to all the Mg-containing β-$Ca_3(PO_4)_2$ structures, we will have information which will reveal the structural role of differing amounts of impurity. To our knowledge, this study constitutes the most intensive and accurate studies of impurity effects. The procedure is applicable to other materials where the effect of impurity warrants study.

$Ca_8H_2(PO_4)_6 \cdot 5H_2O$ (octacalcium phosphate)

$Ca_8H_2(PO_4)_6 \cdot 5H_2O$ is important as a calcium phosphate which has a pronounced tendency to enter into an epitaxial relationship with $Ca_5(PO_4)_3OH$, hydroxyapatite, and thus is often intimately involved

with $Ca_5(PO_4)_3OH$. The details of a previously determined structure (1960, W. E. Brown) are too coarse for many applications and we are refining the structure with advanced techniques available to us in this laboratory. About 2500 weak x-ray reflections have been collected. The crystal used is small, but is the largest found in years of growing $Ca_8H_2(PO_4)_6 \cdot 5H_2O$.

Isotropic refinement of the structure of $Ca_8H_2(PO_4)_2 \cdot 5H_2O$ showed evidence of disorder in the hydrated layer. This was borne out by subsequent anisotropic refinements. Although the disagreement (R_w) between observed x-ray quantities and calculated quantities is very low (4.6%), and the results are therefore excellent at first sight, some changes in the fine details of the structural model as used in the refinement scheme are necessary before the structural parameters can be assumed to have physical significance.

The disorder arises because some water molecules are able to hydrogen bond in more than one way and are therefore in slightly different places in different unit cells. A hydrogen bonding scheme for the waters and two HPO_4 groups in $Ca_8H_2(PO_4)_2 \cdot 5H_2O$ has been worked out and is being tested.

$Ca(BF_4)_2$

In conjunction with Professor T. H. Jordan of the Chemistry Department, Cornell College, Iowa, who has chosen to spend a sabbatical year in our laboratory, we have begun an investigation into BF_4 salts. These salts are important as possible fluoridating agents because they slowly hydrolyse in water to produce fluoride ions. The rate of production of fluoride ions is too slow to allow CaF_2 to precipitate and instead there is a tendency to form the desirable product fluoridated hydroxyapatite $Ca_5(PO_4)_3(OH,F)$. We have collected 6239 x-ray reflections from a spherical single crystal of $Ca(BF_4)_2$. These reflections were merged into a unique set of 2934 reflections of observable intensity and 454 reflections which were not significantly above background. The disagreement between equivalent pieces of data was satisfactorily good at 2.6%.

$Ca(H_2PO_4)_2 \cdot H_2O$

In a previous x-ray diffraction study of $Ca(H_2PO_4)_2 \cdot H_2O$, ideal hydrogen positions were calculated because of the imprecise detail revealed through x-ray diffraction. By neutron diffraction we have confirmed the bifurcated bonding of one hydrogen atom predicted on the basis of x-ray diffraction. On completion of least square refinement, the hydrogen bonding in this salt will be well-characterized and can be related to that in other phosphates.

$SnHPO_4$

From a reported crude determination of the structure of $SnHPO_4$, the $HPO_4^{=}$ ions apparently form dimers $(HPO_4)_2$ by very strong hydrogen bonds. Such entities may also exist in aqueous solutions of phosphates, and their occurrence in the solid state permits them to be well-characterized. Once known, these same characteristics can be sought in aqueous solutions. In conjunction with Prof. Jordan, we have (1) attempted to grow crystals of a size suitable ($\sim 3mm^3$) for neutron diffraction, (2) investigated the infrared and Raman spectra of $SnHPO_4$ and assigned frequencies to the hydrogen and deuterium motions, and (3) established by DTA that decomposition occurs at $\sim$250°C and that there is no first order phase transition above -100°C.

The spectral investigation showed that the hydrogen bond between dimers is not as strong as the structure determination suggests. Further work on crystal growth is in progress. If this effort is successful, the crystals will be used in single crystal Raman work and in neutron diffraction.

Rare Earth Apatites

In collaboration with Professor I. Mayer of Hebrew University in Jerusalem, Israel, who is spending a sabbatical year at NBS, we have been investigating various rare earth apatites with the general formula $RE_xM_{10-2x}Na_x(PO_4)_6F_2$, where RE is a trivalent rare earth ion such as La^{3+} and M is a divalent alkali earth cation such as Ca^{2+}, with all cation sites filled in the apatite structure. The reactions were carried out at 100°C in a sealed platinum tube and

the products were first characterized by x-ray powder diffraction. Lattice constants of a series of rare earth-strontium-sodium, barium-sodium, and calcium-sodium fluoroapatites prepared in this way have been determined. The lattice parameters have been observed to decrease with decreasing ionic radius of the rare earth ion. It is noteworthy that in the Eu-Ca-Na system, the lattice parameters remain constant at all compositions and are the same as those of $Ca_{10}(PO_4)_6F_2$, perhaps because the average of the radii of Eu^{3+} and Na^+ is close to the radius of Ca^{2+}, and these ions are distributed among the crystallographic sites of Ca^{2+} as follows:

	Cations in Compound	Cations in Triangular Sites	Cations in Columnar Sites
in the compound	$[Eu_4Ca_2Na_2]$	$[Ca_2Eu_2Na_2]$	$[Eu_2Na_2]$
" " "	$[Eu_3Ca_4Na_3]$	$[Ca_4EuNa]$	$[Eu_2Na_2]$
" " "	$[Eu_2Ca_6Na_2]$	$[Ca_6]$	$[Eu_2Na_2]$

In case of the Ba-compounds, apatite-like compounds with rare earths smaller than Nd could not be prepared, most probably because the difference in size of the two atoms was too large. Attempts to prepare compounds with composition $Ln_5Na_5(PO_4)_6F_2$ also failed.

In many cases, single crystals of the above compounds were found in the preparations. We plan to investigate the exact locations of the various ions in these compounds.

Several attempts to prepare oxyapatites of the type $RE_2Ca_8(PO_4)_6O_2$ and $RE_2Sr_8(PO_4)_6O_2$ were unsuccessful in spite of great precautions.

Epitaxy

Epitaxy is defined as the oriented overgrowth of one substance on another. Considerable emphasis has been placed in the scientific literature on elucidating the initial nucleation process, mainly through developing techniques for the growth and examination of thin films, and on the mechanisms of misfit accommodations due to lack of complete correspondence of the two substances involved. Because growth of calcium phosphates in an aqueous environment takes place under mild conditions, structural fit is probably more important than misfit requirements, although the degree of misfit which can be accommodated is probably also small. We have written two computer programs with which to search systematically for possible epitaxies in

calcium phosphates, with special reference to apatites. The first program searches out those metric fits (or misfits) which occur within predefined limits. The second, which takes the metric fits and compares the possible structural fits, is still being developed, checked and corrected. Development of both programs is taking place slowly because of the large amount of introspection necessary in developing a new approach. The first program is based mainly on lattice parameters and pays little attention to chemical information. It determines which sections or networks in the unit cell lattices in the two compounds being compared match up with one another within generally accepted or reasonable criteria. At present, these criteria are (1) no network edge is greater than 20Å, and (2) no misfit of networks greater than 15% in length of component vectors defining networks and no misfit of greater than 10° in the angles between vectors is allowed. Only those networks which will give unique planes through the real crystal structure (which usually has lower symmetry than the lattice) are generated. The results between hydroxyapatite and various other compounds of possible or known biological significance are given in the following table:

Other compound	Number of unique matches
$Ca_4(PO_4)_2O$	146
$Ca_5(PO_4)_3OH$	20
$Sn_3PO_4F_3$	111
$CaHPO_4 \cdot 2H_2O$	621
$CaHPO_4$	15*
$Ca_8H_2(PO_4)_6 \cdot 5H_2O$	13
$CaCO_3 \cdot 6H_2O$	90
$Ca(COO)_2 \cdot H_2O$	134
$Ca(COO)_2 \cdot 2.2H_2O$	17
$CaCO_3$ (aragonite)	538
$CaCO_3$ (calcite)	40
$BaCa(CO_3)_2$	774
$CaKAsO_4 \cdot 8H_2O$	201
$MgNH_4PO_4 \cdot 6H_2O$	331

* originally > 1000 so criteria reduced internally by program.

Later work has shown the necessity for reduction of the number of network matches to be considered, so a figure of merit has been assessed for each match and the matches sorted in order for each compound.

The second program takes the sorted matches generated by the first program and checks the match of the structural details. In a recent run (with 16 unsorted matches) the program correctly signalled what we a priori considered the best match, picked the appropriate planes through the two structures and correctly matched up the different kinds of atoms, i.e. columnar Ca ions (Ca(I) in $Ca_5(PO_4)_3OH$) with columnar Ca ions in the second compound, and so on. This was a pleasing result. Because of the computing delay referred to earlier, recent progress has been slow.

Rotation About Scattering Vector

The crystal of $Ca(BF_4)_2$ referred to earlier had weak reflections where we thought there should be none. We showed conclusively that this was an artifact due to double reflection. To do this it was necessary to write a computer program for an accessible time shared computer and to use the angle settings thus calculated on the x-ray diffractometer.

Energetic Calculations

We have resumed calculations of lattice energies. The first step, by no means trivial, is to make the computer program made available by W. R. Busing of Oak Ridge National Laboratory fit on the NBS Univac 1108 computer. Later, we hope to determine and test the transfer ability of the potential parameters of Ca, PO_4, CO_3 and perhaps H_2O. This work will be exploratory in that we do not know how feasible it will be or how precisely the calculations will correspond to experimental determinations. In principle, there could be a tie-in with a third step of the epitaxy calculations in which energies of epitaxy could be calculated. Eventually, calculations of this type should have value relative to the variable composition and solubilities of apatites such as those in enamel.

4.2.2 Physical Chemical Studies of Calcium Salts

Sponsor: NIDR (Grant), ADA

Solubility of $CaHPO_4 \cdot 2H_2O$

The experimental data on the solubility of $CaHPO_4 \cdot 2H_2O$ in the system $Ca(OH)_2$-H_3PO_4-NaCl-H_2O were treated by the adjustment procedure. The results show that both the Debye-Hückel and Davies equations provided suitable means for calculating the activity coefficients of the ions up to NaCl concentrations equal to those in serum. However, it was found that the fit of the data was poorest in the highest range of pH's covered by our measurements at higher NaCl concentrations. The electroneutrality unbalances calculated from the raw data indicated an unaccounted for anionic species could have caused poor adjustments. Reviewing the situation further, it became apparent that this species could be $NaHPO_4^-$. Preliminary calculations give the stability constant for such an ion pair in the range of 8-10 L/mole. Adjustment procedure is being used to estimate its value correctly. It is hoped that the data will fit better at all pH ranges after introducing $NaHPO_4^-$ species. The existence of the ion pair $NaHPO_4^-$ could have considerable physiological significance because the high Na^+ concentration in serum would require that corrections be made in the activity of phosphate ions taking into account the species $NaHPO_4^+$. The fact that our calculations of (1) the solubility product constant, and (2) the electroneutrality unbalances both point to the existence of this species gives us added confidence in the validity of this new feature in our model.

Topical Fluoridation

Our objective of developing a more effective topical fluoride agent has been premised on the condition that one should attempt to form an acidic salt such as $CaHPO_4 \cdot 2H_2O$ within the enamel which, after treatment with a fluoride-containing solution, would be converted to the insoluble salt fluorapatite, $Ca_5(PO_4)_3F$. Formation of fluorapatite in this way would not be limited by the slowness of a solid state reaction which seems to be the limiting factor in presently used treatments. The possibility of achieving this objective was considerably improved in a recent experiment when it was found that hydroxyapatite could be nearly completely converted to fluorapatite with a

solution containing calcium, phosphate and BF_4^- ions. $CaHPO_4 \cdot 2H_2O$ forms during the reaction as an intermediate product which is subsequently converted to fluorapatite by F^- ions resulting from the hydrolysis of BF_4^- ions. We believe that the formation of fluorapatite is favored over that of CaF_2 in this solution by the high calcium and phosphate concentrations, and the low concentration of F^- ions because the major portion of the fluoride is present as the BF_4^- ions.

Coulometry

The preparation and physical chemical study of hydroxyapatite and related calcium phosphates has indicated a need for more sensitive analytical methods of chemical assay. For example, the heats of solution of different apatite preparations were found to vary by as much as 12 K cal/mol. These same preparations were assayed to have nearly identical calcium to phosphate ratios within the limits of present analytical procedures. Therefore, in an effort to improve the accuracy and precision for calcium analysis, to better than 0.5%, considerable time has been devoted to the adoption of a published method using constant current coulometry.

Constant current coulometry relies only on accurate measurements of current and time. Thus, not only is coulometry independent of chemical standards, but offers the additional advantages of pretitration of reagent impurities and the ability to titrate microgram quantities. The method is limited almost entirely by the precision with which the end-point can be located.

The adopted method utilizes the cathodic generation of ethylenediaminetetraacetate anion from its mercury (II) complex.

$$HgEDTA^{2-} + 2e^- \longrightarrow Hg^\circ + EDTA^{4-}$$

For each Faraday of current passed through the titration cell, one-half of an equivalent of titrant is generated. To date, the method has not yielded the desired precision. However, it is anticipated that the remaining experimental difficulties will be eliminated.

Growth of Fluorapatite Crystals from Aqueous Solutions

Although fluorapatite, $Ca_5(PO_4)_3F$, can be grown in good crystalline form at very high temperatures, its properties and composition are

likely to differ somewhat from those grown from aqueous systems at more moderate temperatures. We have chosen conditions of maximum acidity where fluorapatite is still a stable phase. The solutions used are ones which are near the singular point for $Ca_5(PO_4)_3OH$, CaF_2, and $Ca(H_2PO_4)_2$ in the system $Ca(OH)_2$-H_3PO_4-H_2O-HF. The reaction employed is the hydrolysis of $CaHPO_4$ and CaF_2 to form $Ca_5(PO_4)_3F$ and $Ca(H_2PO_4)_2$. After most of the $CaHPO_4$ has been hydrolyzed, the solution is diluted to form more $CaHPO_4$ from the $Ca(H_2PO_4)_2$.

The results to date include successful growth of $Ca_5(PO_4)_3F$ crystals as large as 100 x 10 μm. Although these are still too small for single-crystal x-ray studies, they should be useful for other purposes. Contrary to our experiences with $Ca_5(PO_4)_3OH$ and $Ca_5(PO_4)_3Cl$, both of which show considerable fibrous character in the crystals grown from aqueous solutions, the $Ca_5(PO_4)_3F$ crystals appear to be monolithic.

4.3 Structure and Thermodynamic Studies of Noble Metals and Their Alloys

Sponsor: NIDR (Grant)

Electron microprobe data for alloys in the vanadium-rhodium alloy system have now been obtained and these data will enable us to complete the phase diagram. Similar data are currently being obtained from niobium-osmium alloy samples. Meanwhile, we are concentrating our efforts in the preparation and heat-treating of alloy samples for the tantalum-palladium, niobium-palladium and niobium-platinum alloy systems. These systems were only partially determined in previous studies at other laboratories and it is our intention to complete these diagrams.

As our systematic study of these phase diagrams approaches its logical conclusion, we feel compelled to review the data which have been acquired to see if useful trends are emerging. It seems desirable already that certain alloy systems should receive further study in efforts to develop useful dental alloys. These systems offer the possibilities of improved mechanical properties, adequate corrosion

resistance, and biocompatibility with the oral tissues. The latter point should certainly receive thorough consideration in view of recent trends toward a more extensive use of implant dentures.

A great deal of our effort at the present time is directed toward writing and publishing our results in reputable scientific journals so that the information obtained will be widely disseminated. Details of the experimental procedures employed are highly desirable in such reports so that the reader can evaluate the quality of the work and decide how much reliance he may place in these results. Many figures and tables are needed and this requires a considerable investment of time and effort in writing, in proof-reading and in editorial reviews. Each binary alloy system is to be published separately since the experimental procedures were varied in order to produce optimum results for each system. Our future plans will emphasize the preparation of suitable publications for all of the data which we have acquired. We shall ultimately try to incorporate all of the existing data on binary systems involving the transition elements into a comprehensive, systematic and compact review so that the data can be readily applied to the development of practical alloys for various applications in dentistry and elsewhere. Finally, we shall continue our experimental work in selected systems or within certain composition regions where previous studies have been inadequate.

4.4 Developmental, Clinical, and Standards-Related Research

4.4.1 Three-Dimensional Panoramic X-Ray

Sponsor: NIDR, ADA

The addition of a third dimension to the panoramic x-ray would provide additional diagnostic and operative information to the oral surgeon and to the endodontist and should be of assistance to an orthodontist.

As a first step in the development of such an instrument, we have reassembled a modified form of the original two-dimensional panoramic x-ray prototype used some years past at NBS. Our aim is to provide instrumentation which can be operated with personnel now familiar with

the presently used panoramic x-ray equipment. The major change in procedure will involve splitting the x-ray beam or devising a procedure for incorporating an additional x-ray source. The two routes we are exploring are (1) simultaneous non-interfering exposure of two films and a special viewing technique, e.g. stereo glasses, etc., and (2) a lenticular lens technique using one x-ray beam. Because the latter technique is not envisaged as requiring stereo glasses or stereo viewing equipment and thus has potentially greater usefulness, we have been expending our effort in this direction.

In this report period, we have prepared a number of lenticular plate-optical grid-cassette combinations, but the results have not approached the full potential of this system.

We are modifying some of the stationary x-ray grids which we will test to see if exposures can be made to register with the lenticular plates.

While we are emphasizing the lenticular lens approach, we are continuing design and construction of a camera for recording two separate exposures at different angles (method (1) above) since it will probably be necessary to compare results and tissue radiation exposure for the two methods before deciding on the optimal system for producing stereoscopic x-rays.

4.4.2 Composite Restorative and Pit and Fissure Sealant Materials

Sponsor: ADA, NIDR (Grant), NIDR

Work has been commenced on developing materials for use in preventive dentistry, and work has continued to further improve composite restorative materials. The latter were first invented and developed in the Dental Research Section of the National Bureau of Standards and manufacturers were provided with synthetic methods and suitable formulations. These dental filling materials are being sold in this country under trade names* such as Adaptic, Blendant, Concise, Compodent, Compolite Composite Restorative, DFR, Exact, HL-72, Posite, Prestige, and Smile. Foreign markets are developing rapidly. While the consensus is that these materials are more durable than the silicate

- - - - - -

*Identification of commercial products in this report is done so only for clarity and does not imply recommendation or endorsement by the National Bureau of Standards.

cements they are replacing, it is nonetheless true that certain properties leave something to be desired. Among these are (a) storage stability, (b) color stability, (c) dimensional stability during hardening, and (d) resistance to wear on incisal or occlusal surfaces of the teeth. The challenge of discovering means for adequate and stable (e) bonding to the hard tooth tissues has still not been met.

(a) Stabilizers - Storage stability of the dimethacrylate monomer liquids or their pastes requires phenolic polymerization inhibitors or "antioxidants." One such compound, BHM, (3,5-di-t-butyl-4-hydroxybenzyl methacrylate) was synthesized and evaluated; its properties were described in "A Stabilizing Comonomer I. Synthesis and Confirmation of Structure" and "II. Stabilization and Polymerization Characteristics", J. Dent. Res. 51:1071, 1614 (July, Nov.) 1972. Attempts were made to synthesize a similar compound, MP, [2,6-di-t-butyl-4-(2-methacryloxyethoxy)phenol] that, theoretically, should be more effective than BHM. The preparation of MP requires a two-step synthesis. The first step was done successfully in high yield. The second step, however, has frustrated numerous attempts at what would appear to be a straightforward Williamson synthesis procedure. Alternative routes are being sought for this potentially valuable compound.

(b) Color stability - Color stability of composite materials appears to be enhanced if a small amount of an ultraviolet absorbing compound is included in the formulation. It is deemed desirable that all possible ingredients be capable of copolymerization, thus becoming part of the polymeric network and hence unable to diffuse out of the hardened material. This is expected to minimize untoward tissue reactions and possibly improve certain physical properties. Accordingly, an ultraviolet absorbing compound that contains a methacrylate group in the molecule was synthesized. This compound, HB, [2-hydroxy-4(2-methacryloxy ethoxy)benzophenone] and its properties are described in a manuscript currently being prepared for publication in the Journal of Dental Research.

Color stability, however, requires more than protection against UV-induced color-producing chemical reactions. For example,

previous mention was made of a yellow complex formed between aromatic amine accelerators and one or more phthalate monomers that are under consideration as possible binders for composite restorative materials. The investigation of the nature of the complex using ultraviolet and visible absorption spectroscopy has been completed and shows that a very weak complex is formed in cyclohexane (the solvent of choice) between N,N-dimethyl-p-toluidine, one of the most commonly used amine accelerators, and each of the three phthalate monomers. In each case, the absorption maximum (the wavelength at which maximum absorption occurs) of the complex is at approximately 350 nm (in the ultraviolet region of the spectrum) with some absorption extending into the visible region (400-800 nm). A comparison of solutions containing an equimolar concentration of each ester and one concentration of amine (in large excess) shows that the absorption of light is greatest in the case of the terephthalate monomer complex and least in the case of the phthalate monomer complex; i.e., in the order, para derivatives > meta derivatives > ortho derivatives.

Work is in progress in correlating the values of the absorption maxima of complexes formed between various benzene derivatives and N,N-dimethyl-p-toluidine with the nature of the substituents on the benzene ring. Correlations of this type can be useful in predicting discoloration caused by admixture of monomers containing benzene groups with N,N-dimethyl-p-toluidine or similar amine accelerators.

One means to circumvent the charge transfer complex problem is to employ somewhat similar isomeric crystalline monomers that possess diminished π-acid character. Three such monomers, the bis(2-methacryloxyethyl) ether of hydroquinone, resorcinol and catechol, respectively, were prepared and studied. Since these three each are crystalline solids that melt slightly above room temperature, they, like the phthalate isomers, are capable of forming a liquid ternary eutectic mixture. A manuscript, "Dimethacrylate Monomers of Aromatic Diethers", has been drafted and is being prepared for publication in the Journal of Dental Research.

(c) Dimensional stability during hardening - Shrinkage (or the

development of stress if strain is prevented) during hardening is one of the major obstacles that must be overcome if high values of adhesion are to be obtained. Although too preliminary to enumerate at present, a number of concepts are under study with the aim of eliminating or compensating for polymerization shrinkage, and a test method is being developed to evaluate these ideas.

(d) Resistance to wear - Although composite materials were developed for use in anterior teeth (where silicate cements would otherwise be used), it is nonetheless a fact that a number of dentists are using these materials (prompted by some commercial advertising) on occlusal surfaces. Phillips and others (J. Pros. Den. 28:164, 1972) have observed that about half of the composites suffered from occlusal wear by two years. A number of composite formulations are being readied in anticipation of measurements of wear by laboratory equipment now under development.

Additional study was made of certain metal powders as reinforcement materials for experimental composites. Aluminum, zirconium, tantalum and gold powders were evaluated and results described in a manuscript entitled "Metal-Filled Resin Composites" that is being prepared for publication in the Journal of Dental Research. Appropriate coupling agents applied to the metal powders prior to incorporation into the resin improved strength and other properties. Additional metal powders (titanium, niobium, iron, zinc, tin and certain alloys and combinations of metal and metal oxide) were treated with various coupling agents and various physical properties of their corresponding composites are being measured. The preliminary observations of such materials burnished on their surface with a steel instrument, and viewed with the aid of the scanning electron microscope, supports the contention that the malleability of certain metal reinforcing fillers may result in composites with greater resistance to wear and attrition than the present glass-filled composites. Materials of this type may find use in posterior teeth containing incipient carious lesions, when utilized in conjunction with resins that are capable of sealing developmental pits and fissures.

Not only the wear resistance, but also most other desirable

properties of composites and "sealant" resins depend on the attainment of the most thorough cure or greatest possible degree of polymerization of the formulation. In those with an amine-peroxide initiator system, the ratio of these ingredients is fundamental to the hardening reaction. In this context, one of the previously developed tertiary aromatic amine polymerization accelerators (that is also capable of copolymerizing with the resin monomers) was further studied during this period. It was used in a study that was primarily aimed at determining the optimum benzoyl peroxide to amine ratio for the self-curing of resins and composite materials. It was found that about 1.5 molecules of benzoyl peroxide are required for each molecule of amine accelerator for the optimum hardening of the resin. This work is described in a manuscript entitled "A Method for Determining the Optimum Peroxide to Amine Ratio for Self-Curing Resins" that has been accepted for publication in the Journal of Applied Polymer Science.

(e) Bonding to hard tooth tissues - Attempts were made to observe adsorption of NPG-GMA on synthetic hydroxyapatite (repeatedly washed with hot water) from aqueous 10% alcohol solution. The adsorption was studied spectrophotometrically at 251 mμ at pHs of 3.3, 5.8 and 7.6, within the concentration range of 1×10^{-3} to 1×10^{-6} m/l. No adsorption was observed under these conditions. Similarly, there was no adsorption of di(2-methacryloxyethyl)dimethyl ammonium bromide or of ammonium bromide using an EMF method of measurement. However, when the synthetic hydroxyapatite was exposed to aqueous solutions of Zn, Cu, Fe, Hg, Co, Ni, Mn, La or Th nitrate or Cr chloride, it appeared to acquire the color of the respective metal phosphates, which color did not wash off. This is the beginning of a study involving pretreatments of the tooth surface with "mordants" to improve adhesive bonding by way of appropriate coupling agents.

There is extensive laboratory data showing the effectiveness of the coupling agent, NPG-GMA, in improving adhesion between hard tooth tissues and resinous materials. Now results of a clinical study are available. Fifty-four pairs of Class III and V restorations were

placed in adult patients using an experimental composite filling material. One of each pair of the cavity preparations was treated with a 5.0% solution of [N-(2-hydroxy-3-methacryloxypropyl)-N-phenylglycine] (NPG-GMA) in acetone. The other of each pair was treated with acetone alone as a control.

The restorations were evaluated by three dentists at 0, 1, 2.5 and 3.5 years on the basis of general sensitivity, secondary caries, marginal notch and stain and whether one of each pair was better, the same, or worse in its overall condition than its mate.

There was a significant difference in the incidence of marginal notching in favor of the NPG-GMA pretreatment; however, there was not a significant trend of increased notching with time with either the pretreated or control restorations.

The increase in marginal staining with those restorations placed over the NPG-GMA pretreatment ranked less than the controls.

All evaluators indicated a significantly higher number of those restorations placed over the NPG-GMA solution were better as compared to those placed over the control liquid. In addition, each evaluator rated a higher percentage of the NPG-GMA associated restorations as being better at all four time intervals, with one exception, at which they were rated equal.

The results clinically demonstrate the effectiveness of an adhesion promoting tooth-restoration coupling agent through improved margins of composite restorations.

Pit and Fissure Sealant Materials

A novel class of methacrylate monomers has been discovered and was studied further during this period. Since these compounds will probably become the subject of patent application, full details may be obtained only in confidence; however, generically they comprise methacrylate or acrylate monomers or their polymers which are capable of releasing fluoride ion when exposed to moisture. A number of these monomers and their homopolymers and copolymers were prepared. The rate of fluoride ion release was measured simultaneously with weight gain (or loss) as a function of the copolymer immersed in water

over a prolonged period. Various combinations of monomers were used. It is hoped that the incorporation of one or more of these compounds into pit and fissure "sealant" resins will prove to be of benefit in reducing the incidence of carious attack on the surrounding hard tooth tissues.

Clinical Research

Forty-six pairs of Class II and V composite restorations were placed in adult patients. One, (A), of each pair was restored with a composite material consisting of a resin binder of a ternary eutectic dimethacrylate and a reinforcing filler of two parts fused silica and one part radiopaque BaF_2-containing glass. The other, (B), of each pair was restored as a control with a composite material based on an earlier NBS development of Bis-GMA (the adduct of Bis phenol A and glycidylmethacrylate) as resin binder.

The cavity preparations in restorations (A) were treated with N-(2-hydroxy-3-methacryloxypropyl)-N-phenylglycine, an adhesion promoting coupling agent. Those in (B) were treated with a liner known to have no adhesive promoting ability.

The restorations were examined by three dentists at 0, 1, 2.5 and 3.5 years on the basis of sensitivity, gross fracture, restoration loose or missing, secondary caries, need for replacement, color, surface texture, surface stain, marginal notch, marginal stain, and marginal flushness.

Evaluations for color, texture and flushness were made with the aid of newly developed evaluation guides.

The materials behaved similarly with respect to general sensitivity, sensitivity to percussion, gross fracture, loose or missing restorations, secondary caries, need for replacement, surface staining and marginal flushness.

Restorative A appeared slightly improved with respect to color change, surface texture, marginal notch and marginal stain.

Restorations made from both materials were still clinically sound in a high percentage of cases after 3.5 years. However, further

improvements in color stability are needed.

4.4.3 Dental Ceramics

Sponsor: ADA

The effort this period has been directed toward devising satisfactory strength tests for dental porcelains. Statistical evaluation of various methods for measuring compressive and tensile strengths and the fracture modulus are being made. Both dimetral compression and pull tensile tests have been performed.

Dimetral and pull tensile strength and fracture moduli have been determined on restorative dental porcelain to which anti-balling liquids have been applied. Also, Rockwell 15N Brale superficial hardness and Knoop micro-hardness measurements have been made. In all these tests for identical fires, porcelains to which the anti-balling additive has been applied are as strong as those to which it has not been applied.

Thermal expansion measurements of additive porcelains between ice water and hot coffee temperatures reveal that they match or better the match of non-additive porcelain. Solubility measurements are now being performed at boiling temperatures in an azeotropic HCl solution. Measurements of compressive green strength have shown that green strengths at least two to three times that of the non-additive porcelains are possible. No decay of this strength occurs with time as occurs with non-additive porcelains. Non-additive porcelains lose about half their green strength on standing 12 hours.

A new additive composition has been devised which gives even greater green strength and more reduced balling. It appears that this porcelain may almost double tensile strength.

Efforts to obtain a patent for the additive porcelain technique have continued. The technique is important because it can accomplish what the current aluminous porcelain seeks to do without the aluminous porcelain's loss in translucency, but also with reduction in processing

difficulty. The additive porcelain technique shows promise of being applicable to Veneer porcelains.

4.4.4 Dental Amalgam Studies

Sponsor: ADA, NIDR (Grant)

4.4.4.1 Studies of Dental Amalgam with Various Additions

The use of copper or gold additions to conventional dental amalgam alloys has been shown to be effective in suppressing the weak and corrosion-prone $\gamma 2$ phase. Unfortunately, the copper-containing alloy has a rather low tensile strength and the gold-containing alloy has the undesirable feature of a somewhat higher cost than conventional alloys.

We have made up several experimental alloys in which manganese is used to suppress the formation of the $\gamma 2$ phase. Manganese is an inexpensive element which is apparently non-toxic in biological systems. In fact, trace amounts have been reported to be essential to a normal metabolism. The alloys have so far exhibited negligible dimensional changes during the setting reaction and give high early strengths. Fully hardened samples have been tested using the ADA flow test and these results have revealed significantly less flow than is observed in a contemporary commercial alloy advertised to have unusually low flow properties. Further studies are in progress and these include studies of corrosion resistance as compared with the other alloys in which $\gamma 2$ phase formation has been suppressed.

4.4.4.2 Study of $\gamma 2$ Phase Distribution at Amalgam Surfaces

Our study of the tin distribution on free surfaces of dental amalgam is continuing. During the past six months, we have extended the work to several new amalgams and to various types of finishing procedures. The experimental data are still incomplete, however, and we must await the acquisition of these data before we may reach conclusions as to the relative effectiveness of the various finishing procedures and types of alloys in producing a desirable tin distribution. The most desirable tin distribution will probably be revealed by our planned supplementary clinical study, which will be designed to reveal differences in corrosion behavior and marginal breakdown among the various alloys.

4.4.4.3 Correlation of Dimensional Change on Hardening in Amalgam with Marginal Breakage and Recurrent Caries

Clinical restorations continue to be placed and observations on previously placed restorations are being made. Restorations have been under surveillance for up to 18 months.

4.4.5 Dental Cements

Sponsor: NIDR

Reinforced Polycarboxylate Cements

The aim of this study is to develop improved dental carboxylate cements by incorporating reinforcing agents or by partial substitution of poly(acrylic acid) by other polycarboxylic acid polymers such as itaconic or maleic acid containing copolymers. In this study, powder to liquid ratios were maintained that could be used in dental practice either as a base or as a cementing media. The hardening times of the mixed cements varied from 5 to 10 minutes at 37°C, 100 RH.

The results show that addition of certain reinforcing agents such as stainless steel, silver, aluminum or alumina powder to the commercial zinc oxide (90%)-magnesium oxide (10%) powder markedly increases the tensile strength of the cements obtained on mixing these powders with commercial, aqueous poly(acrylic acid) or acrylic acid-itaconic acid copolymer solutions. Even greater improvements in physical properties are obtained with 20 to 30% potassium titanate in the powder. Thus, the compressive and tensile strength of a product containing 27% potassium titanate-63% zinc oxide-magnesium oxide powder mixed to a base consistency (powder-liquid ratio 1.5) were 916 kg/cm^2 and 152 kg/cm^2, respectively. This compares to a compressive strength of 600 to 690 kg/cm^2 and tensile strength of 68 kg/cm^2 for commercial polycarboxylate cements, an increase of over 30% in compressive and over 120% in tensile strength. Further improvements in compressive strength were reached on addition of 8% graphite, but the resulting products showed a dark shade which is undesirable for some clinical applications. Incorporation of small percentages of silicon carbide whiskers or silane treated glass did not yield products with improved properties. An effort to use an aromatic nylon type fiber

having a very high tensile strength and modulas per unit weight as reinforcing agent proved unsuccessful. The fiber is only available as a yarn. Chopping the film into small strands proved not only laborious, but the resulting fibrils clumped together - which could not be overcome. This clumping made it impossible to obtain a homogeneous mix on blending with zinc oxide. While compressive strength was not affected by changing the rate of loading from 0.2"/min to 0.5"/min, a 15 to 20% decrease in tensile strength was observed at the higher loading rates.

On heating commercial polycarboxylate stored in water from 10 to 63°C at a rate of 3°C/min, the cement shrinks considerably. Further studies to explain this behavior are needed.

Two polycarboxylate copolymers were synthesized. Itaconic acid (35 mol percent) was copolymerized with glacial acrylic acid (65 mol percent) in an aqueous solution containing ammonium persulfate initiator. After removal of some of the water, a 40% aqueous solution of the copolymer was obtained which, on mixing with zinc oxide, hardened in 2 minutes. A 60% aq solution of the copolymer set even faster, whereas a 25% solution had a considerably slower setting time. The copolymer of acrylic acid and maleic anhydride in approximately 2:1 molar ratio was also prepared. A dilute aq solution containing 20% of copolymer set within 2 minutes. More concentrated solutions form turbid suspensions. Further properties of the cements obtained on mixing with zinc oxide-magnesium oxide and appropriate reinforcing agents will be studied.

Some further thought was given to the setting mechanism of zinc polyacrylate and the adhesion of this cement to hard tissues. It has been assumed that poly(acrylic acid)-zinc oxide cement adheres to enamel by chelate formation of pendant carboxylate groups with the calcium present at the enamel surface (D. C. Smith, Brit. Dent. J. 125:381 (1968). A literature survey showed that metal polyelectrolyte complexes such as the poly(acrylic acid)-copper complex form despite the large ring size of this chelate. This may result from the large electrostatic interaction of the polyelectrolyte coil which nullifies

the steric effect and allows the formation of a complex as stable as those composed of five and six-membered rings. However, the complex formation constants for various metals such as zinc with poly(acrylic acid) are much smaller than with copper and even smaller with those of the alkaline earths (Ca, Mg) (H. P. Gregor, L. B. Luttinger and E. M. Loebl, J. Phys. Chem. 59:990 (1955). There is considerable contraversy regarding the method used for calculating these values. Nevertheless, the complex stability constant for calcium was lower by an order of several magnitudes from that of copper. It was reported recently by Jurecic and Fairhurst (IADR Abstracts 1972, No. 379) and Beech (Arch. Oral Biol. 17:907 (1972)) that the infrared absorption peak on hardening of polycarboxylate cement and on reaction of poly-(acrylic acid) with enamel shifts from 1770 cm^{-1} to 1540 cm^{-1}, indicating the formation of ionized carboxyl groups on reaction with zinc. Similarly, calcium ions in enamel and the polycarboxylate cement interact electrostatically. Chelate formation, if it occurs at all, takes place only to a very limited extent.

These data suggest the setting mechanism of zinc polyacrylate cement is complex and involves neutralization of the polycarboxylic acid by the metal oxide and strengthening of the polymeric network by ionic interactions between carboxylate groups in the side chain of the polymer and zinc and magnesium ions and by the reinforcing action of excess metal oxide. The small values of the formation constants for zinc and calcium acrylate make it doubtful whether interaction of the metal takes place to any appreciable extent with carboxylic acid groups located in juxtaposition on the same polymer chain (chelation). However, attachment of metal ions can also occur on carboxyl groups located at some distance on the same polymer chain (intramolecular interaction) or on different polymer chains (intermolecular interaction or crosslinking). Present experimental techniques do not allow a ready elucidation of which mode of attachment prevails both in the setting reaction of the carboxylate cement and in its attachment to enamel.

4.4.6 Polymeric Stabilization of Orthopedic Implants

Sponsor: Cooperative project with George Washington Medical Center

The aim of this project is to provide the clinician with basic information as to the nature, optimal working conditions and techniques of resins used as hip prosthesis material and as implants for other orthopedic applications.

Chemical Properties

Procedural methods were developed for chemical characterization of the in situ-polymerizing methacrylate cement used to stabilize hip prostheses. These included infrared, ultraviolet and nuclear magnetic resonance techniques, refractive index and gas-liquid chromatography. Methanol and ether extractable materials are also determined on the powder component.

Methods to determine total benzoyl peroxide from the extracted residue were not successful. Apparently, some decomposition of peroxide takes place during extraction or removal of the solvent, and low values are obtained in the spectrophotometric determination for benzoyl peroxide in the original polymer powder. A method based on the addition of benzoyl peroxide to solutions containing various concentrations of resin powder in chloroform was developed which allowed the estimation of the peroxide. An effort will be made to determine more accurately the small amount of styrene copolymer. Furthermore, the molecular weight of polymer powder and cured resin and the water sorption and solubility of the cured product will be studied.

Physical and Mechanical Properties

Tensile strengths of 4700 psi (32.4 MN/m^2) and 4200 psi (29.0 MN/m^2) were determined respectively on transparent and radiopaque specimens prepared from mixes using manufacturer-recommended powder/liquid ratios. The incorporation of $BaSO_4$ did not affect the

compressive strength (13,500 psi; 93.1 MN/m^2) or Young's Modulus (330,000 psi; 2275.4 MN/m^2). Mixes of the cement showed shrinkage on polymerization with the amount of bulk shrinkage ranging from about 1 to 5% depending upon the degree of porosity in the specimen.

Preliminary results indicated that the dough time (time from initial contact of powder and liquid until cement is ready for insertion), setting time, handling time (period between dough and setting time), and peak temperature of polymerization can be controlled to some extent by the technique of preparation of the mix of cement. Increased temperature of the mixing container reduces dough, handling and setting times. High powder-liquid ratios apparently reduce dough time, setting time and peak temperature. Continued kneading of the mix reduces setting time. The effects of variations in relative humidity appear to be small, as do difference between cements with and without $BaSO_4$.

4.4.7 Specifications and Standards

Chairmen of both the FDI-ISO and ADA-ANSI Alloy for Dental Amalgam Committee prepared two revised recommendations with accompanying ballots for the FDI-ISO task group consideration. For the ADA-ANSI, a series of round-robin tests were completed and a revised specification circulated for consideration and ballot.

Chairman of the ANSC-Z156 Committee on Denture Base Resins completed a 6th and 7th draft of the 4th revision of specification No. 12. This revised specification includes pour type resins. Processing techniques were modified and employ tinfoil substitutes to approximate more closely dental laboratory conditions. The 7th revision has been approved by the subcommittee and is being reviewed by ANSC-Z156 before final approval. Drafts for review of the FDI specification for Denture Base Resin have been reviewed.

4.4.8 Miscellaneous

A correspondence course on dental materials was reviewed and suggested revision made to the Navy Graduate Dental School.

Assistance was provided graduate dental students of the Navy Graduate Dental School on four projects: (1) Effect of heat during trituration on certain physical properties of dental amalgam, (2) Evaluation of bonding or amalgamation of amalgam to various alloy formulations used in pin manufacture, (3) Strain evaluation of various clasp designs used in removable partial dentures, and (4) Design of cast surfaces for optimum retention of Pyroplast.

NATIONAL BUREAU OF STANDARDS REPORT

NBS PROJECT 311.05-3110561

September 20, 1972

NBS REPORT 10 916

Progress Report

on

THE CRYSTAL STRUCTURE OF V_3Rh_5

R. M. Waterstrat* and Brian Dickens**

*Research Associate, American Dental Association Research Unit at the National Bureau of Standards, Washington, D. C. 20234

**Research Chemist, Dental Research Section, National Bureau of Standards, Washington, D. C. 20234.

This investigation was supported in part by research grant DE02455 to the American Dental Association from the National Institute of Dental Research and is part of the dental research program conducted by the National Bureau of Standards in cooperation with the American Dental Association; the United States Army Medical Research and Development Command; the Dental Sciences Division of the School of Aerospace Medicine, USAF; the National Institute of Dental Research; and the Veterans Administration.

U.S. DEPARTMENT OF COMMERCE

NATIONAL BUREAU OF STANDARDS

Abstract

The crystal structure of the phase V_3Rh_5 has been elucidated. The unit cell is orthorhombic with $a = 5.420$ Å, $b = 9.276$ Å, $c = 4.320$ Å and $Z = 2$; the space group is either Cm2m or Cmcm. The structure is close-packed and contains both ordered and disordered atomic sites. It is intermediate between the structures of the Cu_3Au and CuAu types except that it possesses a two-layer stacking sequence.

The Crystal Structure of V_3Rh_5

Richard M. Waterstrat and Brian Dickens

Greenfield and Beck[1] have reported the existence of a close-packed hexagonal structure in an alloy having the nominal composition $V_{40}Rh_{60}$ after annealing at 1200°C. However, the authors state that due to the small size of their samples they could not claim a very high degree of accuracy for their stated alloy compositions.

In a recent investigation[2] of the entire vanadium-rhodium alloy system, no close-packed hexagonal structure was found. Instead it was observed that a phase having the cubic Cu_3Au type structure exists over the approximate compositional range of 24 to 33 atomic % V and a tetragonal CuAu type structure exists over the range of approximately 41 to 47 atomic % V. These two ordered phase regions are separated from each other by a narrow single phase region which occurs at the approximate composition $V_{37.5}Rh_{62.5}$ (i.e., V_3Rh_5), close to the composition $V_{40}Rh_{60}$ studied by Greenfield and Beck[1].

Large crystals were obtained by fracturing an alloy of nominal composition $V_{37.5}Rh_{62.5}$ which had been annealed at 1300°C for 5 days. A small amount of fine powder of this alloy was also obtained by grinding the ingot with a dental diamond grinding wheel and then removing the admixed diamond crystals by sieving through a 400

mesh screen. The crystals and the fine powder were both reannealed in high vacuum for several minutes at 1300°C in order to relieve any internal strains resulting from cold working.

An x-ray diffraction powder pattern of the alloy V_3Rh_5 showed a strong resemblance to the patterns usually obtained from close-packed hexagonal structures but careful examination revealed that many of the principal "h.c.p. lines" were, in fact, double lines.

Precession photographs obtained from several crystals using MoKα radiation indicated a hexagonal unit cell with $a \cong 5.35$ Å and $c \cong 4.30$ Å but all lines in the powder pattern could not be indexed on the basis of a hexagonal unit cell having these dimensions. However, by introducing a slight distortion to this hexagonal cell we were successful in indexing all lines in the powder pattern on the basis of a C-centered orthorhombic unit cell with $a = 5.420$ Å, $b = 9.276$ Å and $c = 4.320$ Å with 2 formula units per cell. The wavelengths used were $\lambda(CuK_\alpha) = 1.5417$ Å and $\lambda(CuK_{\alpha_1}) = 1.5405$. The observed hexagonal symmetry of the reciprocal lattice must, therefore, have been the result of twinning. Metallographic examination of the crystals revealed a highly striated appearance which seemed to confirm the presence of extensive microtwinning.

By analogy with the adjacent Cu_3Au type and CuAu type

structures in the V-Rh alloy system, it was suspected that the structure of V_3Rh_5 would be an ordered close-packed structure. The observed c-spacing for V_3Rh_5 implies a two layer stacking sequence. The absence of the 001 reflection makes these two layers identical in scattering power. A reasonable assumption is that this equivalence also extends to their compositions, so that each layer contains one formula unit, V_3Rh_5. We were unable to identify this structure with any previously reported structure having a two-layer stacking sequence. The homologous alloy system niobium-rhodium has been reported[3] to contain a narrow single phase region at the composition Nb_3Rh_5 but the crystal structure of this phase possesses a nine-layer stacking sequence[4]. A fully ordered arrangement in the basal planes of Nb_3Rh_5 would satisfy the composition requirements of V_3Rh_5, but would not satisfy the C-centered condition imposed by the x-ray powder data. C-centering would require disordering of some sites to make them crystallographically equivalent. It was therefore critical to determine whether or not the structure was C-centered. The powder intensities are only qualitative, at best, due to x-ray absorption by the sample and because of the non-linear film response. On the other hand, the twinned crystal x-ray photographic data are unreliable due to the very strong x-ray absorption in these large crystals.

Smaller crystals were cut from the larger ones but these crystals gave very poor x-ray patterns due to the presence of streaking produced by cold work associated with the cutting procedure. It was therefore decided to examine the possibility of C-centering by collecting neutron diffraction data since neutron absorption would not be serious. Further, as a consequence of the favorable neutron scattering factors for rhodium and vanadium, the atomic ordering in the sample could be investigated. However, the preparation of the relatively large amount of fine powder required for a neutron diffraction powder pattern was considered too time-consuming and expensive (in terms of diamond wheels). Polycrystalline samples are composed of grains which are too coarse to provide the desired resolution. Therefore, it was decided to elucidate the C-centering by collecting neutron data from the large twinned crystals, even though analysis of the atomic ordering would be effectively prevented by the extensive micro-twinning. The neutron diffraction data, which included two sets of equivalent reflections, indicated a hexagonal unit cell with no systematic extinctions, similar to the one suggested by the precession photographs. There were no observed reflections with $h+k = 2n+1$ for the orthorhombic cell. Thus, the powder pattern may be

referred to a C-centered orthorhombic cell which is being revealed only by the higher resolution in the powder data. The hexagonal "single" crystal data was apparently produced by a superposition of several C-centered orthorhombic reciprocal lattices oriented by means of 60° rotations in the a*b* plane. The annealing treatment of both powder and crystals made it probable that both were of the same phase, and that no effects from cold working during grinding of the powder remained. Further, if the stoichiometry V_3Rh_5 is to be fitted in one layer in a hexagonal unit cell all atoms except one per layer must be disordered, which is considered unlikely to occur.

Only one layer arrangement is consistent with a C-centered cell of the size dictated by the powder data and this is shown in Fig. 1. As regards the stacking sequence, one may locate the vanadium atoms as shown in Fig. 1, in which case the space group would be Cm2m, or one may interchange vanadium and disordered sites in the second layer, in which case the space group is Cmcm. One may also move the second layer so that rhodium atoms occupy the sites shown as vanadium in Fig. 1, but this last model can be ruled out on the basis of a comparison of observed and calculated intensities. We prefer the first possibility, Cm2m, (shown in Fig. 1), since this model would produce a larger number of unlike near

neighbors. The x-ray powder data are not sufficiently accurate to permit a selection between the Cm2m and Cmcm models and because there are no h0ℓ reflections with $\ell = 2n+1$, Cmcm can not be ruled out. The relative intensities for both of these two models are given in Table 1 and the atomic parameters in Table 2. Thus, the twinning mechanism, which is such that [100] sometimes becomes [110]/2, corresponds to an interchange of ordered and disordered sites. The disordering in site occupancy which is necessary to account for the stoichiometry was included in the structure factor calculations by assuming that each disordered site was populated by one half of a vanadium atom and one half of a rhodium atom. The accuracy of the x-ray powder data is insufficient to justify a more sophisticated treatment designed to distinguish between short and long range order.

The crystal structure of V_3Rh_5 may, therefore, be described as a new structural type which contains both ordered and disordered sites in a two-layer stacking sequence in a pseudo-hexagonal unit cell. The structure can be visualized as being intermediate between the Cu_3Au and the CuAu types as regards the atomic ordering, but the Cu_3Au and CuAu structures possess a three-layer (cubic) stacking sequence

whereas the V_3Rh_5 structure has a two-layer (hexagonal) stacking sequence. The existence of V_3Rh_5 over a narrow region of the phase diagram separating the Cu_3Au and CuAu type phases is somewhat surprising. One possible explanation for this abrupt occurrence of hexagonal stacking is that for this type of ordered layer one obtains a slightly larger number of unlike near neighbors in hexagonal stacking rather than cubic. Otherwise there appears to be no reason why a phase of A_3B_5 stoichiometry and identical layer type should not also occur with a cubic stacking sequence.

Ritter, Giessen and Grant[4] have previously recognized the possible existence of both a fully ordered and a partially disordered atomic layering at the A_3B_5 stoichiometry. These are shown in Fig. 2 (II and III) of their paper. These authors[4] were unable to determine which of the two types of ordered layers was the correct one for Nb_3Rh_5 owing to the similarity of the atomic scattering factors for niobium and rhodium atoms. This restriction does not apply in the case of V_3Rh_5. Therefore, by analogy we have selected the layer marked II as being the most probable description for Nb_3Rh_5. The reason for the nine-layer stacking sequence in Nb_3Rh_5 may be connected in some way with the greater difference in atomic size between Nb and Rh atoms (~9%) as compared with V and Rh (<1%).

Acknowledgment

We thank E. Prince of the Reactor Division, National Bureau of Standards, for collecting the neutron data and for helpful discussion.

This investigation was supported in part by research grant DE02455 to the American Dental Association from the National Institute of Dental Research and is part of the dental research program conducted by the National Bureau of Standards in cooperation with the American Dental Association; the United States Army Medical Research and Development Command; the Dental Sciences Division of the School of Aerospace Medicine, USAF; the National Institute of Dental Research; and the Veterans Administration.

References

1. P. Greenfield and P. A. Beck, Trans. AIME, 206 (1956) 265.
2. R. M. Waterstrat, unpublished data (1972).
3. D. L. Ritter, B. C. Giessen and N. J. Grant, Trans. AIME, 230 (1964) 1250.
4. D. L. Ritter, B. C. Giessen and N. J. Grant, Trans. AIME, 230 (1964) 1259.

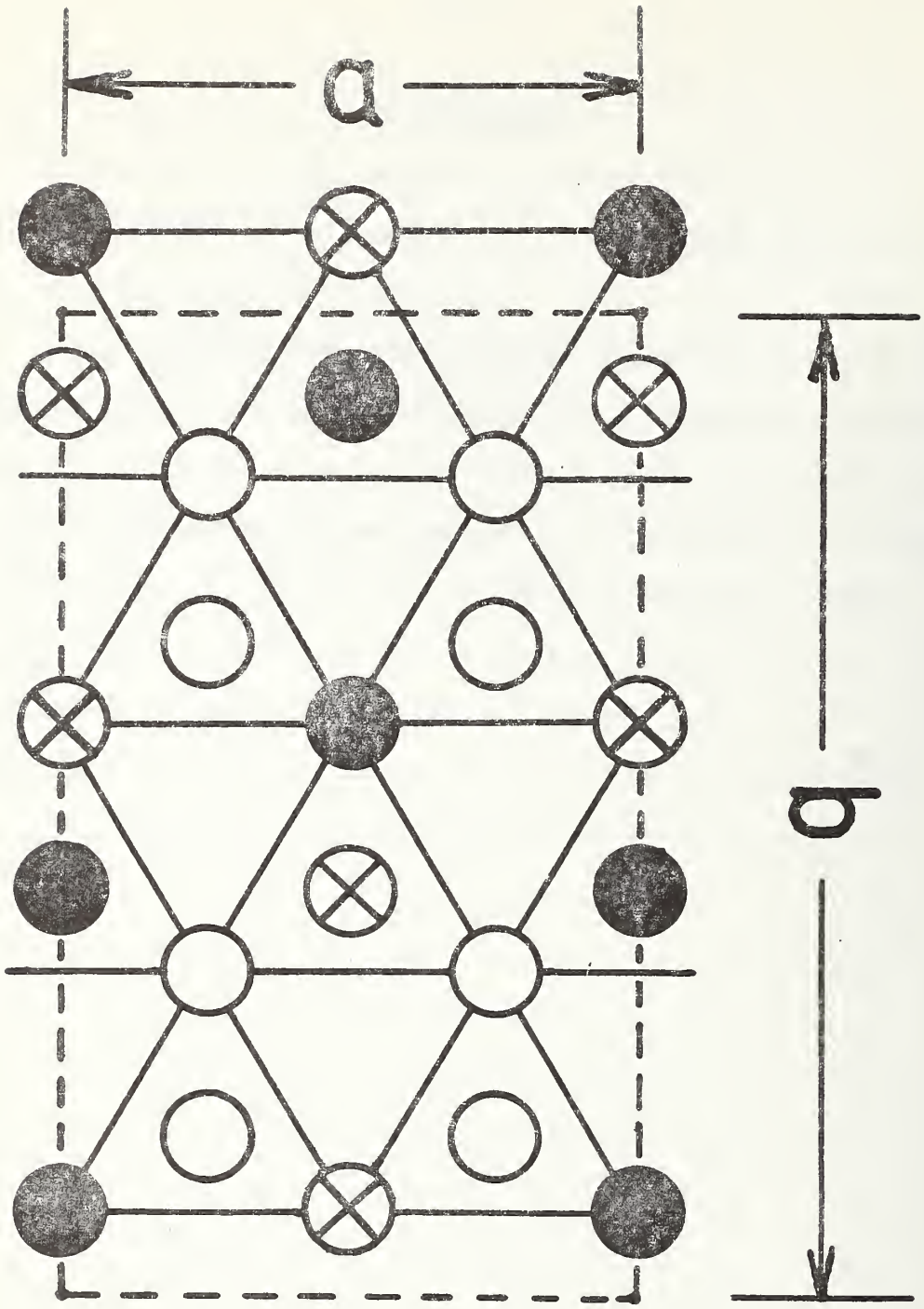

Figure 1.

Proposed crystal structure of V_3Rh_5. The space group is Cm2m. Filled circles represent vanadium atom sites; open circles represent rhodium atom sites; crossed circles represent atomic sites which are populated equally by vanadium and rhodium atoms. The interconnected atom sites are at z = 0. Unconnected sites are at z = 1/2. The unit cell outline is shown by dashed lines.

Table 1. X-ray diffraction data for V_3Rh_5

(orthorhombic cell with a = 5.420 Å, b = 9.276 Å, c = 4.320 Å assuming $\lambda(CuK_\alpha)$ = 1.5417 Å and $\lambda(CuK_{\alpha_1})$ = 1.5405 Å)

	interplanar spacings (Å)		relative intensities		
				calc.	
hkℓ*	obs.	calc.	obs.+	Cm2m	Cmcm
110	-	4.680	-	1	3
020	-	4.638	-	5	5
001	-	4.320	-	0	0
111	-	3.174	-	2	1
021	3.153	3.161	MW	10	10
200	2.713	2.710	W	5	5
130	-	2.686	-	1	0
220	2.345	2.340	M	25	25
040	2.319	2.319	MW	12	12
201	-	2.296	-	0	0
131	-	2.281	-	0	1
211**	2.187**	2.228	W	0	0
002	2.162	2.160	M	39	39
221	2.058	2.057	S	100	100
041	2.045	2.043	M	49	49
112 }	1.924	1.961	VW	<1	<1
022 }		1.958		1	1
*					
240	1.762	1.762	VVW	1	<1
202	1.691	1.689	VW	2	2
241	1.634	1.631	VW	3	3
222	1.590	1.587	M+	13	13
042	1.583	1.581	MW	6	6
400	1.357	1.355	MW	7	7
260	1.344	1.343	M+	14	14
223	1.228	1.226	MS+	14	14
043	1.225	1.223	MW+	7	7
440	1.171	1.170	W	2	2

Table 1 (Cont.)

402	1.149	1.148	MW+	8	8
262	1.141	1.140	M	15	15
441	1.131	1.129	MW+	11	11
081	1.120	1.120	MW	5	5
004	1.080	1.080	MW	3	3
442	1.030	1.029	MW	3	3
224	.9803	.9806	MW	2	2
044		.9790		1	1
443	.9088	.9080	M	7	7
083	.9029	.9031	MW	3	3
2·10·0	.8779	.8776	W	1	1
621	.8704	.8686	M+	7	7
481	~.8639 (broad line)	.8632	M+	7	7
513		.8623		<1	<1
2·10·1		.8600		7	7
404	.8453	.8446	M	5	5
264	.8416	.8416	MS	10	10
622	.8220	.8203	VW	3	3
1·11·1		.8182		<1	<1
482		.8157		3	3
2·10·2	.8131	.8131	VW	3	3
225	.8108	.8105	M	9	9
045		.8096		5	5
444	.7944	.7936	MW	1	1
084		.7903		2	2
660	.7816	.7800	MS	37	37

* All lines compatible with C-centering are listed from 010 to 022. Only the observed lines are listed beyond 022. Unlisted lines all had calculated relative intensities less than 1.

+ The observed relative intensities are strongly affected by an unknown absorption factor which decreases with decreasing interplanar spacing. A direct comparison between

Table 1 (Cont.)

observed and calculated intensities is, therefore, valid only for groups of lines having similar "d" values.

** This observed line is probably due to a small percentage of a second phase in our sample. Its interplanar spacing does not agree well with the calculated value, and its relative intensity seems to vary with the annealing treatment while the relative intensities of all other lines in the patterns remain nearly constant. The 211 reflection has zero intensity in a C-centered space group.

Table 2. Structural parameters for V_3Rh_5

(i) in space group Cm2m (C_{2v}^{14})

	x	y	z	special position	symmetry
V	0	-1/12	0	2a	mm
Rh	1/4	1/6	0	4d	m
$\frac{1}{2}$V+$\frac{1}{2}$Rh	1/2	-1/12	0	2a	mm
V	1/2	1/12	1/2	2b	mm
Rh	1/4	1/3	1/2	4e	m
$\frac{1}{2}$V+$\frac{1}{2}$Rh	0	1/12	1/2	2b	mm

special positions: -

2a: (0,0,0; 1/2,1/2,0) + 0,y,0.

2b: (0,0,0; 1/2,1/2,0) + 0,y,1/2.

4d: (0,0,0; 1/2,1/2,0) + x,y,0; -x,y,0.

4e: (0,0,0; 1/2,1/2,0) + x,y,1/2; -x,y,1/2.

(ii) in space group Cmcm (D_{2h}^{17})

	x	y	z	special position	symmetry
V	0	-1/12	1/4	8f	m
Rh	1/4	1/6	1/4	8g	m
$\frac{1}{2}$V+$\frac{1}{2}$Rh	1/2	-1/12	1/4	8g	m

special positions: -

8f: (0,0,0; 1/2,1/2,0) + 0,y,z; 0,-y,-z; 0,y,1/2-z; 0,-y,1/2+z.

8g: (0,0,0; 1/2,1/2,0) + x,y,1/4; -x,y,1/4; x,-y,3/4; -x,-y,3/4.

All temperature factors assumed to be 1 $Å^2$ and isotropic.

NATIONAL BUREAU OF STANDARDS REPORT

NBS PROJECT
311.05-3110561

December 29, 1972

NBS REPORT
10 978

Progress Report

on

$Ca(H_2PO_4)_2$, A CRYSTAL STRUCTURE CONTAINING UNUSUAL HYDROGEN BONDING

B. Dickens, E. Prince, L. W. Schroeder*, and W. E. Brown**

* Research Associate of the American Dental Association Research Unit at the National Bureau of Standards, Washington, D. C. 20234.

** Director, American Dental Association Research Unit at the National Bureau of Standards, Washington, D. C. 20234.

U.S. DEPARTMENT OF COMMERCE

NATIONAL BUREAU OF STANDARDS

Abstract

$Ca(H_2PO_4)_2$ crystallizes in the triclinic unit cell $\underline{a}$ = 7.5577(5) Å, $\underline{b}$ = 8.2531(6) Å, $\underline{c}$ = 5.5504(3) Å, α = 109.87(1)°, β = 93.68(1)° and γ = 109.15(1)° at 25°C with $\underline{Z}$ = 2. The structure was determined by an automated Σ_2 method from x-ray data and refined by least-squares to $R_w(F)$ = 0.048, R(F) = 0.020 using 3678 observed x-ray data and to $R_w(F)$ = 0.055, R(F) = 0.048 using 843 observed neutron data. Corrections were made for absorption, isotropic secondary extinction and anomalous dispersion in the x-ray case and for anisotropic secondary extinction in the neutron case. Least-square refinements proceeded to the limits of the data sets in space group $P\bar{1}$.

Rudimentary chains Ca...(P(1)O_4)-H(1)...(P(2)O_4)...run parallel to [1$\bar{1}$0]. Adjacent chains are joined by Ca...O bonds on one side and by O(8)-H(5)-O(8′) hydrogen bonds on the other. Alternatively, the structure may be considered to contain hydrogen bonded layers of PO_4 groups; these layers are held together by hydrogen bonds on one side and by Ca...O bonds on the other.

There are two very strong hydrogen bonds in the structure; O(7)--H(4)--O(7′),O(7)...O(7′) = 2.434(2) Å and O(8)--H(5)--O(8′), O(8)...O(8′) = 2.423(2) Å. These hydrogen bonds join the P(2)O_4 groups together to form an infinite chain. The very strong hydrogen bonds are across nominal centers of symmetry,

and diffraction results indicate that each of the H(4) and H(5) protons is effectively centered in a broad symmetric potential well, possibly with a central barrier. A combination of diffraction and IR spectral considerations suggests that the central barriers in the wells, if they exist, probably lie below the zero point energy of the hydrogens.

Introduction

Our earlier studies of calcium phosphates have included refinements of the crystal structures of the hydrogen-containing salts $Ca(H_2PO_4)_2 \cdot H_2O$ (Dickens and Bowen, 1971 and $CaHPO_4$ (Dickens, Bowen and Brown, 1971a). Here we have extended our studies of hydrogen bonding in calcium phosphates and related compounds by determining and refining the crystal structure of $Ca(H_2PO_4)_2$ using both x-ray and neutron data. $Ca(H_2PO_4)_2$ alters to randomly oriented crystallites of $Ca(H_2PO_4)_2 \cdot H_2O$ in moist air (Smith, Lehr and Brown, 1955); perhaps because of this it has been studied comparatively little. It is an important constituent of freshly made superphosphate fertilizer.

Experimental details

Clear colorless platy crystals of $Ca(H_2PO_4)_2$ were prepared according to the method of Smith, Lehr and Brown (1955). An ellipsoidal crystal with axes of 0.15, 0.15 and 0.18 mm was the result of an attempt to grind a sphere. This crystal was mounted in a borate glass capillary with clear

household cement and was used in the x-ray study. Crystal data are as follows: ideal formula: $Ca(H_2PO_4)_2$; cell at 25°C: triclinic with $\underline{a}$ = 7.5577(5) Å, $\underline{b}$ = 8.2531(6) Å, $\underline{c}$ = 5.5504(3) Å, α = 109.87(1)°, β = 93.68(1)°, γ = 109.15(1)°, cell volume = 302.01 Å^3; space-group $P\bar{1}$; cell contents $2[Ca(H_2PO_4)_2]$; calculated density 2.57 g·cm^{-3}; observed density 2.546 g·cm^{-3} (Bassett, 1908). Standard deviations are given in parentheses after the cell parameters, which were calculated by least-squares methods from 30 2θ values observed at 25°C on an x-ray diffractometer equipped with a highly oriented graphite monochromator. Care was taken to use only the Kα_1 peak in determining these 2θ values. The wave-length λ(Mo, Kα_1) = 0.70926 was assumed.

The x-ray data were measured and processed as described by Dickens and Bowen (1971) with the exception that the diffractometer setting program used was written by Lenhert (1970). 12,043 reflections (maximum $\sin\theta/\lambda$ = 0.907 Å^{-1}) comprising two complete sets from one hemisphere and one set from the other hemisphere were measured and merged into a unique set of 3756. Of these, 3690 were 'observed' and 66 were 'unobserved' (unobserved reflections are those less than 2σ(I) above background). The average disagreement between equivalent or remeasured reflections was 0.8%. Absorption corrections were applied for a sphere with a radius the average of the axes of the elliptical crystal. The maximum

effect on F due to the asphericity of the crystal, is estimated at 4%. Absorption due to the capillary was neglected.

The x-ray structure was solved by Σ_2 methods using the sequence DATRON-DATFIX-SIGMA2-PHASE-FOURR in the XRAY 67 system of computer programs (Stewart, 1967). Seven E maps were calculated. Calculations of distances between the three highest peaks (presumed to be one Ca ion and two P atoms) in these trial structures ruled out all but one. The oxygen atoms were found from a subsequent electron density synthesis with phases based on the Ca and P atoms. The structure with hydrogens excluded was refined isotropically using the program RFINE (Finger, 1968) to R_w = 0.077 and R = 0.064. ($R_w=[\Sigma w(|Fo|-|Fc|)^2/\Sigma w(|Fo|^2)]^{\frac{1}{2}}$ and $R = \Sigma||Fo|-|Fc||/\Sigma|Fo|$.) The maximum shift/error was -6.4. The structure was then refined anisotropically to R_w = 0.065, R = 0.037 (maximum shift/error = 0.90). The scattering factors used were for Ca^{2+} and neutral P, O and H; they were taken from Cromer and Mann (1968) and Cromer and Liberman (1970). Only 'observed' reflections were used in the refinements.

The neutron data were taken on a computer controlled 4-circle diffractometer at the National Bureau of Standards Research Reactor (Alperin and Prince, 1970) according to the procedure described by Prince (1972). The crystal was sealed

with $CaCl_2$ in a silica glass enclosure to protect it from moisture. With a wave-length of 1.232 Å and a limiting 2θ angle of 100°, 1212 independent reflections were accessible; of these 843 had integrated intensities greater than $2\sigma(I)$. The crystal was a plate with dimensions approximately 0.5 x 1.0 x 3.0 mm. The hydrogen positions were obtained from a Fourier synthesis based on the neutron data and signs determined from the x-ray parameters. The structure was then refined further.

In the x-ray refinement of the complete structure, consideration of isotropic secondary extinction was deemed adequate and the refinement on all parameters but the thermal parameters of hydrogen, which were fixed at 1 $Å^2$, gave $R_w = 0.033$ and $R = 0.023$. The isotropic secondary extinction factor, $\underline{r}$, in the notation of Zachariasen (1967) was $0.33(7) \times 10^{-4}$ cm. The standard deviation of an observation of unit weight (SDOUW), 7.81, indicated that improper weights were being applied in the least-squares analysis, so that new weights, $(\sigma_c^2 + .00058\ F_o^2)^{-\frac{1}{2}}$, were applied. Here σ_c is the standard deviation of F_o as estimated from counting statistics. The few reflections with extinction factors less than 0.95 were rejected from the final refinement. The final values are $R_w = 0.048$, $R = 0.020$, SDOUW = 1.84, $r = 0.74(5) \times 10^{-4}$ cm. The largest peaks in a difference synthesis calculated after the last cycle of refinement were 0.63, 0.58 and 0.53 electrons $Å^{-3}$. The lowest value was -0.51 $e \cdot Å^{-3}$. The first

three are all halfway between P and O in PO_4 groups. The fourth is 0.1 Å from Ca.

In the neutron case, anisotropic secondary extinction corrections were deemed necessary. The value of SDOUW, 6.87, showed that once again counting statistics were inadequate. New weights, given by $(\sigma_c^2 + 0.00025\ F_o^2)^{-\frac{1}{2}}$ were applied. The structure was then refined to $R_w = 0.055$, $R = 0.048$, and SDOUW = 2.50. The scattering lengths used were Ca:0.49; P:0.51; O:0.577; H:0.372. (Neutron Diffraction Commission, 1969.)

The components ($x10^{10}$) of the extinction tensors (Coppens and Hamilton, 1970) in the neutron case are 0.29(5), 0.27(4), 0.42(6), -0.11(3), 0.24(4), 0.62(3), and indicate considerable anisotropy. This extinction tensor results from a type II treatment in which extinction is dominated by domain size. Refinements using the type I treatment, where mosaic spread dominates, led to non-positive definite tensors and diverged even when starting from converged isotropic extinction refinements. This can be understood by considering the isotropic extinction parameter for the x-ray case, which as given is equivalent to the mean radius of the domains in the crystal. However, the refined parameter can also represent a mosaic spread parameter. Such a calculation leads to a mosaic spread of ~30 sec, roughly a factor of ten larger than that usually obtained in cases where type I occurs (Coppens and Hamilton, 1970). Thus, our refinements suggest that extinction in $Ca(H_2PO_4)_2$ is dominated by the effect of the domain size.

The largest positive peaks in a difference synthesis with the neutron data were 27, 25 and 25 and the largest negative peaks were -27 and -27 on a scale on which the amplitude of a hydrogen peak is -600. The first four peaks are obviously artifacts, since they do not occupy chemically reasonable positions. The fifth is 1.03 Å from O(1) and 2.04 Å from O(7), and thus could be evidence for very slight disordering of the hydrogen atoms, but is comparable with the background in the map.

The appropriateness of the final weighting schemes was checked by comparison of F_o, F_c and $\sigma(F_o)$ with a normal distribution as suggested by Abrahams and Keve (1971) using an unpublished program written by us. The comparison for the neutron data showed that there was little skewness in the fit of F_o and F_c, implying that the correction of the data for secondary extinction left essentially random errors that could be taken up by the model. The value of the standard deviation of an observation of unit weight obtained from the least-square refinement was confirmed in this comparison. A similar comparison of the x-ray data showed the F_o-F_c distribution to be somewhat skewed with F_c being a little smaller than F_o suggesting that the extinction correction may have been somewhat over-estimated. Similar comparisons of the structural parameters from the x-ray and neutron refinement gave a least-squares line of $\underline{Dm} = 0.18 + 1.12\underline{x}$ for the positional parameters and $\underline{Dm} = 0.12 + 1.14\underline{x}$ for the thermal parameters, where

$\underline{Dm} = \| p(1)_i | - | p(2)_i \| / (\sigma^2 p(1)_i + \sigma^2 p(2)_i)^{\frac{1}{2}}$, and the p's are parameters.

The experimental points fell satisfactorily close to the line. Dm is the quantity described by Abrahams and Keve (1971) and x is the appropriate quantile from a normal distribution. The ratio of the neutron to x-ray standard deviations is so large that the above plot is essentially a test of the standard deviations assigned to the neutron parameters.

In the neutron case, the largest correlation coefficient was 0.83 between components of the extinction tensor. Coefficients between the extinction parameters and the scale factor were in the range 0.56 to 0.69. Other coefficients in the range 0.56 to 0.69 involved the B's of H_5, but as Fig. 1 shows, the tensor is oriented with respect to the crystal coordinate system in such a way that fairly large correlations are expected. In the x-ray refinement the three largest coefficients were 0.64 to 0.65 between the scale factor and B_{11} of Ca(1). The three next largest (~0.62) were between B_{11} of Ca(1) and the corresponding B_{11} of P(1) and P(2). The correlation coefficient between the extinction parameter and the scale factor was 0.57. Both x-ray and neutron refinements proceeded satisfactorily to the limits of the data sets assuming space group $P\bar{1}$. There is therefore no indication from the diffraction data that the crystals are not centrosymmetric. Furthermore, similar crystals did not show any piezoelectric resonances when tested by the transmission method (Blume, 1962).

The structural parameters for $Ca(H_2PO_4)_2$ are given in Table 1. The observed and calculated structure factors are given in Table 2 for the x-ray data and in Table 3 for the neutron data.

Description of the structure

There are two formula units of $Ca(H_2PO_4)_2$ in a nominally centrosymmetric unit cell. There are five crystallographically different hydrogen bonds, two of which cross nominal centers of symmetry. If these hydrogen bonds are centered, all atomic sites would be fully occupied and there would be no positional disorder as there is for the hydrogen atoms in $CaHPO_4$ (Jones and Cruickshank, 1961; Curry, Denne and Jones, 1968; Dickens, Bowen and Brown, 1971a). The question of whether the hydrogen bonds in $Ca(H_2PO_4)_2$ are actually centered or not is discussed later.

There are several ways of describing the $Ca(H_2PO_4)_2$ structure. Many calcium phosphates can be described in terms of Ca...PO_4 chains which are linked into sheets, usually puckered or corrugated but occasionally planar, and which are bonded to each other either directly or by some chemically different intermediate layer. In $Ca(H_2PO_4)_2$ (Fig. 1), rudimentary chains with the repeat unit Ca...(P(1)O_4) — H(1)... (P(2)O_4)...exist parallel to $[1\bar{1}0]$. A series of corrugated sheets may then be imagined parallel to (100). Adjacent chains are joined by Ca...O bonds on one side and by O(8)--H(5)--O(8′) bonds on the other. There is hydrogen bonding along the surfaces of the sheets involving H(3) between neighboring chains. The corrugated sheets are bonded together by hydrogen bonds involving H(2) and H(4).

An alternative description is that the PO_4 groups are

held in layers parallel to (010) by hydrogen bonds. These layers are bonded to each other by hydrogen bonds on one side and by Ca ions on the other.

Two striking features of the structure (Fig. 1) are (i) $H_2P(2)O_4$ ions linked into infinite chains by centered hydrogen bonds involving H(4) and H(5) and (ii) pairs of $H_2P(1)O_4$ ions linked into dimers across centers of symmetry by the O(4)—H(2)...O(2) hydrogen bond. The latter feature may be seen at the lower left front corner of figure 1.

The Ca ion environment

The Ca ion is coordinated (Table 4) to eight oxygen atoms including the [O(1′), O(4)] edge of the $P(1)O_4$ group. This edge and the PO_4 apexes O(1), O(5), and O(6) are arranged in an approximate pentagon about Ca. Oxygen atom O(7) and the midpoint of the O(5′)...O(2) vector occupy apical positions of an approximate pentagonal bipyramid. Bipyramidal coordination of Ca is common in calcium phosphates. As judged from the Ca...O distances (Table 4) six of these Ca...O bonds are strong; those to O(4) and O(6) are weaker.

In the 'normal' Ca...O coordination in sheet-containing calcium phosphates the shortest distances are from Ca to oxygen atoms in neighboring chains, the intermediate ones are to oxygens in the same chain but with no covalently attached hydrogen, and the longest are to oxygens covalently bonded to hydrogen (Dickens, Bowen and Brown, 1971a). While vestiges of this pattern persist in $Ca(H_2PO_4)_2$, strong hydrogen bonding has apparently modified it, as is the case in $CaHPO_4$

(Dickens, Bowen and Brown, 1971a). The two oxygens O(4) and O(6), which are covalently bonded to hydrogen atoms in 'normal' hydrogen bonds (see later), have the largest Ca...O distances, 2.665 and 2.826 Å, respectively, in some agreement with the normal pattern. The Ca...O(7) distance, 2.429 Å, is relatively short for an oxygen covalently bonded to hydrogen. Oxygens O(3) and O(8), which are also bonded to hydrogens, are not within the primary coordination of Ca.

The PO_4 groups and their environments

The details of the two unique PO_4 groups and their environments are given in Table 4. The longest P-O distances in the phosphate groups are those where the oxygen has a covalently bonded hydrogen. The P(2)-O(7) and P(2)-O(8) distances are intermediate in length, which is consistent with the 'half' hydrogens found to be associated with O(7) and O(8). The P-O bond lengths are expected to be in some proportion to the strength of the interaction of each oxygen with its environment. In some instances this expectation is realized but in others it is not.

The O-P-O angles in the unusually distorted $P(1)O_4$ group may be explained as follows. The smallest angle, O(1),P(1),O(4) (102.07°), is in accord with Pauling's rule (Pauling, 1960) since the O(1),O(4) edge is coordinated to Ca. The O(3),P(1),O(4) angle (103.17°) is expected to be small because O(3) and O(4) are both covalently bonded to hydrogen and P(1)-O(3) and P(1)-O(4) are both long (see, for example, Table 11 of Baur and Khan, 1970). Conversely, the O(1),P(1),O(2) angle is expected to be large (the observed value is 117.59°) because P(1)-O(1) and P(1)-O(2) are both short. In the $P(2)O_4$ group, the angles involving O(5) are the largest, as expected because P(2)-O(5) is the shortest P-O distance in this group. However, it is not clear why the O(6),P(2),O(7) angle (102.41°) is considerably different from the O(6),P(2),O(8) angle (108.42°), or why the O(5),P(2),O(7) angle is different from the O(5),P(2),O(8) angle.

The O(1),O(4) edge and the O(1) and O(2) apexes in the $P(1)O_4$ group and the O(5), O(6) and O(7) apexes in the $P(2)O_4$ group are coordinated to Ca. No edge in the $H_2P(2)O_4$ ion is coordinated to Ca.

The hydrogen bonds

In our x-ray studies of calcium phosphates, the positions of the hydrogen atoms are known only imprecisely owing to known systematic error in the scattering factors of hydrogen. It has become our practice to calculate "ideal hydrogen positions". In Table 1 we report similarly calculated hydrogen positions for comparison with the positions from the neutron diffraction results. The calculated positions were obtained by assuming that the O-H distance is 1.000 Å and the P-O-H angle is 114°, averages of the values found by neutron diffraction here and in $CaHPO_4 \cdot 2H_2O$ (Jones, 1970). The calculated positions for H(1), H(2) and H(3) are close to those found by neutron diffraction, and justify the procedure for use in cases of non-centered hydrogen bonds where neutron studies may be unavailable.

The variation of the O-H distance with the O...O distance for the non-centered hydrogen bonds is consistent with the curve given by Pimentel and McClellan (1971; Fig. 4, therein). The O(6)-H(3) distance of 0.97 Å is the value expected for an O...O distance of 2.82 Å. Likewise, the O(3)-H(1) and O(4)-H(2) distances of ~1.03 Å are those expected for O...O distances of 2.62 and 2.68 Å.

While the precision of our neutron study does not equal that of our x-ray work, the orientations of the ellipsoids representing the vibrational motion of H(1) and H(2) are

reasonable in that the smallest principal axis is in each case approximately parallel to the O-H bond, and the largest amplitude of motion is perpendicular to the P-O-H...O plane. This is to be expected since motion of the hydrogen out of this plane (derived from OH libration about the P-O bond) is known to be of low frequency (~950 cm^{-1}) and thus of relatively large amplitude (Chapman and Thirlwell, 1964).

The orientation of the thermal ellipsoid for H(3) is not as easily understood as those of H(1) and H(2). The large errors (~20°) in the orientation angles for H(3) suggest that the motion of this hydrogen may not be adequately described by the usual thermal ellipsoid.

Hydrogen atoms H(4) and H(5) are both involved in very short hydrogen bonds, the O...O distances being 2.434 and 2.423 Å, respectively, and link $P(2)O_4$ groups together to form a chain with the repeating unit $-\overset{\lceil}{H}(4)\text{--}O(7)P(O_2H)O(8)\text{--}\overset{\rceil}{H}(5)-$ (see Fig. 1). The apparent positions of these protons on centers of symmetry may be examined in terms of three models. (i) The protons could be ordered in a chain so that each one is associated with only one PO_4 group. Thus, H(4) and H(5) would not be on centers of symmetry, but the sense of neighboring chains would be random to give an average picture of two half-hydrogens about the center. This situation is very unlikely in view of the very short O...O distances; asymmetric distributions have been found only for O...O distances greater than 2.54 Å (Pimentel and McClellan, 1971).

(ii) Each proton could be located in a symmetrical double minimum potential with the very short O...O distance implying a low central barrier and consequently a high tunneling rate. (iii) Each proton could be in a potential well with a central barrier, if any, below the zero point energy.

The difficulty of deciding from diffraction data alone whether the potential has a single or double minimum has been discussed by Hamilton and Ibers (1968). Using the neutron data on $Ca(H_2PO_4)_2$, we carried out a series of refinements in which H(4) and H(5) were displaced off center along the O(7)...O(7′) and O(8)...O(8′) vectors respectively in steps of 0.05 Å and only the vibrational amplitudes of the protons and associated oxygens O(7) and O(8) were allowed to vary. The apparent amplitudes of vibration for H(4) and H(5) along the O...O vectors decreased as the protons were moved further off center while the corresponding amplitudes for O(7) and O(8) remained constant. No significant change in the value of R_w occurred until the protons were 0.17 Å off center, when negative amplitudes of vibration were obtained for both protons. Fig. 2 gives the results of these refinements and shows that an upper bound for the off-center distances is ~0.15 Å assuming the proton vibrational amplitude along the O...O vector must be at least that of the oxygens. This is a good assumption since the only motions where the

proton does not move with the oxygen atoms are modes in which the oxygen motions maintain the center of symmetry and these optic modes are known to have very small amplitudes. This reasoning restricts the protons to within 0.15 Å of the centers.

More insight into the nature of these short hydrogen bonds can be gained by considering both spectroscopic and diffraction information. The exact frequency of the OH stretching vibration for very short (~2.45 Å) hydrogen bonds is still under discussion, but is generally associated with absorptions in the range 600-1500 cm^{-1} (Hadzi, 1965). The infrared spectrum of $Ca(H_2PO_4)_2$ in the range 400-4000 cm^{-1} is shown in Fig. 3. Our spectrum confirms an earlier one by Lehr *et al.* (1967). Although we do not intend to delve into detailed assignments, some absorption bands can be assigned by analogy with other phosphates (Chapman and Thirlwell, 1964) and $Ca(H_2PO_4)_2 \cdot H_2O$ (Berry, 1967). The absorptions at 3450 and 3320 cm^{-1} are O-H stretching frequencies expected for an O...O distance of~2.82 Å (Pimentel and McClellan, 1971), while absorption at 2950 cm^{-1} is similarily expected for O...O distances of ~2.6 Å. This leaves open the question of the OH stretching frequency for the very short (~2.45 Å) hydrogen bonds, which are expected to absorb in the 500-1700 cm^{-1} region (Hadzi, 1965). However, many absorptions including in-plane and out-of-plane OH bends, which hinder

assignments via deuterium shifts, absorb in this region and make it difficult to uniquely assign the OH stretching frequencies associated with the short hydrogen bonds. The spectrum indicates that the highest stretching frequency the OH vibrations in the centered hydrogen bonds could have is ~1400 cm^{-1}, assuming the absorption at ~1400 cm^{-1} is due to OH stretching rather than to OH in-plane bending. One can construct an approximate double minimum potential for these protons using both spectroscopic and diffraction data. As the extreme case, we can take an upper bound to the OH stretching frequency as 1400 cm^{-1}, and using the relationship (Hamilton and Ibers, 1968)

$$\langle u^2 \rangle = \frac{h}{8\pi^2 mc\nu}$$

for the harmonic oscillator in the ground state, we obtain $\langle u^2 \rangle \approx 0.012 Å^2$, where $\langle u^2 \rangle$ is the mean-square amplitude of vibration in $Å^2$ and ν is the frequency in cm^{-1}. If we make the assumption that the total mean-square amplitude of each proton is at least that of the bonded oxygens, the potential minimum could be 0.15 Å off center (Fig. 2). Fig. 4 shows that in this extreme case (highest OH stretching frequency, no allowance for other vibrational modes, i.e., no oxygen motion considered, harmonic potential), the central barrier is below the ground state vibrational level, i.e., the zero-point energy. Allowance for the anharmonity associated with hydrogen bonds would lower the barrier.

A more reasonable potential might be one constructed assuming $\nu_{0\,H}$ ~1150 cm^{-1} because the spectrum shows intense absorption characteristic of hydrogen bonding in this region. (This assignment is not unique because PO_4^{3-} vibrations also absorb in this region.) Then $\langle u^2 \rangle$ would be 0.015 $Å^2$, $\langle u^2 \rangle_0$ as estimated from the diffraction results is 0.009$Å^2$, and the total mean-square amplitude, $\langle u^2 \rangle_0 + \langle u^2 \rangle_H$ would be approximately 0.015 + 0.009 = 0.024 $Å^2$. This puts the potential minimum 0.11 Å off center (Fig. 2) and Fig. 4 shows the central barrier would again be much lower than the ground state vibrational level.

One might assume a value for the OH stretching frequency lower than that given here, but this leads to a larger mean-square-amplitude of vibration and thus the separation of the potential minima must be smaller to fit the diffraction data. Hence, the central barrier would be still lower. Thus, we conclude that the H(4) and H(5) atoms in $Ca(H_2PO_4)_2$ are in centered hydrogen bonds. The conclusion that the central barrier lies below the ground state vibrational level for these hydrogen bonds agrees with the prediction that the proton displays a centrosymmetric distribution when R(O...O) <2.47 Å (Pimentel and McClellan, 1971), and is supported by recent <u>ab initio</u> calculations on short hydrogen bonds (O...O ~2.45 Å) in $H_5O_2^+$ and $H_3O_2^-$ (Kollman and Allen, 1970; Newton and Ehrenson, 1971). These calculations indicate that the central barriers in the potential wells are significantly below the zero-point energies (~700 cm^{-1}) for O...O separations up to 2.487 Å. It therefore appears best to consider the

delocalized proton in hydrogen bonds of this type as a "particle in a box" since the proton moves in a rather broad and flat potential exhibiting considerable anharmonicity.

General discussion

The general details found in the structure of $Ca(H_2PO_4)_2$ are also present in $Ca(H_2AsO_4)_2$ (Ferraris, Jones and Yerkness, 1972), which was investigated independently. The overall structural type is expected to be uncommon because the great excess of anions over cations will make three dimensional bonding unavailable for most combinations of ions. Possible candidates for this type of structure will probably consist chiefly of anions with at least one and more probably two hydrogens (i.e., $H_2PO_4^-$, $H_2AsO_4^-$, $H_2VO_4^-$, HSO_4^-, $HCrO_4^-$, etc.) with which to form hydrogen bonds. If an acid molecule (with zero net charge) derived from a tetrahedral anion can be induced to crystallize in the structure, the cation need not be more than monovalent. Salts of the type $Ca(BF_4)_2$ are also possibilities. The salts $Sr(H_2PO_4)_2$ and $Ba(H_2PO_4)_2$ are known to crystallize in two forms each (Lehr et al., 1967). The reduced cells (Mighell, Santoro and Donnay, 1969) of their triclinic forms, together with a permutation of the cell of $Ca(H_2PO_4)_2$, are:

	a	b	c	α	β	γ
$Ca(H_2PO_4)_2$	5.550 Å	8.253 Å	7.558 Å	109.15°	93.68°	109.87°
$Sr(H_2PO_4)_2$	6.70	7.10	7.84	104.7	96.9	109.3
$Ba(H_2PO_4)_2$	7.03	7.24	8.10	105.0	96.2	108.6

While the Sr and Ba salts appear to be structurally related to each other, they do not seem to be simply related to the Ca salt. Perhaps Ca is not able to sustain the large cation coordinations undoubtedly required in the Sr and Ba structures, and a relationship of distortion obtains similar to the relationship between the $Ba_3(PO_4)_2$ (Zachariasen, 1948) or $Ba_3(VO_4)_2$ (Süsse and Buerger, 1970) type structures and $\beta Ca_3(PO_4)_2$ (Gopal and Calvo, 1971; Dickens, Bowen and Brown, 1971b). In the apatite series, Ca is just within the stability field which includes Ba and Sr. For cations with ionic radii less than that of Ca, the wagnerite (Mg_2PO_4F) structure is preferred (Kreidler, 1967).

The linking of PO_4 groups through symmetrical hydrogen bonds to form chains running throughout the crystal is one of the more novel features of the structure of $Ca(H_2PO_4)_2$. To our knowledge this is one of only two examples of such extended linkages involving centered hydrogen bonds, the arsenate analog, $Ca(H_2AsO_4)_2$ (Ferraris et al., 1972), apparently being a similar case. Such linkages suggest possible ferroelectric behavior especially in view of the fact that

other salts of $H_2PO_4^-$, e.g., KH_2PO_4, are well known ferroelectrics. Present theories of hydrogen-bonded ferroelectrics (Kobayashi, 1968) emphasize the ordering of the protons in a double well. In general, these theories lead to the result that the higher the tunneling rate (i.e., the lower the barrier), the lower the temperature of the phase transition, which is often second order.

In the case of $Ca(H_2PO_4)_2$, our unsuccessful attempt to reduce extinction in the crystal used for neutron diffraction by dipping it in liquid nitrogen indicates that there is probably no first-order phase change in $Ca(H_2PO_4)_2$ between room temperature and ~77°K, although there is still the possibility of a second-order phase transition. However, the barriers are seemingly well below the zero-point energies even at room temperatures, and contraction on cooling would be expected to decrease the barriers by more overlapping of the component potential wells. Thus, we conclude that the existence of a ferroelectric phase of $Ca(H_2PO_4)_2$ is unlikely.

The existence of hydrogen bonded dimers of PO_4 groups in $Ca(H_2PO_4)_2$ may have some bearing on species present in aqueous solutions of phosphates. The existence of a dimeric species $[H_4(PO_4)_2]^{2-}$ in fairly dilute aqueous solutions of alkali metal orthophosphates has been suggested (Childs, 1969, 1970) on the basis of studies of ionic equilibria. Similar postulates have been made for solutions of H_3PO_4 more concentrated than 0.1 m (Elmore et al., 1965). The presence of the ion pairs $[CaHPO_4]^\circ$ and $[CaH_2PO_4]^+$ has been suggested (Moreno, Gregory and Brown, 1966) via solubility studies of calcium phosphates.

Our observation of $H_2P(1)O_4$ ions linked into dimers and $H_2P(2)O_4^-$ ions linked together by symmetrical hydrogen bonds to form polymeric chains suggests that the possibility that small polymers of phosphate ions exist in aqueous solution be given serious consideration. The related case of the hydration of $H^+ \cdot nH_2O$ to $H^+ \cdot (n+1)H_2O$, has been studied by Kerbarle et al. (1967) who showed by mass spectrometry that no unique value of n dominates. Indeed, in the crystal structure studies of $(H^+ \cdot nH_2O)\ X^-$ compounds (Lundgren and Olovsson, 1968), $H_5O_2^+$ and higher complexes were found. Thus, further investigations into the existence of dimeric, trimeric, etc., species involving $H_2PO_4^-$ seems warranted. The dissociation constants of H_3PO_4, $10^{-2.12}$, $10^{-7.21}$ and $10^{-12.67}$, reveal considerable affinity of the PO_4 group for its second and especially its third hydrogens. Thus phosphates, being polybasic, might be expected to contain unusual but chemically important hydrogen bonds which result in the formation of unusual complexes.

Acknowledgment

We thank J. S. Bowen and P. B. Kingsbury for technical help. Fig. 1 was drawn using the ORTEP program of C. K. Johnson. This investigation was supported in part by research grant DE00572 to the American Dental Association, General Research Support Grant RR05689 funds made available to the American Dental Association, and by contract NIDR-02 to the National Bureau of Standards from the National Institute of Dental Research.

References

Abrahams, S. C. and Keve, E. T. (1971). Acta Cryst. A27, 157-165.

Alperin, H. and Prince, E. (1970). J. Res. Natl. Bur. Stds. 74C, 89-95.

Bassett, H. (1908). Zeit. anorg. Chem. 59. 1-55.

Baur, W. H. and Khan, A. A. (1970). Acta Cryst. B26, 1584-1596.

Berry, E. E. (1968). Spectrochim. Acta 24A, 1727-1734.

Blume, R. J. (1962). Rev. Sci. Instr. 22, 598-599.

Chapman, A. C. and Thirlwell, L. E. (1964). Spectrochim. Acta 20, 937-947.

Childs, C. W. (1969). J. Phys. Chem. 73, 2956-2960.

Childs, C. W. (1970). Inorg. Chem. 9, 2465-2469.

Coppens, P. and Hamilton, W. C. (1970). Acta Cryst. A26, 71-83.

Cromer, D. T. and Mann, J. B. (1968). Acta Cryst. A24, 321-324.

Cromer, D. T. and Liberman, D. (1970). J. Chem. Phys. 53, 1891-1898.

Curry, N. A., Denne, W. A. and Jones, D. W. (1968). Bull. Soc. Chim, Fr., 1748-1750.

Dickens, B. and Bowen, J. S. (1971). Acta Cryst. B27, 2247-2255.

Dickens, B., Bowen, J. S. and Brown, W. E. (1971). Acta Cryst. B28, 797-806.

Dickens, B., Bowen, J. S. and Brown, W. E. (1971). Abstract G3, American Crystallographic Association winter meeting, Columbia, S. C.

Elmore, K. L., Hatfield, J. D., Dunn, R. L. and Jones, A. D. (1965). J. Phys. Chem. 96, 3520-3525.

Ferraris, G., Jones, D. W. and Yerkness, J. (1972). Acta Cryst. B28, 209-214.

Finger, L. W. (1968). Carnegie Institute of Washington, unpublished.

Gopal, R. and Calvo, C. (1971). Canadian J. Chem. Soc. 49, 1036-1046.

Hamilton, W. C. and Ibers, J. A. (1968). Hydrogen Bonding in Solids Chap. 3, New York; Benjamin.

Hadzi, D. (1965). Pure Appl. Chem. 11, 435-453.

Jones, D. W. (1970). (Private communication.)

Jones, D. W. and Cruickshank, D. W. J. (1961). Z. Krist. 116, 101-125.

Kerbale, P., Searles, S. K., Zolla, A., Scarborough, J. and Arshadi, M. (1967). J. Am. Chem. Soc. 89, 6393-6399.

Kobayashi, K. K. (1968). J. Phys. Soc. Japan. 24, 497-508.

Kollman, P. A. and Allen, L. C. (1970). J. Am Chem. Soc. 92, 6101-6107.

Kreidler, E. R. (1967). Ph.D. Thesis, Penn. State University. Dissertation 68-3549, University Microfilms, Ann Arbor, Mich.

Lenhert, P. G. (1970). Abstract M8, American Crystallographic Association winter meeting, New Orleans, La., March.

Lehr, J. R., Brown, E. H., Frazier, A. W., Smith, J. P. and Thrasher, R. D. (1967). Crystallographic Properties of Fertilizer Compounds, Chem. Eng. Bull. 6, TVA, p.118.

Lundgren, J. O. and Olovsson, I. (1968). J. Chem. Phys. 49, 1068-1074, and references therein.

Mighell, A. D., Santoro, A. and Donnay, J. D. H. (1969). International Tables for X-ray Crystallography, Vol. I, Kynoch Press; Birmingham, p. 534.

Moreno, E. C., Gregory, T. M. and Brown, W. E. (1966). J. Res. Natl. Bur. Stds., 70A, 545-552.

Newton, M. D. and Ehrenson, S. (1971). J. Am. Chem. Soc. 93, 4971-4990.

Pauling, L. (1960). The Nature of the Chemical Bond, 3rd Edition, p. 559, Ithaca, New York; Cornell University Press.

Pimentel, G. C. and McClellan, A. L. (1971). Annual Rev. Phys. Chem., "Hydrogen Bonding", 22, 347-385.

Prince, E. (1972). J. Chem. Phys. 56, 4352-4355.

Smith, J. P., Lehr, J. R. and Brown, W. E. (1955). Amer. Min. 40, 893-899.

Stewart, J. M. (1967). XRAY 67 System of Computer Programs, Technical Report 67-58. University of Maryland, College Park, Maryland 20742.

Süsse, P. and Buerger, M. J. (1970). Zeit. Krist. 131, 161-174.

The Neutron Diffraction Commission (1969). Acta Cryst. A25, 391-392.

Zachariasen, W. H. (1967). Acta Cryst. 23, 558-564.

Zachariasen, W. H. (1948). Acta Cryst. 1, 263-265.

Table 1. Atomic parameters in $Ca(H_2PO_4)_2$

Atom		x	y	z	B^*_{11}	B_{22}	B_{33}	B_{12}	B_{13}	B_{23}
Ca	a	0.31392(2)	0.41915(2)	0.18764(3)	0.835(6)	0.767(6)	0.597(6)	0.219(4)	0.088(4)	0.233(4)
	b	0.3139(6)	0.4190(5)	0.1877(6)	1.0(1)	1.0(1)	0.9(1)	0.2(1)	0.3(1)	0.3(1)
P(1)	a	0.25687(3)	0.15967(3)	0.51764(4)	0.693(7)	0.590(7)	0.534(7)	0.124(5)	0.073(5)	0.209(5)
	b	0.2569(5)	0.1596(5)	0.5171(5)	1.8(1)	0.7(1)	0.7(1)	0.1(1)	0.14(8)	0.18(9)
O(1)	a	0.42553(8)	0.31905(8)	0.5122(1)	0.80(2)	0.83(2)	0.91(2)	0.05(1)	0.09(1)	0.38(1)
	b	0.4259(4)	0.3189(4)	0.5122(5)	0.8(1)	0.8(1)	1.1(1)	-0.08(8)	0.20(8)	0.37(9)
O(2)	a	0.17951(9)	0.18764(8)	0.76582(1)	1.04(2)	1.02(2)	0.63(2)	0.14(1)	0.25(1)	0.20(1)
	b	0.1802(4)	0.1888(4)	0.7671(5)	1.0(1)	1.0(1)	0.7(1)	0.1(1)	0.3(1)	0.1(1)
O(3)	a	0.2902(1)	-0.02827(9)	0.4366(1)	1.72(2)	0.84(2)	0.96(2)	0.63(2)	0.22(2)	0.32(1)
	b	0.2905(4)	-0.0270(4)	0.4384(6)	1.8(2)	0.9(1)	1.2(1)	0.6(1)	0.38(9)	0.3(1)
O(4)	a	0.10443(9)	0.12477(9)	0.2801(1)	0.98(2)	1.08(2)	0.95(2)	0.11(1)	-0.17(1)	0.49(1)
	b	0.1035(4)	0.1237(4)	0.2795(5)	0.9(1)	1.1(1)	1.3(1)	0.1(1)	-0.1(1)	0.5(1)
H(1)	a	0.306(3)	-0.053(3)	0.566(5)	1.00					
	b	0.3239(9)	-0.0622(8)	0.586(1)	2.8(3)	2.1(3)	2.3(2)	1.1(2)	-0.0(2)	0.7(2)
	c	0.317	-0.064	0.587						
H(2)	a	0.021(4)	0.038(3)	0.235(5)	1.00					
	b	-0.0152(8)	0.0123(8)	0.237(1)	1.5(2)	1.5(2)	2.4(2)	-0.1(2)	-0.1(2)	0.5(2)
	c	-0.013	0.011	0.236						
P(2)	a	0.73538(3)	0.31138(3)	0.17145(4)	0.651(7)	0.650(7)	0.624(7)	0.210(5)	0.029(5)	0.211(5)
	b	0.7356(4)	0.3116(5)	0.1710(6)	0.6(1)	0.8(1)	1.1(1)	0.3(1)	0.3(1)	0.4(1)
O(5)	a	0.60344(9)	0.37118(9)	0.04075(9)	1.10(2)	1.05(2)	0.94(2)	0.50(1)	0.05(1)	0.47(1)
	b	0.6026(4)	0.3708(4)	0.0403(5)	1.1(1)	1.1(1)	1.3(1)	0.6(1)	0.2(1)	0.5(1)
O(6)	a	0.91733(9)	0.32349(9)	0.0360(1)	1.12(2)	1.26(2)	1.01(2)	0.47(2)	0.47(1)	0.26(2)
	b	0.9167(4)	0.3234(5)	0.0351(6)	1.1(1)	1.4(1)	1.3(1)	0.4(1)	0.6(1)	0.4(1)
O(7)	a	0.82615(8)	0.44107(9)	0.4552(1)	0.63(2)	1.16(2)	0.67(2)	0.20(1)	-0.01(1)	-0.09(1)
	b	0.8261(4)	0.4407(4)	0.4553(5)	0.5(1)	1.3(1)	0.9(1)	0.2(1)	0.1(1)	-0.1(1)
O(8)	a	0.6416(1)	0.11232(8)	0.1612(1)	1.24(2)	0.71(2)	1.19(2)	0.05(1)	-0.23(1)	0.46(1)
	b	0.6411(4)	0.1126(4)	0.1610(6)	1.3(1)	0.8(1)	1.3(1)	0.1(1)	-0.2(1)	0.5(1)
H(3)	a	0.899(3)	0.248(3)	-0.103(5)	1.00					
	b	0.882(1)	0.233(1)	-0.140(1)	3.6(3)	2.7(3)	2.3(3)	1.6(3)	1.1(2)	0.4(2)
	c	0.888	0.230	-0.147						
H(4)	a	1.000	0.500	0.500	1.00					
	b	1.000	0.500	0.500	3.1(4)	2.1(4)	1.3(3)	0.7(3)	0.4(3)	0.1(2)
	c	0.969	0.490	0.493						
H(5)	a	0.500	0.000	0.000	1.00					
	b	0.500	0.000	0.000	2.5(3)	2.7(4)	2.8(3)	1.4(3)	0.7(3)	1.7(3)
	c	0.526	0.033	0.020						

Figures in parentheses are standard deviations in the last digit(s).

* Thermal parameters are in $Å^2$ and have the form $\exp-[1/4(h^2a^{*2}B_{11} + k^2b^{*2}B_{22} + \ell^2c^{*2}B_{33} + 2hka^*b^*B_{12} + 2h\ell a^*c^*B_{13} + 2k\ell b^*c^*B_{23})]$.

a X-ray values

b neutron values

c calculated hydrogen positions as described in text.

Table 2. Calculated and observed x-ray structure factors for $Ca(H_2PO_4)_2$. Columns are ℓ, 10 F_o, 10 F_c and 10 $\sigma(F_o)$. Unobserved reflections are those with intensity less than 2 $\sigma(I)$ and are marked by *.

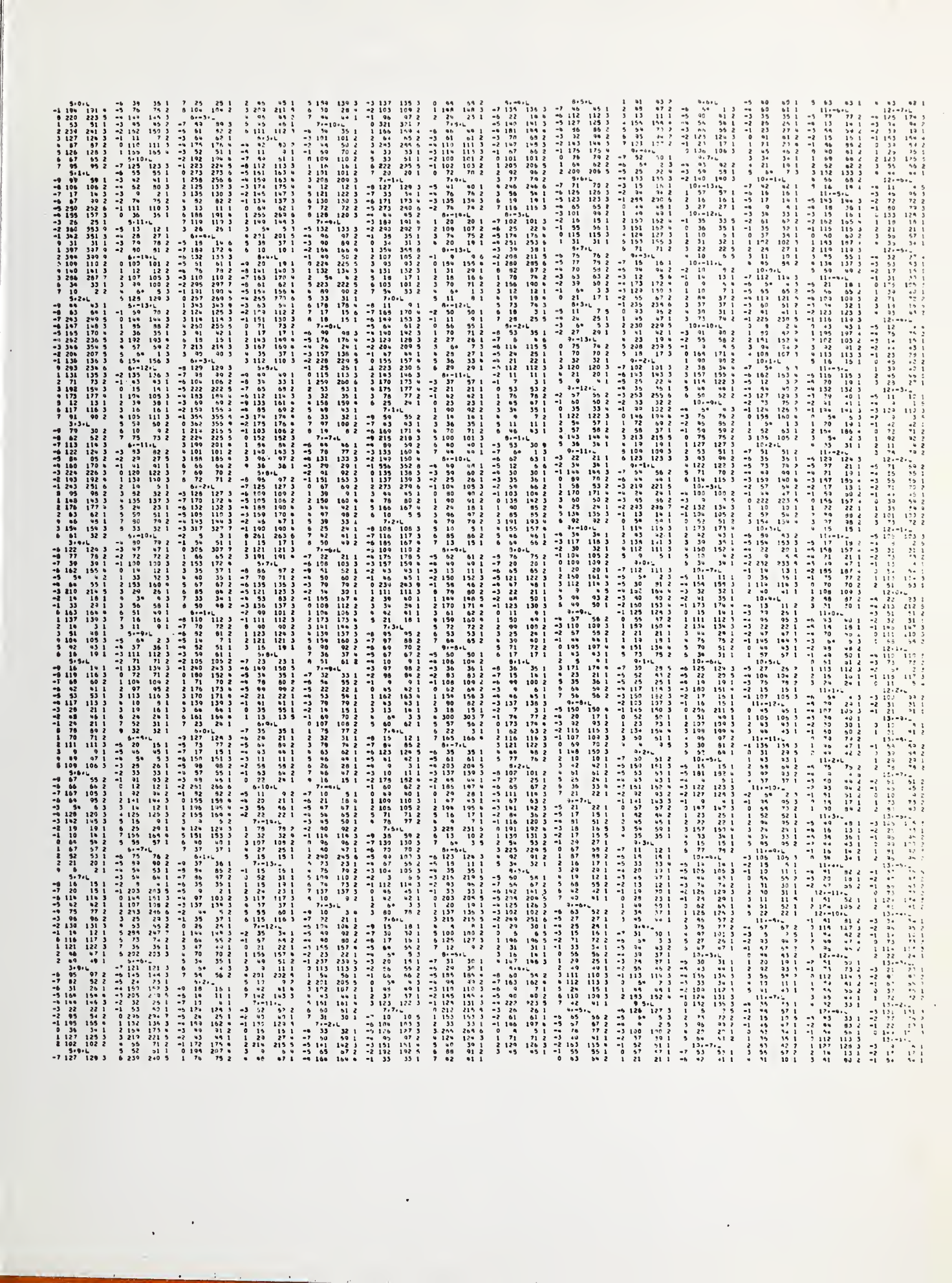

Table 3. Calculated and observed neutron structure factors for $Ca(H_2PO_4)_2$. Columns are ℓ, 100 F_o, 100 F_c and 100 $\sigma(F_o)$. Unobserved reflections are those with intensity less than 2 $\sigma(I)$ and are marked by *.

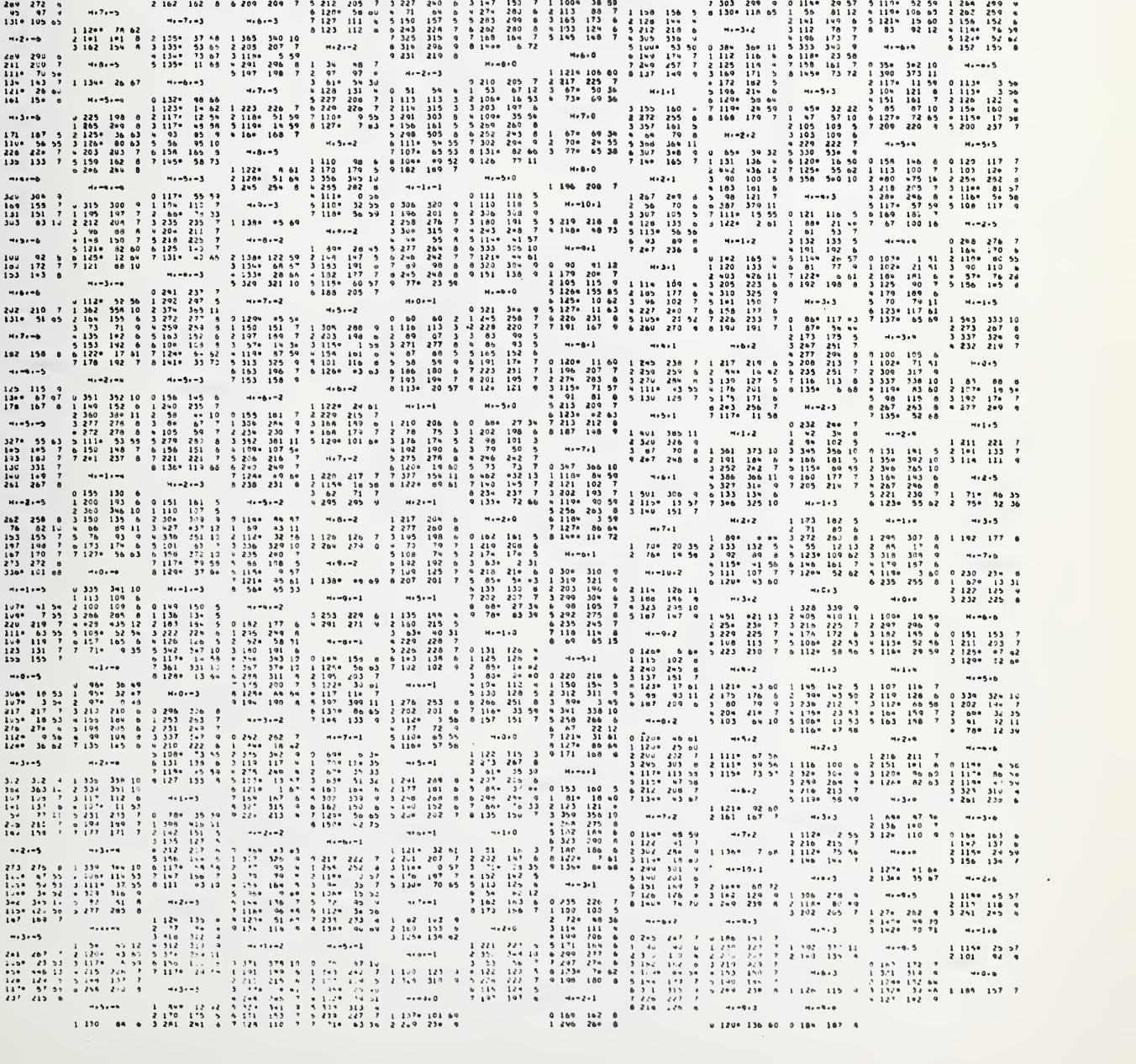

Table 4. Structural details in $Ca(H_2PO_4)_2$

Ca environment	distance, Å or angle, deg. X-ray	neutron ¶
Ca, O(2)	2.3547(6) Å	2.345(4) Å
Ca, O(1)	2.3795(6)	2.379(5)
Ca, O(5)	2.4238(6)	2.426(4)
Ca, O(7)	2.4284(6)	2.423(5)
Ca, O(1')	2.4316(6)	2.433(4)
Ca, O(5')	2.4874(7)	2.483(4)
Ca, O(4)	2.6647(6)	2.670(4)
Ca, O(6)	2.8262(7)	2.831(4)
$H_2P(1)O_4$ group		
P(1), O(1)	1.5125(6)	1.513(4)
P(1), O(2)	1.5061(6)	1.512(4)
P(1), O(3)	1.5709(6)	1.563(4)
P(1), O(4)	1.5742(6)	1.576(4)
O(1), O(2)	2.5818(9)	2.581(4)
O(1), O(3)	2.5773(9)	2.569(4)
O(1), O(4)	2.4003(8)	2.409(4)
O(2), O(3)	2.4849(9)	2.482(4)
O(2), O(4)	2.5533(9)	2.560(4)
O(3), O(4)	2.4643(9)	2.463(4)
O(1), P(1), O(2)	117.59(3)°	117.2(3)°
O(1), P(1), O(3)	113.40(4)	113.3(3)
O(1), P(1), O(4)	102.07(3)	102.5(3)
O(2), P(1), O(3)	107.69(4)	107.6(3)
O(2), P(1), O(4)	111.95(4)	112.0(3)
O(3), P(1), O(4)	103.17(4)	103.4(3)
O(3), H(1) +	0.82(2) Å	1.000(8) Å 1.016(8) *
O(4), H(2) +	0.73(2)	1.000(8) 1.011(8) *
P(1), O(3), H(1)	110(1)°	115.9(4)°
P(1), O(4), H(2)	117(1)	117.0(3)
$H_2P(2)O_4$ group		
P(2), O(5)	1.4959(6) Å	1.499(4) Å
P(2), O(6)	1.6001(6)	1.596(4)
P(2), O(7)	1.5266(6)	1.528(4)
P(2), O(8)	1.5401(6)	1.540(4)
O(5), O(6)	2.5292(9)	2.530(4)
O(5), O(7)	2.5341(8)	2.540(4)
O(5), O(8)	2.5389(9)	2.535(4)
O(6), O(7)	2.4372(9)	2.439(4)
O(6), O(8)	2.5473(9)	2.547(4)
O(7), O(8)	2.4869(9)	2.484(4)

$H_2P(2)O_4$ group Cont.	distance, Å or angle, deg. X-ray	neutron
O(5), P(2), O(6)	109.52(4)°	109.6(3)°
O(5), P(2), O(7)	113.95(4)	114.1(3)
O(5), P(2), O(8)	113.49(4)	113.0(3)
O(6), P(2), O(7)	102.41(3)	102.7(3)
O(6), P(2), O(8)	108.42(4)	108.6(3)
O(7), P(2), O(8)	108.38(3)	108.1(3)
O(6), H(3) +	0.78(2) Å	0.957(8) Å 0.985(8) *
O(7), H(4)	1.2171(5)	1.218(3)
O(8), H(5)	1.2116(6)	1.210(3)
P(2), O(6), H(3)	116(1)°	111.7(5)°
P(2), O(7), H(4)	113.75(4)	113.6(2)
P(2), O(8), H(5)	121.59(5)	121.9(2)
H_2PO_4 environments		
O(1), Ca	2.3795(6)	2.379(4)
O(1), Ca'	2.4316(6)	2.433(4)
O(2), Ca	2.3547(6)	2.346(4)
O(2), H(2)	1.70, 1.98(2) ‡	1.710(6)
O(2), O(4)	2.6778(9) *	2.677(5) *
O(3), O(8)	2.6210(9) *	2.620(4) *
H(1), O(8)	1.62, 1.80(2) ‡	1.625(7)
O(3), H(1), O(8)	177°, 175(1)° ‡	173.6(6)°
O(3), H(3)	1.90, 2.11(2) Å ‡	1.922(8) Å
O(3), O(6)	2.8101(9)	2.817(4) *
O(4), Ca	2.6647(6)	2.671(5)
O(4), O(2)	2.6778(9)	2.677(5)
H(2), O(2)	1.70, 1.98(2) ‡	1.710(6)
O(4), H(2), O(2)	164, 161(2)° ‡	162.8(6)°
O(5), Ca	2.4238(6) Å	2.426(4) Å
O(5), Ca''	2.4874(7)	2.483(4)
O(6), Ca	2.8262(7)	2.830(4)
O(6), O(3)	2.8101(9) *	2.817(4) *
H(3), O(3)	1.90, 2.11(2) ‡	1.922(8)
O(6), H(3), O(3)	150, 150(2)° ‡	154.5(6)°
O(7), Ca	2.4284(6) Å	2.429(4) Å
O(7), O(7')	2.434(1) *	2.434(5) *
H(4), O(7')	1.43, 1.217(5) ‡	1.217(3)
O(7), H(4), O(7')	180, 180° ‡	180°
O(8), O(8')	2.423(1) *	2.419(6) *
H(5), O(8')	1.44, 1.216(6) ‡	1.210(3)
O(8), H(5), O(8')	167, 180° ‡	180°

¶ Neutron values for internuclear distances.

Figures in parentheses are standard deviations in the last digit(s) and should not be taken as implying the mean bond distance is known to this precision.

+ O – H distance of 1.000 Å, P – O – H angle of 114° assumed.

‡ first value from calculated hydrogen position, as described in text, second value from x-ray results.

* Riding model correction (Busing and Levy, 1964).

* These O...O distances involve Hydrogen bonds.

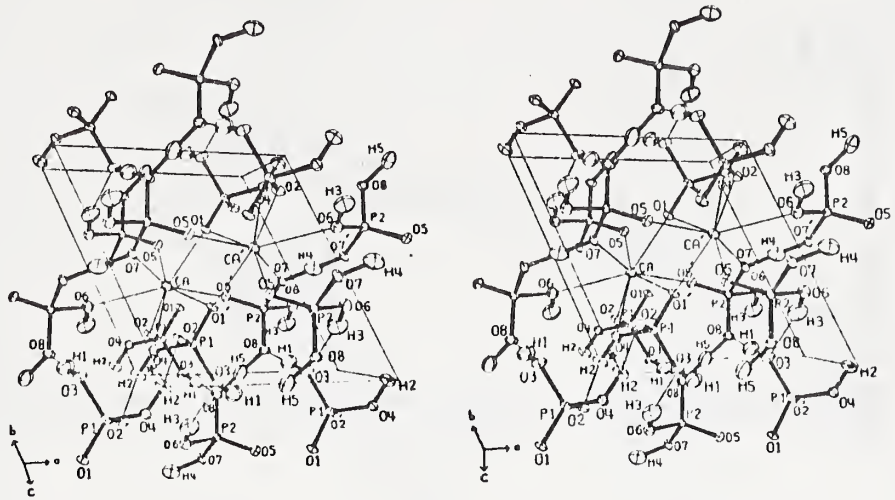

Figure 1 - A stereoscopic illustration of the $Ca(H_2PO_4)_2$ structure. The origin of the crystallographic coordinate system marked by *. $P(1)O_4$ groups hydrogen bonded into dimers may be seen at the lower left front corner. The $P(2)O_4$ hydrogen bonded infinite chain passes near the centers of the bottom and right edges of the unit cell.

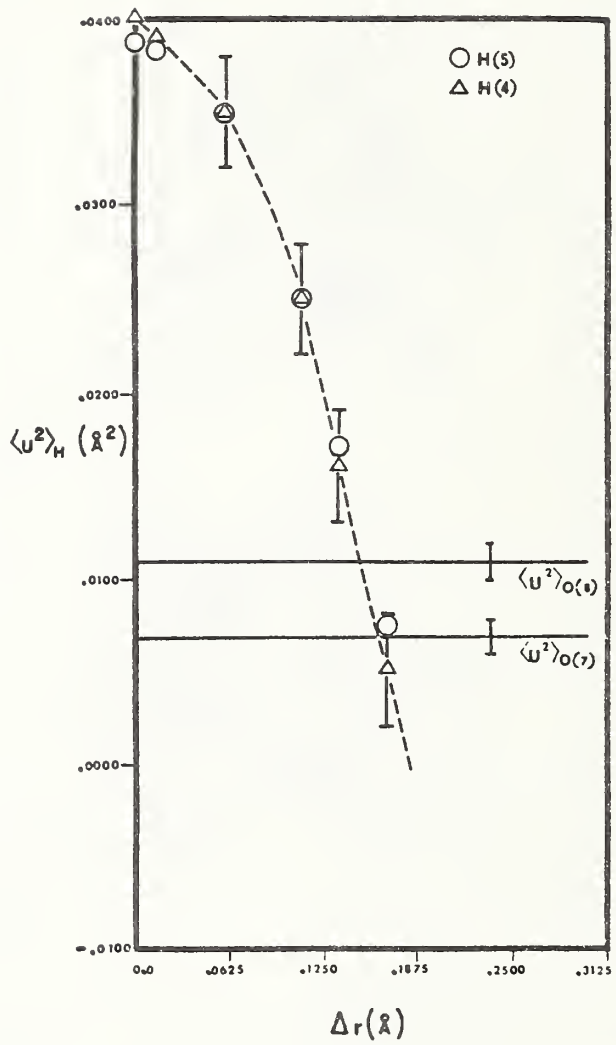

Figure 2 - The variation of the mean-square amplitudes of hydrogen atoms H(4) and H(5) in $Ca(H_2PO_4)_2$ with displacement from the centers of symmetry.

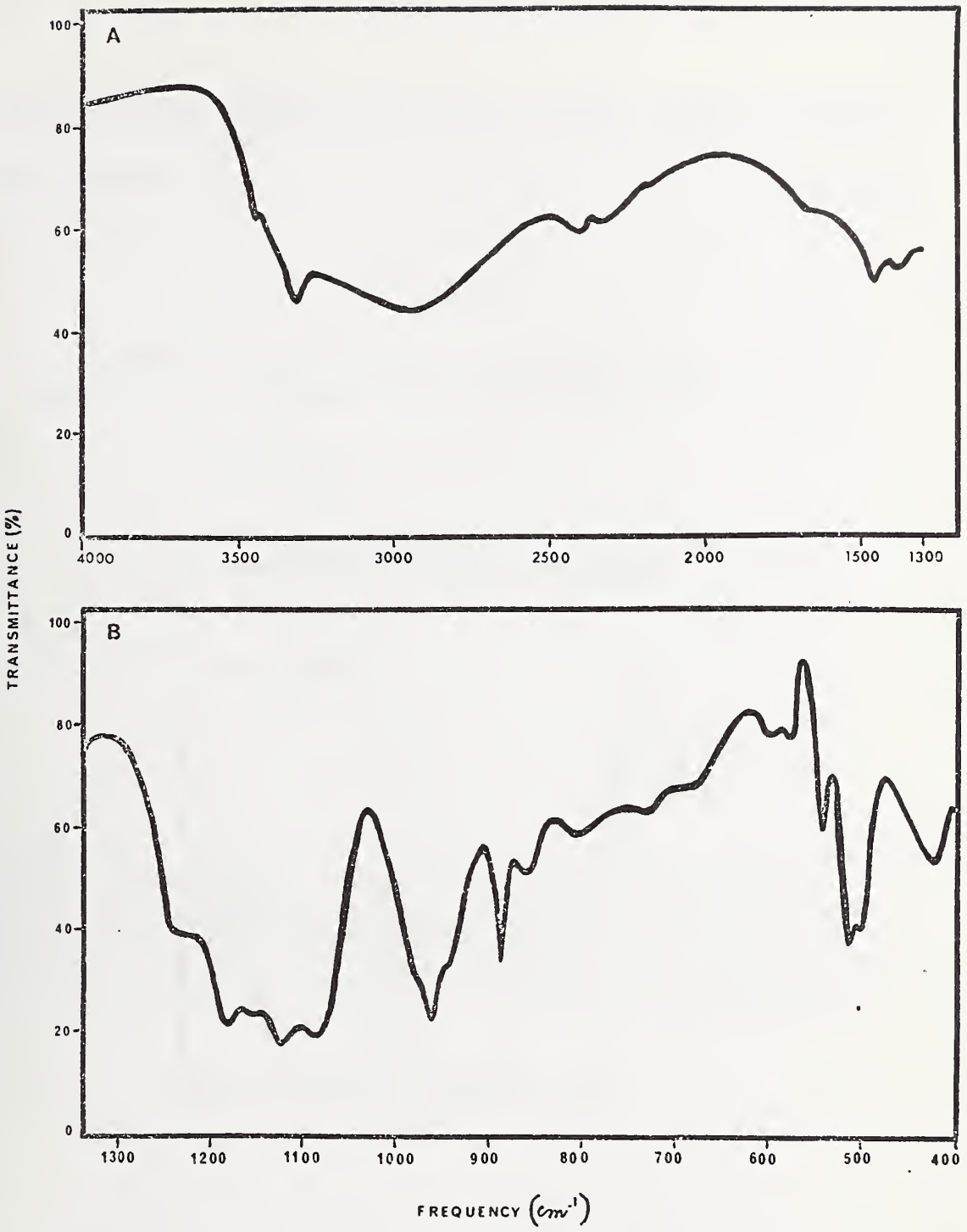

Figure 3

A - Infrared spectrum of $Ca(H_2PO_4)_2$ in the region 1300 to 4000 cm^{-1} taken from a halocarbon oil mull smeared between KBr plates. Particle sizes under 10 μm.

B - Spectrum in the 400 to 1300 cm^{-1} region taken from a Nujol mull. Spectra were run on a grating spectrophotometer using the standard slit program and a scan speed of 33 cm^{-1}/min. Frequencies were checked against a standard 0.05 mm polystyrene film.

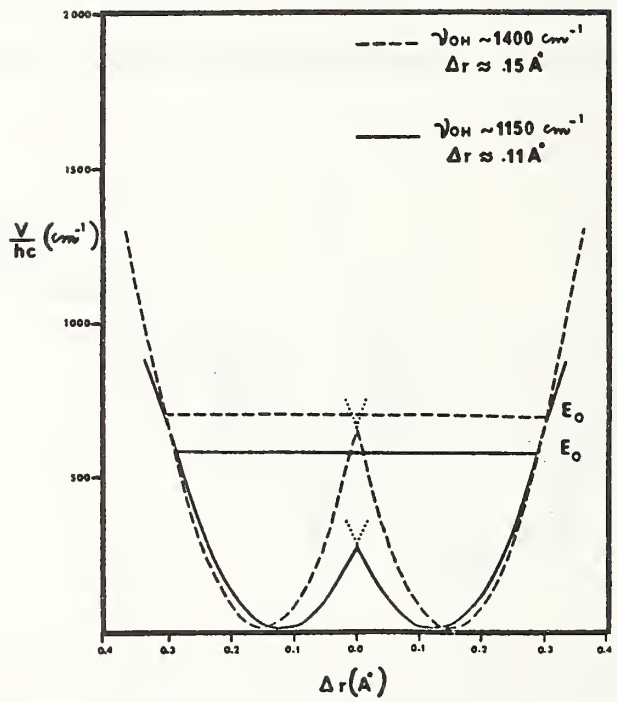

Figure 4 - A comparison of the zero point energy, E_o, and the central barrier of two combined harmonic potential wells for an extreme (dotted lines) case and a more probable (solid lines) case for hydrogens H(4) and H(5) in $Ca(H_2PO_4)_2$.

NATIONAL BUREAU OF STANDARDS REPORT

NBS PROJECT 311.05-3110561

December 29, 1972

NBS REPORT 10 979

Progress Report

on

CLINICAL EVALUATION OF A RADIOPAQUE COMPOSITE RESTORATIVE MATERIAL AFTER THREE AND ONE HALF YEARS

Chandler, H. H.*, DDS; Bowen, R. L.**, DDS;
Paffenbarger, G. C.***, DDS; and Mullineaux, A. L.****

* Research Associate American Dental Association Research Unit at the National Bureau of Standards, Washington, D. C. 20234 on leave of absence from the Ohio State University College of Dentistry, Columbus, Ohio 43210.

** Associate Director American Dental Association Research Unit at the National Bureau of Standards, Washington, D. C. 20234.

*** Senior Research Associate American Dental Association Research Unit at the National Bureau of Standards, Washington, D. C. 20234.

**** Research Associate American Dental Association Research Unit at the National Bureau of Standards, Washington, D. C. 20234.

This investigation was supported in part by NIH Research Grants DE02742-01 thru -05 and DE02494-02 thru -06 to the American Dental Association from the National Institute of Dental Research and is part of the dental research program conducted by the National Bureau of Standards in cooperation with the American Dental Association; the Dental Research Division of the United States Army Medical Research and Development Command; the Dental Sciences Division of the School of Aerospace Medicine, USAF; the National Institute of Dental Research; and the Veterans Administration.

U.S. DEPARTMENT OF COMMERCE

NATIONAL BUREAU OF STANDARDS

Clinical evaluation of a radiopaque composite restorative material after three and one half years

Synopsis

A clinical comparison was made of an experimental radiopaque composite restorative material and Addent®35. The radiopaque experimental formulation contained a novel ternary eutectic dimethacrylate as the resin binder and fused silica and a novel BaF_2-containing glass as the reinforcing fillers. Forty-six pairs of Class III and V restorations were placed.

Results of the evaluations indicate that the experimental material compared favorably with the commercial material over the course of the investigation. At 3.5 years, a significantly greater number of the restorations made of the experimental material were rated as being better compared to those of Addent®35.

The need for radiopaque dental materials has been discussed previously[1,2] and is based primarily on the necessity for accurate and prompt diagnosis using radiographic methods. Examples are: the detection of secondary caries around dental restorations and the localization of ingested or aspirated denture base materials.

Physical properties of one such experimental composite material developed at the National Bureau of Standards were reported previously.[3] That report indicated that the properties measured were within ranges that would make it suitable for at least limited clinical evaluation as an esthetic anterior restorative material. Therefore, a clinical study was initiated using a material essentially identical to that reported except that the silica particles in the filler had been spheroidized. This report gives the results of the evaluation for the first 3.5 years. The results are compared with those obtained using Addent®35* which, although no longer being sold, was at the time of placement (1968-69) a commercially available material.

---

* 3M Co., St. Paul, Minnesota

Materials*

With the exception of benzoyl peroxide contained in both, the ingredients of the two composite materials were completely different. The composition of the liquids[4,5] and powders[6] used to make the experimental formulations is given in Table 1. Seventy-nine parts by weight of the reinforcing filler and 21 parts by weight of monomer were mixed on a glass slab for one minute prior to insertion.

As with most of the commercial dental composite materials, Addent®35 had a resin matrix of the BIS-GMA type[7,8] {i.e., based on 2,2-bis[4(2-hydroxy-3-methacryloxy propoxy)phenyl] propane}. It contained an inorganic filler of spheres of soda-lime glass, short rods of Type E glass and a finely divided lithium aluminosilicate. It was comparatively radiolucent.

To facilitate color change evaluations, only one shade of each material was used.

All of the cavity preparations to receive the experimental composite were treated with the NPG-GMA solution, the ingredients of which are listed under "Coupling Agent Formulation" in Table 1.

---

* Certain commercial materials and equipment are identified in this paper to specify the experimental procedure. In no instance does such identification imply recommendation or endorsement by the National Bureau of Standards or that the material or equipment identified is necessarily the best available for the purpose.

The solution is not a pulp protecting cavity liner in the traditional sense but could be partially effective in this respect if it successfully seals the interface between the restoration and tooth. The results of a clinical test of this material are reported elsewhere.[9] The cavity preparations for Addent®35 were treated with the liner supplied by the manufacturer who described it as a synthetic vinyl copolymer designed to minimize pulp response.[10] The liner was removed from the cavo-surface margin as directed by the manufacturer.

Clinical methods

Forty-six pairs (one of each pair, selected at random, being the experimental material and the other, Addent®35) of Class III and V restorations were placed in adult patients selected on their probable availability for recall for as long as five years. In order of decreasing preference, the restorations in each pair were matched using approximating surfaces on adjacent teeth, the same surfaces on contralateral teeth, the same surfaces on different teeth in the same quadrant or different surfaces in the same quadrant.

An oral prophylaxis was performed on the teeth in areas to receive the restorations. A rubber dam was always used and cavity preparation procedures followed conventional techniques. Where cavity depth was judged to be greater than 1 mm in dentin, a commercially available calcium hydroxide liner or base* was applied. After washing with a stream of tap water, the preparations for the experimental material were treated with the solution of NPG-GMA carried on a cotton pledget. The excess was immediately removed with a dry pledget. Methods of insertion and finishing have been described earlier.[1]

Evaluation methods

The restorations were evaluated by three dentists (three of the authors) on the basis of sensitivity to percussion, general sensitivity or pain, gross fracture, restoration loose or missing, secondary caries, the need for replacement, color, surface texture, marginal notch, marginal stain, and degree of marginal flushness. Finally, the restorations of each pair were evaluated to determine if one was better, the same or worse than the other in its overall condition.

---

* Hydrex - Kerr Manufacturing Co., Romulus, Michigan 48174

Sensitivity was determined by questioning each patient as to his experiences. Teeth were percussed with a mirror handle by at least one of the evaluators at each examination. Scores were given from "0" for no sensitivity up to "10" for severe sensitivity.

Gross fracture (as opposed to minute marginal fracture), loose or missing restorations, and secondary caries were recorded as was the need for replacement. The latter evaluation was based solely on the evaluator's clinical judgment.

Surface texture evaluations were made by comparing the texture of the restoration with the texture of a series of glass blocks, Figure 1. The blocks were of increasing roughness and were designated "0" - polished glass, "2" - glass ground with aluminum oxide of 20 μm particle size, "4" - ground with silicon carbide, 50 μm, "6" - ground with silicon carbide, 100 μm, and "8" - ground with silicon carbide, 250 μm. If the surface roughness of the restoration was greater than the block designated as "8," a score up to "10" could be given. Comparisons were made by alternately "feeling" the restoration and the various blocks with a dental explorer until the evaluator perceived similar

roughness. Intermediate scores could be given if the evaluator perceived roughness between those in the series of blocks.

Surface staining evaluations were given from "0" for no visible stain up to "10" for severe stain. These evaluations were made on the facial surface where possible and were recorded only when the stain was greater than that on the surrounding tooth enamel. If the facial surface was not visible, the evaluation was made on the lingual surface.

Color evaluations were made by comparing the restorations with a shade guide containing ten anterior porcelain tooth crowns of increasing darkness numbered from "0" to '9," Figure 2. If darkness greater than "9" was perceived, a score of "10" could be given. Evaluations were made on the facial surface where possible.

Notch, stain, and flushness evaluations were made on labial, lingual, gingival and incisal margins of Class III restorations and mesial, distal, gingival and incisal or occlusal margins on Class V restorations.

Notch evaluations were made by tactile sensation with a dental explorer. Scores could range from "0" for no notch

up to "10" for a notch estimated to be 1 mm wide. Although not used in this investigation, a notch guide was developed during the study with which the operator, using a dental explorer, could make direct comparisons of the notch existing at the cavo-surface margin with that of the "V" shaped (triangular) notch in the guide block, Figure 3.

Marginal stain evaluations were made similar to those of surface staining in that each evaluator could give scores of "0" for no stain up to "10" for severe stain.

Marginal flushness scores were determined by comparing the lack of flushness with a step block, Figure 4. A score of "0" was given if the restoration was flush with the tooth and up to "10" for a lack of flushness similar to that of the 1 mm step on the guide block. If the tooth was higher than the restoration, the score was preceded by the letter "U" (up) and if lower, the letter "D" (down).

Finally, the better, same or worse evaluations were based solely on clinical judgment with no limiting criteria but were usually made on differences in margins, stain, color or flushness.

Because of a subtle difference in color between the experimental and commercial materials it was possible for the evaluators to distinguish them in some cases during the evaluation procedures. Therefore, the study was not entirely blind.

The first evaluation was made as soon as possible after the restorations were finished. Additional evaluations were made at approximately 1, 2.5 and 3.5 years.

Results and discussion

The patients available for recall at 3.5 years had 36 pairs of restorations or about 78% of the original sample. Eight pairs in two patients were lost due to crown and bridge placement and two pairs due to two patients' unavailability. This low sample mortality (the twenty patients were workers at the National Bureau of Standards) is very desirable as it reduces the need for a large initial sample.

General evaluations: Evaluations for sensitivity, secondary caries, and the need for replacement are listed in Table 2.

None of the restorations fractured, became loose or were missing.

Only three teeth exhibited any kind of sensitivity at any time during the investigation. In two cases the sensitivity had disappeared at the time of the next recall. The other instance was noted at the 3.5 year recall. Because of the insensitive nature of the evaluation method, no conclusion should be made concerning the overall clinical pulpal response to these materials. One report indicates that the pulpal response to developmental formulations of Addent®35 was more than to silicate cement with a zinc phosphate cement base but less than to cold curing plastic materials with commercially available liners; the use of the liner supplied with the material did not eliminate the response.[11]

Pulpal response to the experimental formulation used in this study has not been determined. However, acute oral toxicity of the monomer was evaluated by gastric intubation

Of 1.0, 3.16, 10.0, and 31.6 ml/kg of body weight to four pairs (each dosage to one pair) of albino rats. The 31.6 ml/kg dose was fatal to one rat. Thus, the formulation is considered relatively harmless by this route.

Acute irritation to rabbit eyes was determined by applying 0.1 ml of the monomer to one eye of each of three albino rabbits. No irritation was produced in one eye and slight irritation in two eyes. The irritation disappeared by 72 hours. Thus, the monomer was considered to be essentially non-irritating to rabbit eyes.

There were 11 evaluations noting caries associated with four different patients and eight different restorations. Five of the restorations were of Addent® 35 and three were of the experimental formulation. There was only one instance where all three evaluators noted caries involved with the same restoration. In the remainder of cases only one evaluator noted caries at any specified time. The differences among evaluators with respect to caries incidence probably occurred because the caries involvement was in a very incipient stage and was difficult to distinguish from marginal breakdown and stain.

Of the 72 restorations available for examination at 3.5 years, two (one of each material) were in need of replacement because of secondary caries.

Color and surface evaluations: The results of the color, surface texture and surface stain evaluations, given in Table 3, are the average given by each investigator for the specified material and time.

Color - All three evaluators noted a shift toward darker colors with the passage of time but not all to the same degree. Evaluator 1 noted less change than evaluators 2 or 3. The most change occurred during the first year, with less change per year noted at subsequent recalls. The darkening of Addent®35 was significantly greater than was the discoloration of the experimental material ($p<0.02$).[12]

Both materials were subjected to the color stability test as outlined in American Dental Association Specification No. 12 for Denture Base Polymers.[13] There was a slight discoloration of Addent®35 but no perceptible darkening of the experimental material from exposure to the sun

lamp. Thus, there is correlation to the extent that the material that darkened more under the sun lamp also darkened more in clinical use.

The experimental material discolored somewhat clinically but not under the sun lamp. This may or may not be related to color formation that appears to occur upon combining the phthalate monomers and the amine accelerators; this slight coloration is suspected of being related to charge transfer complex formation and is currently being investigated.

Surface texture - The data in Table 3 indicate that evaluators 1 and 2 perceived little difference in the change in surface roughness of the experimental and commercial materials with the passage of time. Evaluator 3 detected considerable change toward roughening.

If a direct comparison is made of the surface texture evaluations between the two materials for each evaluator and for each time interval, it may be seen that the experimental formulation was rated smoother than Addent®35 in 10 out of 12 instances. This would not occur unless

there was a significant difference in smoothness ($p < 0.02$).[12] The clinical significance of this smoothness is not known but did not result in appreciably less surface stain (Table 3). However, smoothness in all dental restorations is desirable.

Surface staining - During this study there was no apparent trend in the average evaluations of surface staining (Table 3). In many instances there was more stain detected earlier in the investigation than at later recalls and all evaluators reported similar amounts. There were 22 evaluations greater than "0" on the test material and 26 on Addent®35. Each evaluator reported staining on seven patients, five of whom were smokers.

In some patients it was difficult to differentiate surface staining and discoloration of the material itself. Several patients (most of whom were smokers) presented no stain on the labial surface but did have stain on the lingual surface. Evidently, the presumed better brushing that occurred on labial surfaces was effective in removing the stain.

Also, more stain is deposited on lingual surfaces of smokers than on labial surfaces.

Marginal evaluations: Table 4 lists results of evaluations for marginal notching, staining and flushness. Evaluations on incisal and gingival margins of Class III restorations were not used because their accuracy was in doubt due to poor visibility beneath the gingival margin and because the exact area to be evaluated on the incisal was difficult to determine. Notch values for evaluator 3 were not used because of a marked change in his procedure midway in the investigation. This was due to the development and his use of the marginal notch evaluation guide (Fig. 3) in a separate, concurrent clinical study of other materials.

Marginal notch: There was no significant difference between the two materials with respect to the degree of marginal notching at any given time. Neither was there a noticeable trend of increased notching with time. In other words, there was as much notch at the beginning or 0 year examination as there was at 3.5 years. Margins exhibiting some degree of notching averaged about 9% of the total

sample. The materials were about equal in this respect on the labial margin but on the lingual margins there were three times as many Addent®35 restorations exhibiting notch as compared to the experimental formulation.

Marginal Stain - All evaluators noted an increase in marginal staining with time. The amount of change was somewhat greater with Addent®35 than with the experimental formulation ($p<0.05$).[12] At 3.5 years, some degree of marginal stain was noted in 45 out of 175 restorations of the test formulation compared to 74 of 175 of Addent®35. Statistical examination reveals this difference to be significant ($p<0.01$).[14]

Several instances of marginal stain were noted at the first evaluation. This can probably be attributed to retained stained enamel since there was not yet time for the deposition of stained material at the interface. There was considerable difference among the investigators as to the incidence and degree of staining. This may be in part due to the arbitrary nature of this evaluation and the lack of a guide to which constant referral could be made by all three evaluators.

Marginal flushness - Flushness evaluations indicated there was little difference between materials and little change with time. In most cases the tooth margin was slightly higher than the restoration even at the initial examination indicating that the restorations were over-finished.

■ Better, same and worse evaluation: Table 5 lists the percentage of experimental and Addent®35 restorations that were rated better than their matching restorations at each time period and by each evaluator. Evaluator 1 rated about equal percentages of both materials better at 0 and 3.5 years. Evaluator 2 rated equal numbers better at 0 years but between two and three times as many of the test formulation better after 3.5 years. Evaluator 3 rated more Addent®35 restorations better at 0 years but at 3.5 years rated twice as many of the test material restorations as better.

All three evaluators recorded a decrease in the percentage of restorations rated the same with the passage of time. Evaluator 1 rated 85% the same at 0 years, evaluator 2, 82% and evaluator 3, 57%. These percentages had

changed to 53, 31 and 25, respectively after 3.5 years.

Pooled results of all investigators at 3.5 years showed that there were 45 notations rating the experimental restorations "better" as compared to 24 for the Addent®35. This difference is significant at a 99% confidence level.[14]

Summary and conclusions

Forty-six pairs of Class III and V composite restorations were placed in adult patients. One of each pair was restored with an experimental composite material consisting of a resin binder of a ternary eutectic dimethacrylate and a reinforcing filler of two parts fused silica and one part radiopaque BaF_2-containing glass. The other of each pair was restored with Addent® 35 a commercially available material at the time of placement (1968-69).

The cavity preparations for the experimental material were treated with N-(2-hydroxy-3-methacryloxypropyl)-N-phenylglycine an adhesion promoting coupling agent. The preparations for Addent®35 were treated with the liner supplied by the manufacturer.

The restorations were evaluated by three dentists at 0, 1, 2.5 and 3.5 years on the basis of sensitivity, gross fracture, restoration loose or missing, secondary caries, need for replacement, color, surface texture, surface stain,

marginal notch, marginal stain, marginal flushness and whether it was better, the same or worse than its mate in the pair.

Evaluations for color, texture and flushness were made with the aid of newly developed evaluation guides.

Results of the evaluations indicated there was essentially no difference in the two materials with respect to general sensitivity, sensitivity to percussion, gross fracture, loose or missing restorations, secondary caries, need for replacement, surface staining and marginal flushness.

There was a slight difference in the restorations in favor of the experimental material with respect to color change, surface texture, marginal notch and marginal stain.

A significantly greater number of the restorations made of the experimental material were rated as being better compared to those of Addent®35.

Restorations made from the material were still clinically sound in a high percentage of cases after 3.5 years and compared favorably with a commercial material. However, further improvements in color stability are needed.

Table 1 ■ Composition of the experimental materials

Weight %	Ingredient	Source
	Liquid Monomer Formulation	
45.70	HEMA isophthalate[4]	Lee Pharmaceuticals
36.90	HEMA phthalate[4]	Lee Pharmaceuticals
14.54	HEMA terephthalate[4]	Lee Pharmaceuticals
2.19	Permasorb®MA	National Starch & Chemical Co.
0.32	N,N-dimethyl-sym-m-xylidine (DMSX)[5]	3M Co.
0.20	2,6-di-tert-butyl-4-methylphenol (BHT)	Eastman Kodak
0.1555	Di-tert-butyl-sulfide (DTBS)	K & K Laboratories, Inc.
	Reinforcing Filler Formulation	
65.79	Fused silica	Corning Glass Works
32.89	BaF_2-containing glass[6]	Corning Glass Works
0.82	Lauroyl peroxide	Pennwalt Corp.
0.50	Benzoyl peroxide	Pennwalt Corp.
	Coupling Agent Formulation	
84.56	Acetone	Allied Chemical
6.43	N-(2-hydroxy-3-methacryloxypropyl)-N-phenylglycine, (NPG-GMA)*	Lee Pharmaceuticals
4.13	HEMA isophthalate	Lee Pharmaceuticals
3.34	HEMA phthalate	Lee Pharmaceuticals
1.32	HEMA terephthalate	Lee Pharmaceuticals
0.19	Permasorb®MA	National Starch & Chemical Co.
0.01-0.02	2,6-di-tert-butyl-4-methylphenol (BHT)	Eastman Kodak
0.01	Di-tert-butyl-sulfide (DTBS)	K & K Laboratories, Inc.

* Recrystallized from acetone

Table 2 ■ General evaluations

Material	Evaluator	Sensitivity to Percussion				General Sensitivity				Secondary Caries				Restorations needing Replacement			
		Years															
		0	1.0	2.5	3.5	0	1.0	2.5	3.5	0	1.0	2.5	3.5	0	1.0	2.5	3.5
Experimental	1	0*	0	0	0	0	0	0	0	0	0	0	2	0	1	1	1
	2	0	0	0	0	0	0	0	0	0	1	0	0	0	0	0	0
	3	0	0	0	0	0	0	0	0	0	0	2	1	0	0	0	0
Addent®35	1	0	0	0	0	0	0	0	0	0	0	0	0	0	0	1	1
	2	0	0	0	0	1	0	0	1	0	1	0	0	0	1	0	0
	3	1	0	0	0	0	0	0	0	0	1	3	0	0	0	1	1

* Each entry represents the number of teeth or restorations exhibiting the property indicated.

Table 3 ■ Color and surface evaluations

Material	Evaluator	Restoration Color				Surface Texture				Surface Stain			
		years											
		0	1.0	2.5	3.5	0	1.0	2.5	3.5	0	1.0	2.5	3.5
Experimental	1	1.7* (1.1)†	2.7 (1.7)	2.8 (1.9)	3.0 (1.9)	2.11 (0.38)	2.03 (0.49)	2.70 (0.96)	2.36 (0.72)	0.11 (0.74)	0.3 (1.6)	0.12 (0.76)	0.3 (1.7)
	2	2.16 (0.74)	3.8 (1.3)	4.3 (1.2)	4.8 (1.2)	2.58 (0.56)	2.85 (0.23)	2.78 (0.33)	3.01 (0.35)	0.0 (0.0)	0.3 (1.2)	0.11 (0.62)	0.4 (1.8)
	3	2.9 (1.1)	4.2 (1.2)	5.3 (1.3)	5.5 (1.3)	2.78 (0.81)	3.13 (0.52)	4.28 (0.63)	4.55 (0.97)	0.0 (0.0)	0.3 (1.3)	0.4 (1.2)	0.14 (0.83)
Addent®35	1	1.5 (1.1)	2.3 (2.0)	2.7 (2.3)	3.0 (2.3)	2.15 (0.56)	2.08 (0.42)	2.86 (0.99)	2.47 (0.94)	0.0 (0.0)	0.5 (2.0)	0.3 (1.2)	0.3 (1.3)
	2	1.66 (0.76)	3.5 (1.4)	4.2 (1.4)	4.8 (1.7)	3.24 (0.52)	2.97 (0.40)	2.96 (0.26)	2.94 (0.23)	0.0 (0.0)	0.3 (1.3)	0.14 (0.63)	0.06 (0.23)
	3	2.2 (1.0)	4.3 (1.7)	5.9 (1.2)	6.0 (1.7)	2.78 (0.79)	3.67 (0.77)	4.86 (0.68)	5.53 (0.91)	0.0 (0.0)	0.3 (1.3)	0.4 (1.3)	0.17 (0.85)

* Each entry represents the average score given by each investigator for the indicated time and property. Higher numbers indicate darker color, rougher surfaces or more severe staining.

The number of evaluations in each cell is 46 at 0 years, 39 at 1.0 years, 43 at 2.5 years, and 36 at 3.5 years.

† Standard deviation.

Table 4 ■ Margin evaluations

Property	Material	Evaluator	Labial (incisal on Class V's)				Lingual (distal on Class V's)			
			years				years			
			0	1	1.5	3.5	0	1	1.5	3.5
Notching	Experimental	1	0.5* (1.9) †	0.4 (1.7)	0.15 (0.67)	0.22 (0.63)	0.00 (0.00)	0.04 (0.19)	0.00 (0.00)	0.06 (0.22)
		2	0.4 (1.8)	0.6 (1.8)	0.6 (1.9)	0.2 (1.1)	0.06 (0.24)	0.07 (0.38)	0.06 (0.25)	0.00 (0.00)
	Addent®35	1	0.3 (1.0)	0.26 (1.36)	0.18 (0.81)	0.14 (0.71)	0.25 (0.84)	0.00 (0.00)	0.10 (0.24)	0.14 (0.45)
		2	0.3 (1.6)	0.4 (1.5)	0.3 (1.0)	0.35 (0.99)	0.18 (0.53)	0.07 (0.27)	0.17 (0.49)	0.20 (0.65)
Staining	Experimental	1	0.00 (0.00)	0.06 (0.34)	0.15 (0.80)	0.12 (0.55)	0.00 (0.00)	0.11 (0.42)	0.26 (0.73)	0.4 (1.6)
		2	0.01 (0.08)	0.32 (0.73)	0.28 (0.55)	0.47 (0.66)	0.03 (0.17)	0.8 (1.9)	0.19 (0.52)	0.32 (0.56)
		3	0.12 (0.32)	0.44 (0.96)	0.38 (0.67)	0.41 (0.78)	0.31 (0.74)	0.9 (1.4)	0.40 (0.67)	0.8 (1.3)
	Addent®35	1	0.00 (0.00)	0.00 (0.00)	0.31 (0.86)	0.6 (1.4)	0.00 (0.00)	0.00 (0.00)	0.37 (0.96)	1.0 (2.4)
		2	0.15 (0.53)	0.7 (1.3)	1.0 (1.2)	1.5 (2.0)	0.06 (0.24)	0.6 (1.6)	0.42 (0.71)	0.22 (0.50)
		3	0.28 (0.73)	0.9 (1.5)	0.8 (1.0)	1.1 (1.3)	0.37 (0.71)	0.7 (2.0)	0.7 (1.0)	1.2 (1.4)
Flushness	Experimental	1	-0.03 (0.11)	0.00 (0.36)	0.09 (0.25)	-0.02 (0.23)	-0.06 (0.39)	-0.02 (0.49)	0.00 (0.23)	-0.18 (0.32)
		2	0.11 (0.33)	0.06 (0.26)	0.12 (0.29)	0.17 (0.35)	0.09 (0.52)	0.13 (0.55)	0.23 (0.34)	0.28 (0.52)
		3	0.05 (0.28)	0.10 (0.33)	0.03 (0.13)	0.05 (0.18)	0.12 (0.31)	0.22 (0.38)	0.13 (0.16)	0.14 (0.24)
	Addent®35	1	-0.012 (0.077)	-0.03 (0.17)	0.06 (0.23)	-0.14 (0.71)	0.03 (0.12)	-0.04 (0.19)	0.08 (0.52)	-0.18 (0.32)
		2	0.12 (0.77)	0.03 (0.12)	0.06 (0.17)	0.21 (0.31)	0.20 (0.30)	0.19 (0.37)	0.33 (0.37)	0.50 (0.64)
		3	-0.04 (0.20)	0.06 (0.29)	0.01 (0.17)	0.08 (0.16)	0.16 (0.30)	0.27 (0.49)	0.15 (0.19)	0.19 (0.17)

Footnotes to Table 4:

* Each entry represents the average score given by each investigator for the indicated time and property. Higher numbers indicate greater notching, staining and lack of flushness. For flushness, negative numbers indicate that the restorations were higher than the tooth and positive numbers indicate the restorations were lower than the tooth.

The number of evaluations ranges from 43 ± 3 at 0 years to 33 ± 1 at 3.5 years for the labial margin and 32.5 ± 0.5 at 0 years to 25 at 3.5 years for the lingual margin.

† Standard deviation.

Table 5 ■ Better, same or worse evaluation

Evaluator	Material	Time (years)			
		0	1.0	2.5	3.5
		%*	%	%	%
1	Experimental	9	8	14	25
	Addent®35	6	15	23	22
2	Experimental	9	10	30	50
	Addent®35	9	26	32	19
3	Experimental	13	36	46	50
	Addent®35	30	28	21	25

* Each entry represents the percentage of restorations rated better than their matching restoration for the indicated material and time. The balance were rated the same.

Bibliography

1. Chandler, H. H.; Bowen, R. L., Paffenbarger, G. C., and Mullineaux, A. L. Clinical investigation of a radiopaque composite restorative material. JADA 81:935 Oct 1970.

2. Chandler, H. H.; Bowen, R. L., and Paffenbarger, G. C. The need for radiopaque denture base materials: A review of the literature. J Biomed Materials Res 5:245 July 1971.

3. Barton, J. A., Jr.; Burns, C. L.; Chandler, H. H., and Bowen, R. L. An experimental radiopaque composite material: An in vitro study. [Manuscript submitted to J Dent Res for publication]

4. Bowen, R. L. Crystalline dimethacrylate monomers. J dent Res 49:810 July-Aug 1970.

5. Bowen, R. L., and Argentar, H. Diminishing discoloration in methacrylate accelerator systems. JADA 75:918 Oct 1967.

6. Bowen, R. L., and Cleek, G. W. X-ray-opaque reinforcing fillers for composite materials. J dent Res 48:79 Jan-Feb 1969.

7. Bowen, R. L. Properties of a silica-reinforced polymer for dental restorations. JADA 66:57 Jan 1963.

8. Bowen, R. L. Dental filling material comprising vinyl silane treated fused silica and a binder consisting of the reaction product of bisphenol and glycidyl acrylate. U. S. Patent 3,066,112 Nov 1962.

9. Chandler, H. H.; Bowen, R. L.; Paffenbarger, G. C., and Mullineaux, A. L. Clinical evaluation of a tooth-restoration coupling agent. [Manuscript submitted to JADA for publication.]

10. Advertising brochure - 3M Co.

11. Langeland, Leena K.; Guttuso, James; Jerome, David R., and Langeland, Kaare. Histological and clinical comparison of Addent with silicate cements and cold-curing materials. JADA 72:373 Feb 1966.

12. Siegel, S. Nonparametric statistics for the behavioral sciences. New York, McGraw-Hill Book Co., Inc., 1956, pp 36-42, 250.

13. Guide to dental materials and devices, 1972-1973, ed 6. American Dental Association Specification No. 12 for Denture Base Polymer. Chicago, American Dental Association, 1972, p 201.

14. Hoel, P. G. Introduction to mathematical statistics. New York, John Wiley & Sons, Inc., 1962, pp 148-151.

15. Hoel, P. G. Introduction to mathematical statistics. New York, John Wiley & Sons, Inc., 1962, pp 104-105.

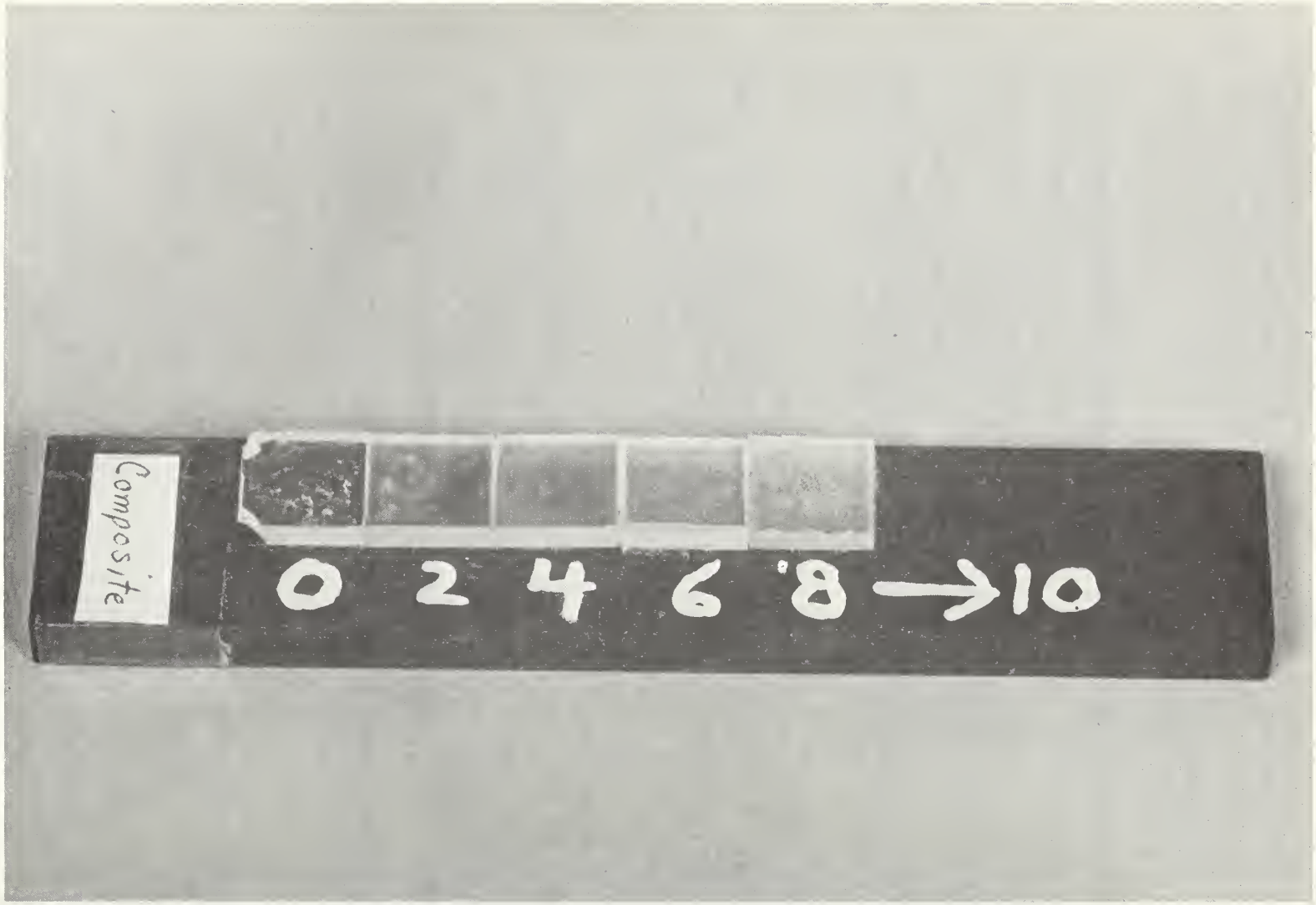

Fig. 1 - Surface texture evaluation guide composed of glass blocks of increasing roughness (see text). The evaluator (using a dental explorer) matches the roughness of the restoration with that of one of the blocks.

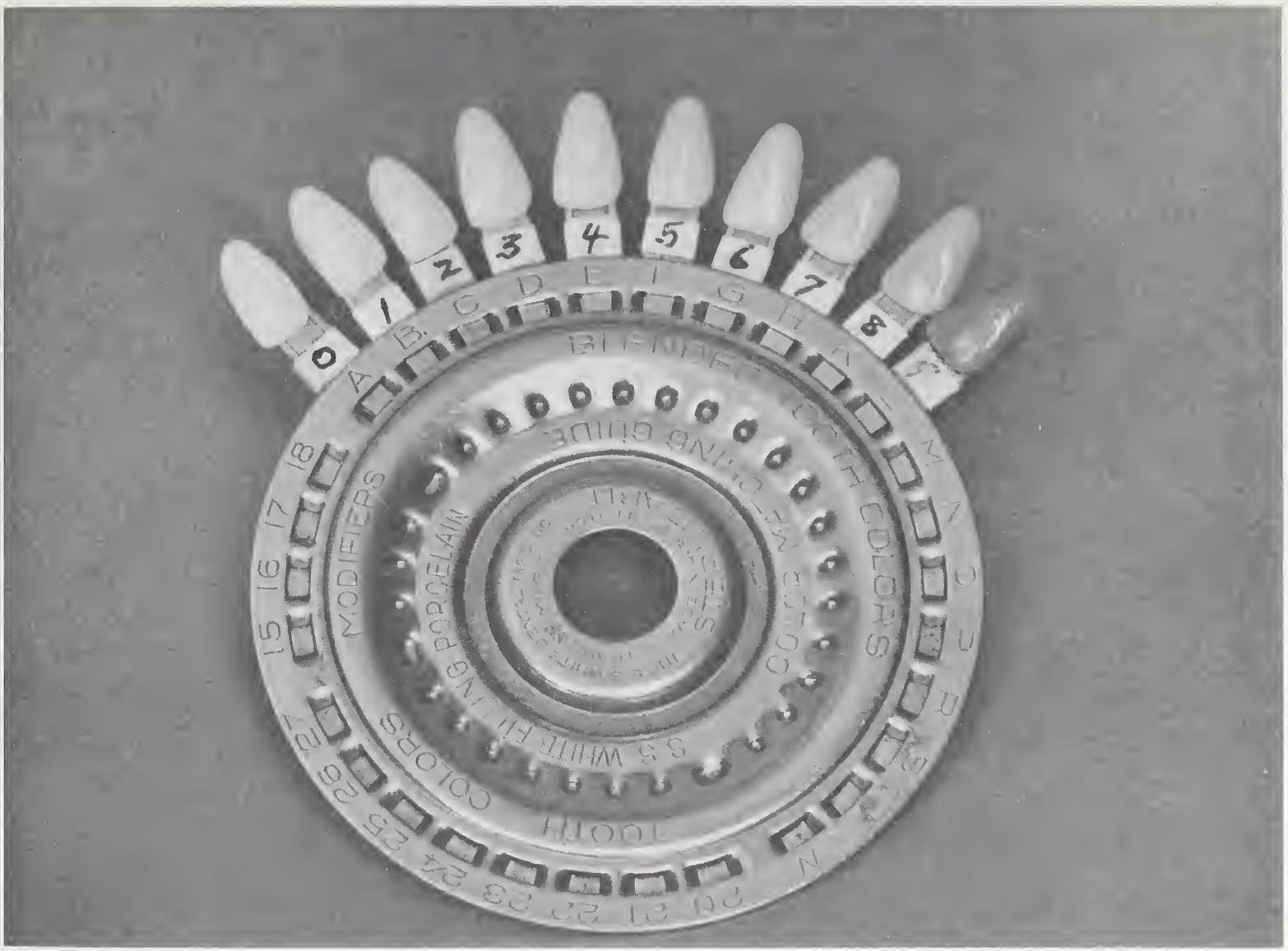

Fig. 2 - Color evaluation guide. The evaluator compares the color of the restoration with the porcelain tooth crowns on the guide.

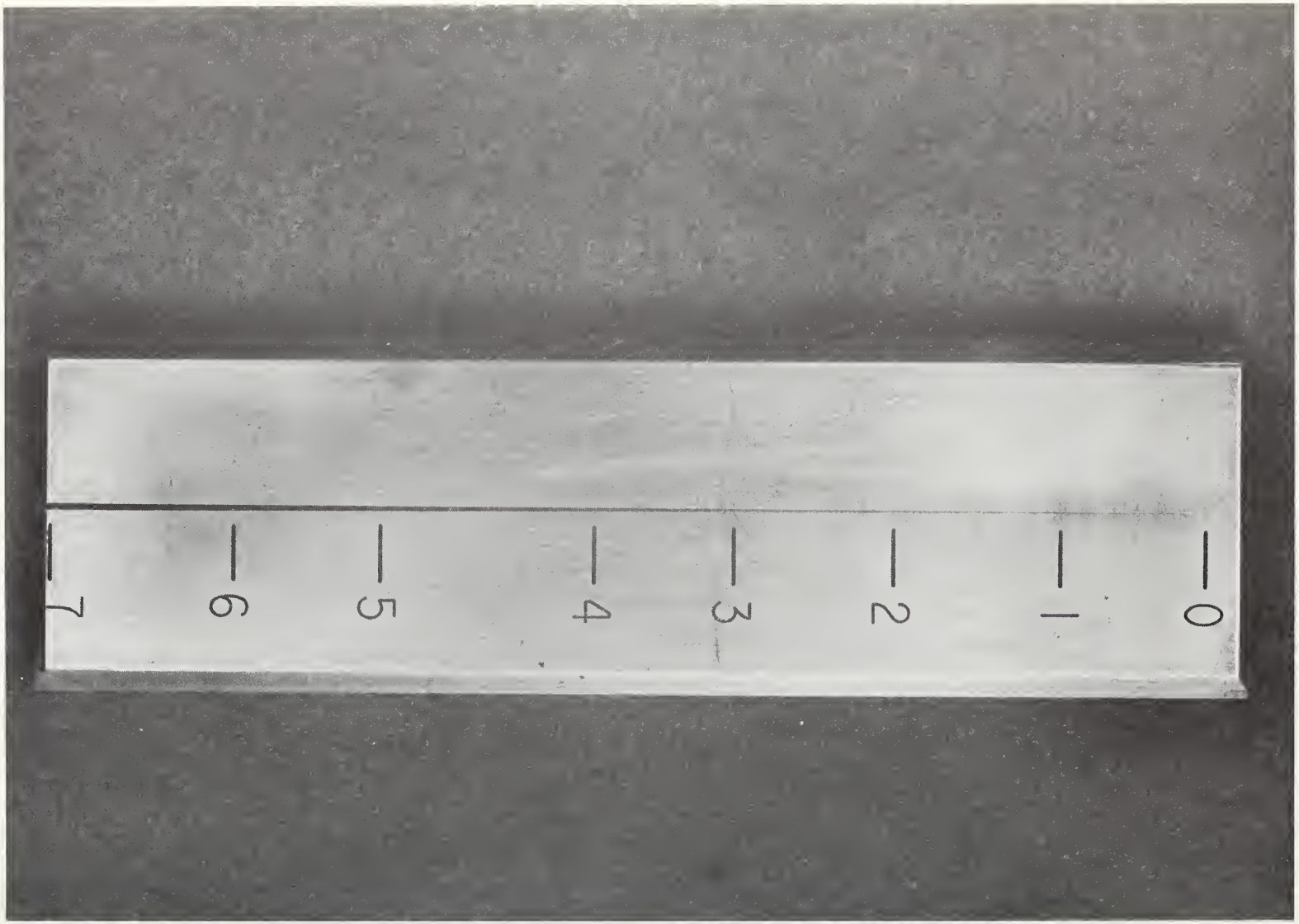

Fig. 3 - Marginal notch evaluation guide. The stainless steel block contains a triangular groove (the sides forming a 60° angle) from 0.0 to 0.7 mm in width. The evaluator compares the marginal notch of the restoration with the notch on the guide using a dental explorer.

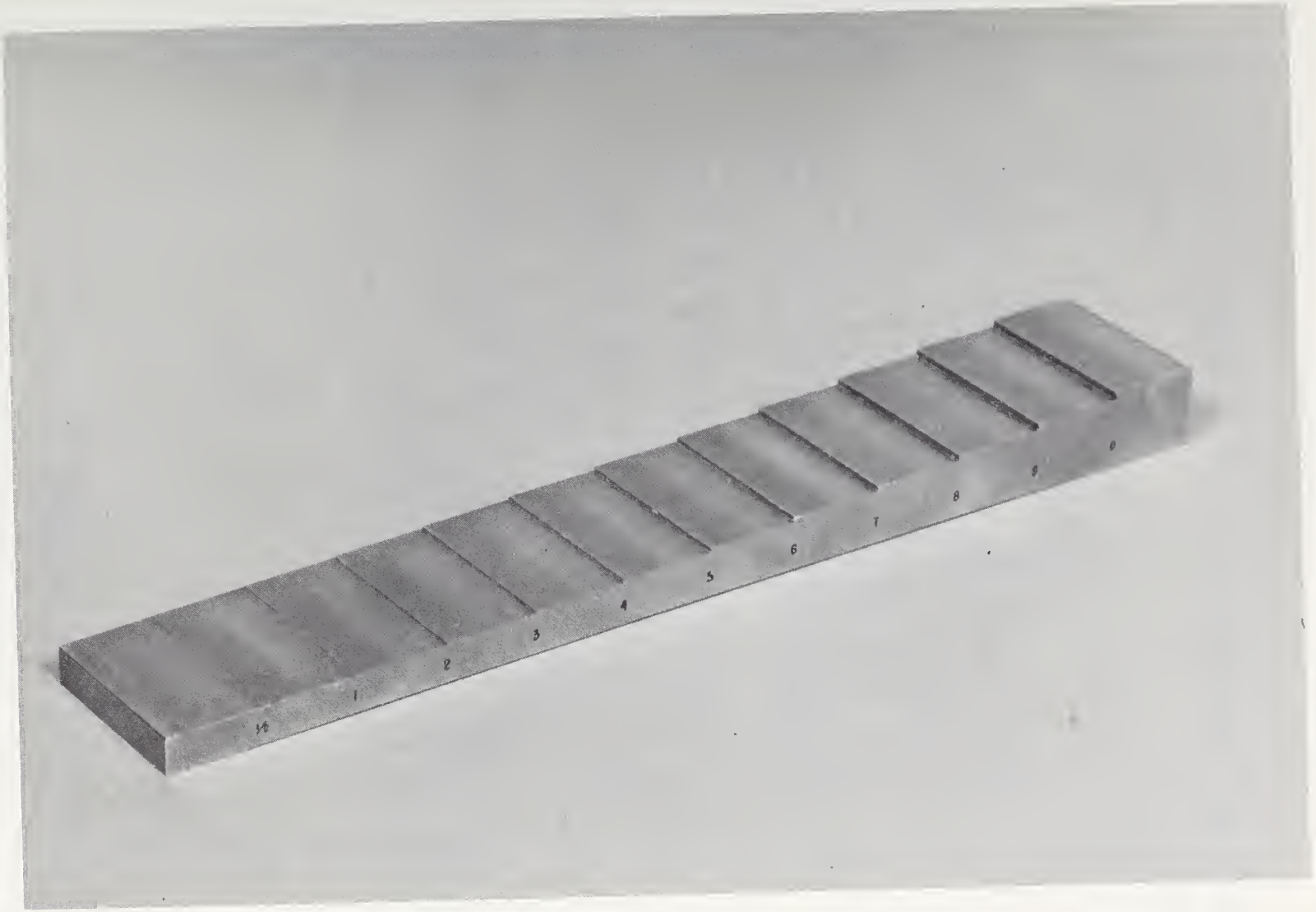

Fig. 4 - Marginal flushness evaluation guide. The stainless steel block contains a series of steps of increasing height. The first step is ~0.05 mm, the next ~0.1 mm and each succeeding step is ~0.1 mm higher than the one preceeding. The evaluator matches the lack of marginal flushness with one of the steps on the block using a dental explorer.

NATIONAL BUREAU OF STANDARDS REPORT

NBS PROJECT
311.05-3110561

December 29, 1972

NBS REPORT
10 980

Progress Report

on

CLINICAL EVALUATION OF A TOOTH-RESTORATION COUPLING AGENT

Chandler, H. H.*, DDS; Bowen, R. L.**, DDS;

Paffenbarger, G. C.***, DDS; and Mullineaux, A. L.****

* Research Associate American Dental Association Research Unit at the National Bureau of Standards, Washington, D. C. 20234 on leave of absence from the Ohio State University College of Dentistry, Columbus, Ohio 43210.

** Associate Director American Dental Association Research Unit at the National Bureau of Standards, Washington, D. C. 20234.

*** Senior Research Associate American Dental Association Research Unit at the National Bureau of Standards, Washington, D. C. 20234.

**** Research Associate American Dental Association Research Unit at the National Bureau of Standards, Washington, D. C. 20234.

This investigation was supported in part by Research Grants DE02742-01 thru -05 and DE02494-02 thru -06 to the American Dental Association from the National Institute of Dental Research and is part of the dental research program conducted by the National Bureau of Standards in cooperation with the American Dental Association; the Dental Research Division of the United States Army Medical Research and Development Command; the Dental Sciences Division of the School of Aerospace Medicine, USAF; the National Institute of Dental Research; and the Veterans Administration.

NBS

U.S. DEPARTMENT OF COMMERCE

NATIONAL BUREAU OF STANDARDS

Clinical evaluation of a tooth-restoration coupling agent

SYNOPSIS

The clinical effectiveness of a tooth-restoration coupling agent (NPG-GMA) was tested by treating 54 Class III and V cavity preparations with an acetone solution of this surface-active comonomer. Fifty-four additional preparations were treated with acetone alone for comparison. The teeth were restored with an experimental composite material.

The restorations were observed by three dentists for 3.5 years. The evaluations indicated that the restorations placed over the NPG-GMA coupling agent had significantly better margins, and a significantly higher number of the NPG-GMA associated restorations were rated better as compared to those placed over the acetone control.

One of the most important advancements in restorative dentistry would be the development of methods and materials that could be used to restore teeth in such a way that there would be no leakage around the restoration. Prevention of leakage could be achieved if the filling material bonded directly to the tooth structure or if there was an intermediary substance that would bond to both the tooth and the filling material. Such bonding must be sufficiently strong to overcome the stresses that occur at the tooth-restoration interface.

Marginal leakage has been demonstrated *in vitro* by penetration of the tooth-restoration interface with radio-isotopes, dyes and air, by artificial caries development and by percolation brought about by thermal cycling in water.[1] *In vivo*, marginal leakage may be at least partially responsible for pulp pathology, a loss of marginal integrity, corrosion of metallic restorations, tooth staining and secondary caries.[2]

The purpose of this investigation was to evaluate clinically the effectiveness of a tooth-restoration coupling agent used in combination with an experimental, composite resin filling material.

Materials*

The composite restorative material was a crosslinked methacrylate polymer as the resin binder and a combination of a radiopaque, BaF_2-containing glass and spheroidized fused silica as the inorganic reinforcing filler. A more complete description of the powder and liquid formulations used to form the composite is reported elsewhere.[3]

The experimental coupling agent was [N-(2-hydroxy-3-methacryloxypropyl)-N-phenylglycine] (NPG-GMA)† recrystallized from acetone; this has been referred to as a "surface-active comonomer."[4] It was applied as a 5.0% solution using acetone as the volatile carrier. The solution also contained 0.14% hydroquinone monomethylether‡ and 0.12% di-t-butyl sulfide§ as stabilizers.

---

* Certain commercial materials and equipment are identified in this paper to specify the experimental procedure. In no instance does such identification imply recommendation or endorsement by the National Bureau of Standards or that the material or equipment identified is necessarily the best available for the purpose.

† Lee Pharmaceuticals, South El Monte, Calif.; (custom synthesis).

‡ Eastman Kodak Co., New York, N. Y.

§ K & K Laboratories, Inc., Plainview, N. J.

Methods

Fifty-four matched pairs of restorations were placed by one operator in 26 adult patients. Methods for selecting the patients and pairs and the clinical procedures were reported.[3,5]

After cleaning the preparations with a stream of tap water, they were dried with compressed air. At random, one of each pair was treated with the NPG-GMA solution carried to the cavity preparation on a cotton pledget. The other was treated in an identical manner except that acetone alone was used for comparison and control. Neither the operator nor the other two evaluators knew which preparations received the NPG-GMA solution.

With methods described elsewhere,[3] the restorations were evaluated by three dentists on the basis of general sensitivity, secondary caries, marginal notch and marginal stain. In addition, each evaluator, using any criteria he thought appropriate, determined if one of the restorations in each pair was better than the other or if they were the same in their overall condition. The evaluations

were carried out as soon as possible after the restorations had been finished (at least 24 hours after insertion) and at about 1, 2.5 and 3.5 years.

Results and discussion

Of the original 26 patients, 23 were available for recall at 3.5 years. This resulted in the loss of seven pairs of restorations or about 13% of the original sample.

Sensitivity: The sensitivity and caries evaluations are listed in Table 1.

There was no significant difference in the sensitivity produced in the teeth that received the NPG-GMA coupling agent and those that received the acetone control. The sensitivity was usually in response to cold but sometimes to heat or sweetness.

There were several instances where the tooth exhibiting sensitivity contained two restorations, one of which had been placed over the NPG-GMA solution and the other over the acetone control. Therefore, it is not known which material, if either, might have been the cause. With one exception, the sensitivity noted at the original examination had disappeared at the first yearly recall.

The cause of the apparently high incidence of sensitivity is not known, but over half (24) of the evaluations noting sensitivity occurred on one patient who had numerous Class V restorations and who reported that his anterior teeth were chronically sensitive to cold.

It is doubtful that an effective tooth-restoration coupling agent would appreciably reduce the type of post-operative sensitivity noted in this investigation. Such sensitivity commonly occurs and is generally attributed to trauma from cavity preparation or initial pulpal response to the materials used. It is more likely that a tooth-restoration coupling agent would help to prevent pulpal response that occurs after a period of time due to long-term leakage. This type of response was not noted in this investigation either with teeth that had received the NPG-GMA or the acetone control.

Caries: There were 12 notations of secondary caries, 9 of which occurred in association with the coupling agent and 3 with the acetone control (Table 1). Ten of these notations were

associated with one patient who exhibited a high degree of marginal notch and marginal stain that was difficult to distinguish from caries. This may account for the poor agreement among the evaluators with respect to caries incidence. For example, one investigator noted no caries at any time, while another noted eight instances of caries at 2.5 years but none at 3.5 years with the same restorations in the same two patients. This indicates that the criteria for defining secondary caries need improvement.

Marginal notch: Marginal notch and stain evaluations given in Table 2 show the average value of each evaluator for each material and at each time. Evaluations are listed for the labial and lingual margins of the Class III restorations and incisal and distal of the Class V's. The notch values of evaluator 3 were not used because of a marked change in his procedure midway in the investigation; this was due to the development and his use of a marginal notch evaluation guide[3] in a separate, concurrent, clinical study of other materials.

There was no apparent time trend with the degree of marginal notching. If one compares the average

notch evaluation for the NPG-GMA and acetone treatment for each evaluator, surface and time, the average notching for those restorations placed over the control treatment is greater than that of the NPG-GMA treatment in 11 out of 16 instances. This difference is significant only at about a 90% confidence level.[6]

There were 57 evaluations noting some degree of marginal notch with those restorations associated with the NPG-GMA solution and 97 with those restorations receiving the acetone control. There were a total of 612 evaluations in each group. To determine if these proportions were significantly different, a normal approximation to the binomial distribution was made.[7] Results indicated that there was a significantly lower incidence of marginal notching with those restorations placed in the NPG-GMA treated teeth (at a level of confidence greater than 99%).

Marginal stain: All evaluators noted a general increase in marginal staining with the passage of time. More stain developed at the lingual than at the labial margins (Table 2).

If a direct comparison is made of the amount of increased staining between 0 and 3.5 years for the NPG-GMA test and acetone control treatments of the labial and lingual margins recorded by each evaluator, there was less change associated with the NPG-GMA treatment in 5 out of 6 instances (Table 2). This would probably occur less than 11 times out of 100 if there were no real difference.[6]

There were 212 evaluations noting marginal stain on the teeth that received the NPG-GMA solution and 237 in teeth that received the acetone control out of a total of 914 evaluations in each group. Statistical evaluation of these results indicated the difference was significant only at about an 80% confidence level.[7]

Better, same, worse: Table 3 lists the percentages of restorations pretreated with the NPG-GMA and acetone solutions that were rated better than their matching restorations for each time period and by each evaluator.

All evaluators rated a higher percentage of the restorations placed over the NPG-GMA solution as better than those placed over the acetone control at all

time periods with one exception (evaluator 1 at 2.5 years). This would indicate a significant difference in the materials at a greater than 99% confidence level.[6]

Although the restorations and teeth were evaluated separately for sensitivity, secondary caries, and marginal notch and stain, there were additional criteria used for the better, same or worse evaluation. In fact no limitation was placed on the criteria that could be used in this rating. Therefore, many of the "better" evaluations were based on such properties as surface stain, color, contour, roughness or the presence of voids. Presumably, such properties could not be influenced by the presence or absence of the NPG-GMA coupling agent. Therefore, the reasons for the "better" evaluations at 3.5 years were compiled to determine if the differences between test and control restorations were caused by differences in marginal integrity or by other factors. Of 132 evaluations where reasons were noted, the restorations associated with the NPG-GMA were rated "better" 60 times. Of the 60, 45 were based on differences in margins and 15 on other factors. Thirty-four pairs were rated "same."

The restorations associated with the control treatment were rated "better" 38 times. Of the 38, 24 were on the basis of margins and 14 on other factors. Therefore, the differences in the better, same or worse evaluations were caused predominantly by differences in marginal integrity and were significant at a 99% confidence level.[8]

Significant improvements were reported in bonding resin-based materials to enamel and dentin with NPG-GMA in laboratory tests.[4] However, the efficacy of improved adhesive bonding by this means under clinical conditions had not been studied previously. Certain differences in test conditions are apparent: 1) the laboratory tests were done on flat tooth surfaces under conditions that minimized tensile stresses induced by polymerization shrinkage. During hardening of the restorative material in clinical preparations, significant tensile stresses should develop.[4] 2) In the laboratory tests, the temperature was approximately constant, whereas under oral conditions it fluctuates widely.[9] 3) In the adhesion tests, the stress to break the bond was applied only once; in the mouth repeated

mechanical or thermal[10] stressing may result in fatigue of the tooth-restoration bond.

In view of these and other challenging conditions of the oral environment, it is worthy of note that significant even though modest improvement was demonstrable clinically with the use of the NPG-GMA coupling agent.

Observations on replacement of restorations: During this and a similar investigation, the operator (H.H.C.) replaced over 125 defective silicate restorations, and a number of unreinforced direct resin fillings. After the outer surfaces of the silicates had been removed, there was seldom any clinical evidence of leakage. If the restoration was not loose, it appeared to be in very close approximation to the cavity wall, and there was no odor of decay. It was usually necessary to remove the last vestiges of the filling material with a bur or by prying it loose with a spoon excavator. This last material was not stained and the underlying tooth appeared dry and hard.

When the unreinforced direct resin fillings were removed, it was not uncommon to observe clinically detectable moisture beneath the restorations and occasionally an odor of decay and a softening of the dentinal wall.

Although there is some shrinkage during hardening,[11] the thermal expansion[12] and stiffness[13] of silicate cement nearly match those of the tooth; this may account for the preceding observations and the low incidence of secondary decay associated with this material.

In the authors' opinions bond strength and permanence would be markedly improved if shrinkage on hardening of the restoration could be eliminated and if its coefficient of thermal expansion and stiffness properties could be made to match those of the dentin or enamel.

Summary and conclusions

Fifty-four pairs of Class III and V restorations were placed in adult patients using an experimental radiopaque composite filling material. One of each pair of the cavity preparations was treated with an experimental tooth-restoration coupling agent consisting of a 5.0% solution of [N-(2-hydroxy-3-methacryloxypropyl)-N-phenylglycine] (NPG-GMA) in acetone. The other of each pair was treated with acetone alone as a control.

The restorations were evaluated by three dentists at 0, 1, 2.5 and 3.5 years on the basis of general sensitivity, secondary caries, marginal notch and stain and whether one of each pair was better, the same or worse in its overall condition than its mate.

Results indicated little difference in the pretreatments with respect to general sensitivity. Lack of reproducibility or agreement among the three evaluators in assessing the presence of secondary caries shows the need for better clinical criteria for such determinations.

There was a significant difference in the incidence of marginal notching in favor of the NPG-GMA pretreatment, however there was not a significant trend of increased notching with time with either the pretreated or control restorations.

The increase in marginal staining with those restorations placed over the NPG-GMA pretreatment ranked less than the controls.

All evaluators indicated a significantly higher number of those restorations placed over the NPG-GMA solution were better as compared to those placed over the control liquid. In addition, each evaluator rated a higher percentage of the

NPG-GMA associated restorations as being better at all four time intervals, with one exception, at which they were rated equal.

The results clinically demonstrate the effectiveness of an adhesion promoting tooth-restoration coupling agent through improved margins of composite restorations.

Table 1 ■ Sensitivity and caries evaluation

Property	Treatment	Evaluator	Years			
			0	1	2.5	3.5
Sensitivity	NPG-GMA	1	6*	1	0	0
		2	7	1	0	0
		3	8	1	0	0
	Acetone	1	9	0	0	0
		2	6	0	0	0
		3	6	0	0	0
Caries	NPG-GMA	1	0	0	0	3
		2	0	0	0	0
		3	0	0	6†	0
	Acetone	1	0	0	0	1
		2	0	0	0	0
		3	0	0	2†	0

* Each entry represents the number of teeth exhibiting the indicated property.

† Since these same teeth were judged non-carious at 3.5 years (the restorations had not been replaced), better criteria to distinguish caries from marginal stain are needed.

Table 2 ■ Marginal evaluations

Property	Treatment	Evaluator	Labial (incisal on Class V's) Years 0	1	2.5	3.5	Lingual (distal on Class V's) Years 0	1	2.5	3.5
Notching	NPG-GMA	1	0.00* (0.00)†	0.24 (0.73	0.3 (1.5)	0.22 (0.57)	0.3 (1.9)	0.2 (1.1)	0.6 (1.6)	0.32 (0.84)
		2	0.15 (0.66)	0.4 (1.3)	0.04 (0.20)	0.14 (0.77)	0.21 (0.62)	0.00 (0.00)	0.5 (1.3)	0.27 (0.94)
	Acetone	1	0.6 (1.8)	0.5 (1.2)	0.24 (0.69)	0.35 (0.77)	0.6 (1.3)	0.21 (0.62)	0 24 (0.58)	0.18 (0.66)
		2	0.22 (0.92)	0.4 (1.3)	0.6 (1.7)	0.4 (1.1)	0.24 (0.74)	0.28 (0.70)	0.29 (0.83)	0.4 (1.3)
Staining	NPG-GMA	1	0.04 (0.27)	0.17 (0.75)	0.21 (1.0)	0.3 (1.5)	0.03 (0.19)	0.4 (1.3)	1.1 (2.4)	1.3 (2.4)
		2	0.22 (0.57)	0.19 (0.51)	0.38 (0.68)	0.6 (1.2)	0.14 (0.35)	0.45 (0.98)	1.3 (1.7)	1.5 (2.5)
		3	0.28 (0.71)	0.32 (0.87)	0.60 (0.90)	0.40 (0.76)	0.7 (1.4)	1.2 (1.8)	2.6 (3.4)	1.6 (2.3)
	Acetone	1	0.00 (0.00)	0.07 (0.38)	0.8 (2.3)	0.5 (1.6)	0.17 (0.93)	0.6 (1.4)	0.9 (1.9)	1.5 (3.1)
		2	0.17 (0.42)	0.31 (0.90)	0.7 (1.2)	1.1 (1.7)	0.07 (0.26)	0.55 (0.91)	0.9 (1.6)	1.5 (2.4)
		3	0.31 (0.61)	0.6 (1.1)	1.3 (2.0)	0.8 (1.7)	0.4 (1.0)	0.9 (1.5)	1.6 (2.2)	1.1 (2.1)

* Each entry represents the average score given by each investigator for the indicated time and property. Higher numbers indicate greater notching and stain.

The number of evaluations ranges from 54 at 0 years to 45 ± 2 at 3.5 years for the labial margins and 29 at 0 years to 22 at 3.5 years for the lingual margins.

† Standard deviation.

Table 3 ■ Better, same or worse evaluations

Evaluator	Treatment	Time (years)			
		0	1.0	2.5	3.5
		%*	%	%	%
1	NPG-GMA	13	19	23	36
	Acetone	2	9	23	30
2	NPG-GMA	15	24	42	49
	Acetone	7	19	26	28
3	NPG-GMA	33	44	54	52
	Acetone	28	33	27	34

* Each entry represents the percentage of restorations rated better than their matching restorations for the indicated material and time. The balance were rated the same.

Bibliography

1. Going, R. E. Microleakage around dental restorations: a summarizing review. JADA 84:1349 June 1972.

2. Bowen, R. L. and Mullineaux, A. L. Adhesive restorative materials. Dent Abstracts 14:80 Feb 1969.

3. Chandler, H. H.; Bowen, R. L.; Paffenbarger, G. C., and Mullineaux, A. L. Clinical evaluation of a radiopaque composite restorative material after 3.5 years. [Manuscript released by Washington Editorial Review Board for publication in J Dent Res]

4. a) Bowen, R. L. Adhesive bonding of various materials to hard tooth tissues. I. Method of determining bond strength. J Dent Res 44:690 July-Aug 1965.

   b) Bowen, R. L. Adhesive bonding of various materials to hard tooth tissues. II. Bonding to dentin promoted by a surface-active comonomer. J Dent Res 44:895 Sept-Oct 1965.

   c) Bowen, R. L. Adhesive bonding of various materials to hard tooth tissues. III Bonding to dentin improved by pretreatment and the use of a surface-active comonomer. J Dent Res 44:903 Sept-Oct 1965.

4. d) Bowen, R. L. Adhesive bonding of various materials to hard tooth tissues. IV. Bonding to dentin, enamel and fluorapatite improved by the use of a surface-active comonomer. J Dent Res 44:906 Sept-Oct 1965.

e) Bowen, R. L. Adhesive bonding of various materials to hard tooth tissues. V. The effect of a surface-active comonomer on adhesion to diverse substrates. J Dent Res 44:1369 Nov-Dec 1965.

f) Bowen, R. L. Adhesive bonding of various materials to hard tooth tissues. VI. Forces developing in direct filling materials during hardening. JADA 74:439 Feb 1967.

5. Chandler, H. H.; Bowen, R. L.; Paffenbarger, G. C., and Mullineaux, A. L. Clinical investigation of a radiopaque composite restorative material. JADA 81:935 Oct 1970.

6. Segel, S. Nonparametric statistics for the behavioral sciences. N. Y., McGraw-Hill Book Co., 1956 pp 36-42, 250.

7. Hoel, P. G. Introductions to mathematical statistics. N. Y., John Wiley & Sons, Inc., 1962 pp 148-151.

8. Hoel, P. G. Introductions to mathematical statistics. N. Y., John Wiley & Sons, Inc., 1962 pp 104-105.

9. Paffenbarger, G. C.; Nelsen, R. J., and Sweeney, W. T. Direct and indirect filling resins: A review of some physical and chemical properties. JADA 47:516 Nov 1953.

10. Brown, W. S., et al. Thermal fatigue in teeth. J Dent Res 51:461 Mar-April 1972.

11. Smith, D. L. and Schoonover, I. C. Direct filling resins: dimensional changes resulting from polymerization shrinkage and water sorption. JADA 46:540 May 1953.

12. Souder, W. H. and Peters, C. G. An investigation of the physical properties of dental materials. Washington, D. C. Govern. Printing Office, 1920 pp 9-19.

13. Bowen, R. L. and Rodriguez, M. S. Tensile strength and modulus of elasticity of tooth structure and several restorative materials. JADA 64:378 Mar 1962.

NATIONAL BUREAU OF STANDARDS REPORT

NBS PROJECT 311.05-3110561

December 29, 1972

NBS REPORT 10 981

Progress Report

on

$Ca_4(PO_4)_2O$, TETRACALCIUM DIPHOSPHATE MONOXIDE; CRYSTAL STRUCTURE AND RELATIONSHIPS TO $Ca_5(PO_4)_3OH$ AND $K_3Na(SO_4)_2$

B. Dickens, W. E. Brown*, G. J. Kruger**, and M. M. Stewart***

* Director, American Dental Association Research Unit at the National Bureau of Standards.

** Postdoctoral fellow, Department of Computer Science, University of Maryland, 1970-1971. Permanent address: National Physical Research Laboratory, South African Council for Scientific and Industrial Research, Pretoria, Republic of South Africa.

*** Department of Chemistry, University of Maryland, College Park, Maryland 20742.

U.S. DEPARTMENT OF COMMERCE

NATIONAL BUREAU OF STANDARDS

Abstract

$Ca_4(PO_4)_2O$, tetracalcium diphosphate monoxide, crystallizes in the monoclinic unit cell $\underline{a}$ = 7.023(1) Å, $\underline{b}$ = 11.986(4) Å, $\underline{c}$ = 9.473(2) Å, β = 90.90(1)° (at 25°C) in space group $P2_1$ with $4[Ca_4(PO_4)_2O]$ per cell. 3288 x-ray data were measured from a single crystal by θ-2θ scans using MoKα radiation; 56 of these reflections were of "unobservable" intensity. The structure was solved by an application of direct phasing methods and subsequent calculation of an E map. It was refined anisotropically by full-matrix least-squares to $\underline{R}_w(F)$ = 0.036, R(F) = 0.037. Allowance was made for isotropic secondary extinction but not for anomalous scattering or absorption.

The dimensions of the unit cells of $Ca_4(PO_4)_2O$ and $Ca_5(PO_4)_3OH$ (hydroxyapatite), an idealized form of the major inorganic phase in the human body, are simply related. Although this 3-dimensional relationship in the unit cell shapes is not carried over into the details of the actual structures, $Ca_4(PO_4)_2O$ does contain a layer which is similar to a layer in $Ca_5(PO_4)_3OH$, and an epitaxial relationship between the two compounds is conceivable. $Ca_4(PO_4)_2O$ is also related to the $K_3Na(SO_4)_2$ (glaserite) structure. In this relationship the oxide ions are "extra" ions.

One Ca ion in $Ca_4(PO_4)_2O$ is coordinated weakly to a

Abstract (Cont.)

face of a PO_4 group, a feature which has been previously observed for Ca only in a disordered cation site in β-$Ca_3(PO_4)_2$. The two crystallographically discrete oxide ions are surrounded by tetrahedra of Ca ions, with Ca...O distances in the range 2.136(4) Å to 2.277(3) Å. Thus, the oxide ions do not lie in a channel formed by cations in the structure and $Ca_4(PO_4)_2O$ cannot be considered to be an oxy-apatite.

The positions of the P atoms and the Ca and oxide ions lie close to those required by space group Pmcn. This explains the appreciable twinning exhibited by $Ca_4(PO_4)_2O$. It also makes the existence of a higher symmetry modification feasible.

Introduction

This investigation is the sequel to an earlier investigation (Brown and Epstein, 1965) on $Ca_4(PO_4)_2O$, tetracalcium diphosphate monoxide. The more usual name for $Ca_4(PO_4)_2O$ is tetracalcium phosphate, from the formula when written as $4CaO \cdot P_2O_5$. Brown and Epstein showed that $Ca_4(PO_4)_2O$ may have a structural relationship to $Ca_5(PO_4)_3(OH,F)$ (Kay, Young and Posner, 1964), the mineral hydroxyapatite, which may be considered an idealized form of the major inorganic phase in the human body. Here we report on the determination of the crystal structure of $Ca_4(PO_4)_2O$ using a small single crystal, and discuss the $Ca_4(PO_4)_2O$ - $Ca_5(PO_4)_3OH$ and $Ca_4(PO_4)_2O$ - $K_3Na(SO_4)_2$ relationships.

Data collection and structure refinement

The crystal used in the data collection was an irregular colorless disc with radius ~0.33mm, thickness ~0.11mm. This was the largest untwinned crystal found in the sample described by Brown and Epstein (1965). The crystal was attached to the goniometer head in our usual way (Dickens and Bowen, 1971a). Crystal data are as follows:

Formula (ideal): $Ca_4(PO_4)_2O$

cell at 25°C: monoclinic

$\underline{a}$ = 7.023(1) Å

$\underline{b}$ = 11.986(4) Å

$\underline{c}$ = 9.473(2) Å

β = 90.90(1)°

volume = 797.3 $Å^3$

space group $P2_1$; cell contents $4[Ca_4(PO_4)_2O]$;

calculated density 3.051 $g \cdot cm^{-3}$;

observed density 3.06 $g \cdot cm^{-3}$ (Bücking and Linck, 1887).

The cell parameters and their standard deviations (given in parentheses) were calculated by least-squares from 20 2θ values observed on a diffractometer using MoKα radiation filtered through 0.025 mm Nb foil. The wavelength λ(MoKα) = 0.710688 Å was assumed. (To make $\underline{b}$ the unique monoclinic axis, the cell $\underline{a}'$, $\underline{b}'$, $\underline{c}'$ given by Brown and Epstein has been transformed here to $\underline{c}$, $\underline{a}$, $\underline{b}$.)

The x-ray data were measured using the θ-2θ procedure described by Alexander and Smith (1962; 1964) and as adapted by Reimann, Mighell and Mauer (1967). Each reflection was measured once only. There were 3288 reflections total of which 56 were "unobserved" [i.e., $I_{hk\ell} < 2\sigma(I_{hk\ell})$]. μ(Mo) was taken to be 30.3 cm^{-1}. Because of the small crystal size, absorption corrections were neglected; the resultant maximum error in F_o is estimated to be 5% for the 2θ range 0 to 80°.

The structure was determined using the sequence

DATRDN - NORMSF - SINGEN - APHASE - TANGEN - FOURR in the XRAY system of Stewart et al (1972). The quasi-normalized structure factor statistics (Dickinson, Stewart and Holden, 1966) were very close (see below) to those expected for an acentric space-group. In the following list, E is the quasi-normalized structure factor and the values in square brackets are the theoretical values for an acentric structure. Quantities enclosed in < > brackets are average values. $\langle|E|\rangle = 0.886$ [0.886], $\langle|E^2-1|\rangle = 0.748$ [0.736], $\langle|E^2-1|^2\rangle = 1.061$ [1.000], $\langle|E^2-1|^3\rangle = 3.186$ [2.000]; %E>3.0 = 0.05 [0.01], %E>2.5 = 0.22 [0.19], %E>2.0 = 1.95 [1.83], %E>1.8 = 4.10 [3.92], %E>1.6 = 7.91 [7.73], %E>1.4 = 14.6 [14.1], %E>1.2 = 23.9 [23.7], %E>1.0 = 35.9[36.8].

The following phases were fixed during the tangent refinement part of the program: [1] 4,0,0(0); [6] 4,4,0(90); [24] 0,1,3(0); [29] 1,0,-13(0); [89] 8,0,3(0), where the values given are [sequence number in ordered list of E values], h, k, ℓ, (phase in degrees). The tangent refinement was carried out in four stages, using 100, 150, 225 and then 300 E values (minimum E's were 1.887, 1.981, 1.661 and 1.563, respectively). The 300 E values from the final cycle were used to calculate an E map which contained peaks at the Ca and P positions as its salient features.

The oxygen atoms were found in a subsequent F_o Fourier synthesis phased from the Ca and P atoms.

The structure was refined isotropically using the XRAY system program CRYLSQ to $R_w = 0.041$, $R = 0.050$, and then anisotropically in a series of block refinements (varying half of the structure at any one time) to $R_w = 0.036$, $R = 0.037$. The y coordinate of Ca(1) was fixed to define the origin along [010]. The scattering factors used were those for the neutral atoms in International Tables for X-ray Crystallography (1962). Before the anisotropic refinements, the weighting scheme was changed from one based on counting statistics, $\sigma_c(F)$, to $w(F) = (\sigma_c^2(F) + 0.0005\ F_o^2)^{-1}$. In the final refinement, the average shift/error was 0.005 and the standard deviation of an observation of unit weight was 0.34. The extinction parameter g, (Zachariasen, 1963; 1967, Larson, 1970) refined to $1.38(6) \times 10^{-4}$ degrees (for an isotropic Gaussian distribution of mosaic blocks). The largest correlation coefficients are 0.64 between the extinction and scale factors, and 0.50 to 0.59 between the y parameters of the pairs of atoms [Ca(4), Ca(5)], [Ca(5), Ca(6)], [Ca(5), Ca(8)], and [Ca(6), Ca(8)]. The three largest peaks and two largest "holes" in a difference electron

density synthesis calculated after the final refinement were ~0.8 electrons·Å^{-3} and ~-0.8 electrons·Å^{-3}, respectively. They are all attributed to the background.

The atomic parameters are given in Table 1 and the observed and calculated structure factors in Table 2.

Description of the structure

The structure of $Ca_4(PO_4)_2O$ is shown in Fig. 1. There are eight unique Ca ions, four PO_4 groups and two oxide ions. The Ca and P atoms lie near four sheets perpendicular to [010], two adjacent sheets being crystallographically related to the other two in the cell by the two-fold screw axis of the space group, $P2_1$. Each sheet contains two cation-anion columns and one cation-cation column. These columns are [Ca(1), Ca(2)], [Ca(3), $P(2)O_4$] and [Ca(4), $P(1)O_4$] in one sheet (Fig. 2) and [Ca(7), Ca(8)], [Ca(5), $P(3)O_4$] and [Ca(6), $P(4)O_4$] in the other (Fig. 3).

The calcium ion environments

Ca(1) is coordinated to seven oxygen atoms (see Fig. 2), including the PO_4 edge [O(21), O(22)] and the oxide ion O(1), arranged in an approximately pentagonal bipyramid (see Table 3 for details of all ionic environments).

Ca(2) is coordinated to seven oxygen atoms, including the PO_4 edges [O(21),O(23)] and [O(41),O(42)], and the

oxide ion O(1). The coordination polyhedron of Ca(2) is irregular.

Ca(3) is coordinated to seven oxygen atoms, including the PO_4 edges [O(12),O(13)] and [O(31),O(34)], and to the oxide ion O(2). Six of the oxygens in the coordination of Ca(3) may be considered to be arranged in a partial pentagonal bipyramid. The seventh member of the coordination polyhedron is O(34), which is necessarily displaced from the remaining equatorial position of the pentagonal bipyramid because it is the second member of the [O(31),O(34)] PO_4 edge. It is the oxygen with the weakest bond to Ca(3).

Ca(4) is coordinated to seven oxygen atoms, including the PO_4 edge [O(32),O(33)], and the O(1) oxide ion. The coordination geometry of Ca(4) is derived from pentagonal bipyramidal, with O(1) occupying one of the axial positions.

Ca(5) is coordinated to seven oxygen atoms (Fig. 3), including the PO_4 edges [O(41),O(44)] and [O(12),O(13)], and the oxide ion O(2). The coordination of Ca(5) is derived from pentagonal bipyramidal with [O(41),O(44)] in the equator.

Ca(6) is coordinated to eight oxygen atoms, including the PO_4 edge [O(11),O(14)], and the oxide ion O(1). The coordination polyhedron of Ca(6) may be considered to

include the PO_4 face [O(32),O(33),O(34)] although the primary ionic bonding of all these three oxygen atoms is to neighboring Ca ions. Coordination of Ca to a PO_4 face is rare; the other known example is in the β-$Ca_3(PO_4)_2$ structure (Dickens, Bowen and Brown, 1971b).

Ca(7) is coordinated to seven oxygen atoms, including the PO_4 edges [O(11),O(13)] and [O(42),O(43)], and the oxide ion O(2). The coordination geometry is irregular.

Ca(8) is coordinated to seven oxygen atoms, including the PO_4 edge [O(31),O(33)], and the oxide ion O(2). The coordination is pentagonal bipyramidal with the above oxygens in equatorial positions, along with O(11) and O(43).

Proceeding on the assumption that any Ca...O distance less than ~2.5 Å denotes a strong Ca...O bond, we note that the bonding of all Ca ions to the oxide ions O(1) and O(2) is strong. The number of strong and less strong bonds to all coordinated oxygens from individual Ca ions are as follows:

Ca(1) 6,1; Ca(2) 3,4; Ca(3) 2,5; Ca(4) 5,2; Ca(5) 4,3; Ca(6) 4,4; Ca(7) 4,3; Ca(8) 6,2.

The PO_4 environments

In the $P(1)O_4$ group (Fig. 2), each oxygen is bonded to three Ca ions. The $P(1)O_4$ edges [O(11),O(13)],

[O(11),O(14)] and [O(12),O(13)] are "shared" by coordination to Ca ions.

In the $P(2)O_4$ group, O(21),O(22) and O(23) are each coordinated to three Ca ions, and O(24) is coordinated to two. The edges [O(21),O(22)] and [O(21),O(23)] are "shared".

In the $P(3)O_4$ group (Fig. 3), O(31) and O(32) are both bonded to three Ca ions, while O(33) and O(34) may be considered to be bonded to four. The edges [O(31),O(33)], [O(31),O(34)] and [O(32),O(33)] are "shared", as is the [O(32),O(33),O(34)] face. As judged from the O...Ca distances for the $P(3)O_4$ group, the bonding of the $P(3)O_4$ oxygens to Ca(8) and Ca(6) is weak, apparently because of repulsion of these Ca ions by the other two Ca ions, Ca(5) and Ca(4), to which the $P(3)O_4$ oxygens are bonded more strongly.

In the $P(4)O_4$ group, each oxygen is bonded to three Ca ions and the edges [O(41),O(42)], [O(41),O(44)] and [O(42),O(43)] are "shared".

In all PO_4 groups, the O-P-O angles less than the tetrahedral angle, 109.5°, are associated with PO_4 edges which are coordinated to Ca, in accord with Pauling's rule (Pauling, 1960).

The oxide ion environments

Oxide ion O(1) is coordinated very strongly to the

Ca(1), Ca(2), Ca(4) and Ca(6) ions, which are arranged in an approximate tetrahedron about O(1). Ca(6) is in a different sheet from the other Ca ions. Oxide ion O(2) is similarly coordinated to Ca(5), Ca(7), Ca(8) in one sheet and Ca(3) in another. The O(1)...Ca and O(2)...Ca distances (Table 3) are unusually small.

Discussion

Cruickshank (1961) has suggested that the average of the P-O distances in PO_4 groups is constant. This has been denied by Baur and Khan (1970). It is commonly observed that the length of an individual P-O bond apparently depends on the environment of the oxygen atom, i.e., whether the oxygen is covalently bonded to hydrogen or ionically bonded to one or more Ca ions. It seems intuitively reasonable that the average P-O bond length will similarly depend on the total environment of the PO_4 group, because the more electropositive the environment, the more electrons will be attached onto the oxygen atoms, affecting the amount of π bonding and the hybridization of the σ bonding in each P-O bond.

The average P-O distance in $Ca_4(PO_4)_2O$ for 3-coordination of oxygen by Ca ions is 1.538(10) Å, where the standard deviation (in parentheses) is estimated from the spread of the individual values. The two examples of possible 4-coordination, O(33) and O(34), average to 1.537(18) Å, practically the same value as for the 3-coordination. The sole example of 2-coordination is O(24), with P(2) - O(24) = 1.511 Å, which is appropriately less than the P-O distances for 3-coordinated oxygens. Examination of the P-O bond distances along the lines described by Baur (1970) does not explain the individual variations.

The average P-O distances in the P(1), P(2), P(3) and P(4) PO_4 groups are 1.533(5), 1.537(19), 1.535(14) and 1.541(8) Å respectively. The standard deviations (in parentheses) were again estimated from the spread of the individual values. From the bond lengths in the $Ca_4(PO_4)_2O$ structure, it appears that the effect (through the valence unit concept) of coordination number alone on P-O bond lengths is relatively wide-spread, yet the average values of individual PO_4 groups are effectively constant. The average for all PO_4 groups is 1.537 Å, with a standard deviation of 0.003 Å when only the spread of the averages is considered, and 0.012 Å when the

spread of the individual values is considered. Corresponding values from our study of magnesium-containing β-$Ca_3(PO_4)_2$ (Dickens, Bowen and Brown, 1971b) are 1.537(10) Å and 1.533(8) Å. The overall average value of 1.537 Å agrees very well with that of 1.539 Å obtained by Baur and Khan by averaging over PO_4 groups in various forms, i.e., $H_2PO_4^-$ etc., in several structures found in the literature. Therefore, even when one or more P-O bonds are increased to ~1.59 Å by the formation of covalent O-H bonds, the remaining P-O bonds apparently decrease to essentially preserve the average value, and any effect of the environment of the PO_4 group is very small.

In the usual considerations of coordination polyhedra, attention is given to the configuration within a covalently bonded group or to the arrangement of oxygen atoms around a central cation. In the case of the

$O(Ca)_4$ groupings in the $Ca_4(PO_4)_2O$ structure, one must instead consider the arrangement of cations around an oxygen atoms. Some light can be shed on the unusually small Ca...O distance of 2.213 Å in the Ca_4O grouping by the following reasoning: CaO (Oftedahl, 1927) has the NaCl structure with a Ca...O distance of 2.406 Å. This octahedral coordination of O by Ca can be compared with tetrahedral coordination of O by Ca by assuming a tetrahedral arrangement of CaO exists with lattice energy comparable to that of the octahedral arrangement. Then the ratio of Ca...O distances is given by $R_o/R_t = [(A_tB_o)/(A_oB_t)]^{1/(n-1)}$ with A being the Madelung constants, B the repulsion constants, and n the exponent of the interatomic distance (n = 8 on average for Ca^{2+} and O^{2-}) in the Born formulation of the lattice energy (see Pauling, 1960, p. 508, p. 509, pp. 537-538). Substitution of R_o = 2.406 Å, A_o = 1.7476, A_t = 1.640 (the average of the Madelung constants for the sphalerite and wurtzite structures) $B_o = 6B'$, $B_t = 4B'$, where both B_o and B_t are considered to be proportional to the number of nearest neighbors, and n = 8, gives R_t = 2.305 Å. In the $O(Ca)_4$ groupings in $Ca_4(PO_4)_2O$ there is actually increased attraction over that calculated using a Madelung constant for tetrahedral coordination because the other oxygen neighbors of the Ca ions tetrahedrally bonded to O^{2-} are

further away than the O^{2-} is. Thus, the groupings will be further contracted, and allowance for this factor would bring the calculated distance close to that observed.

In the coordination of Ca ions to PO_4 ions in $Ca_4(PO_4)_2O$, (i) each oxygen is usually coordinated to three Ca ions; and (ii) the Ca...O bond tends to be in the plane O-P-O' where O' is one of the other three oxygens in the PO_4 group. Thus, the ideal coordination of a PO_4 group appears to be when it shares each of its six edges with a Ca ion (Pauling's third rule not withstanding), making a total PO_4 coordination of six Ca ions. Apex coordination of a PO_4 group would, of course, require twice as many surrounding Ca ions as edge coordination does and the effects of Ca...Ca repulsion would be expected to be important. Because Ca bonded to a PO_4 edge forms twice as many bonds to that PO_4 group as does Ca bonded only to a PO_4 apex, the former are bonded more strongly than the latter and probably govern the arrangement of Ca ions around the PO_4 group through Ca...Ca repulsions. In general, the Ca arrangements in $Ca_4(PO_4)_2O$ are close to those expected when all Ca ions are coordinated to edges. From the point of view of minimizing Ca...Ca repulsions, face sharing would be preferred. This is more undesirable than edge sharing however, because of increased Ca...P repulsions, as Pauling's third rule states. Therefore, edge sharing where possible appears

to be a reasonable compromise in the coordination of Ca to a PO_4 group. In this case, the three Ca ions and one P atom coordinated to each O atom in the PO_4 group are arranged in approximately tetrahedral directions about the oxygen atom.

Although the structure of $Ca_4(PO_4)_2O$ is actually monoclinic and acentric ($P2_1$), and the distribution of the quasi-normalized structure factor compares well with that expected for an acentric structure (see above), the positions of the Ca, PO_4 and oxide ions approximately correspond to the requirements of the centric space group $P2_1/m,2_1/c,2_1/n$, ($Pmcn$-D_{2h}^{16}). All symmetry elements in D_{2h}^{16} except for the 2_1-axis parallel to [010] are pseudo-symmetry elements (designated with primes in the following discussion). These pseudo-symmetry elements are placed in $Ca_4(PO_4)_2O$ as follows:

(i) mirror planes, m′, perpendicular to [100] pass through the P atoms, the Ca(3), Ca(4), Ca(5), and Ca(6) ions and the oxide ions O(1) and O(2).

(ii) a c′-glide plane perpendicular to [010] is at $\underline{y} \sim 0.4$ with the present placement of the origin along [010]. (Because $P2_1$ is a polar space-group, placement of the origin along [010] is arbitrary in the actual structure.)

(iii) an n′-glide perpendicular to [001] is at $\underline{z}=0.5$.

Thus, the pseudo-symmetry in the crystal structure is sufficiently pronounced for the existence of a higher temperature orthorhombic modification to be feasible. Brown and Epstein (1965) noticed appreciable pseudo-orthorhombic symmetry in their x-ray photographs of $Ca_4(PO_4)_2O$ and also concluded that an orthorhombic modification may exist. That the $Ca_4(PO_4)_2O$ structure is capable of absorbing a large amount of energy is revealed by the fact that the melting point of $Ca_4(PO_4)_2O$ is very high (~1710° C, Trömel and Fix, 1961). It is possible that the $Ca_4(PO_4)_2O$ sample studied by Trömel and Zaminer (1959) is an orthorhombic form, stabilized perhaps by some impurity. On the other hand, their sample may have looked orthorhombic because of extensive twinning.

There are eight general positions in space-group Pmcn. Eight Ca ions [Ca(1), Ca(2), Ca(7), Ca(8) and their counterparts generated by the 2_1-axis of $P2_1$] would be crystallographically equivalent and lie in a general position in Pmcn. The remaining atoms under consideration, the equivalent quadruple sets 2[P(1),P(3)], 2[P(2),P(4)], 2[Ca(3),Ca(6)], 2[Ca(4),Ca(5)] and 2[O(1),O(2)], would all be in special positions on mirror planes in the orthorhombic structure. Two oxygens of each PO_4 group would lie on the mirror plane, and the remaining two would be related by the mirror plane. The $\underline{c}'$-glide relationship between $P(1)O_4$ and $P(3)O_4$ groups is such that the equivalency relationships between their oxygen atoms are O(13)≈O(31), O(11)≈O(34), and O(13), O(12)≈O(32),O(33). The relationship between $P(2)O_4$ and

$P(4)O_4$ is less clear, but it appears (Fig. 1) that a rotation of $P(4)O_4$ by about 90° around a (so that it would satisfy the requirements of the mirror plane m′) would bring the two PO_4 groups into a c-glide relationship. Their oxygen atoms would then be related as follows: O(21)≈O(42), O(24)≈O(43), and O(23),O(22)≈O(41),O(44).

The pseudo-symmetry in $Ca_4(PO_4)_2O$ is also of interest because of possible twinning modes. Termier and Richard (1895) state that (001) and (100) (in the present notation) are the lamellar twin planes. This was corroborated by Brown and Epstein (1965), who state that the composition planes for normal twins they observed would be (001) and (100). Twinning in which the (100) and (001) planes are composition planes are the only ones involving pinacoids that could be detected optically. The possible existence of a high-temperature orthorhombic modification with the symmetry elements $2_1/m$ and $2_1/n$ associated with the a and c axes, respectively, lends strong support for twinning by any of these four pseudo-symmetry operations. Of the remaining symmetry operations, $2_1/c$, which are associated with the b axis, only the c-glide could produce twinning in monoclinic $Ca_4(PO_4)_2O$ because the 2_1 axis is present

as a true symmetry element. Twins produced by the c-glide operation, however, would be "optical twins" and would not be detected with the polarizing microscope. Note that the plane of the c-glide lies at the center of the apatite-like layer in $Ca_4(PO_4)_2O$ described below. The existence of a similar layer in $Ca_5(PO_4)_3(OH)$, hydroxyapatite, suggests that the operations corresponding to $2_1/c$ could produce twinning in $Ca_5(PO_4)_3OH$. Although these operations have not been suggested previously for $Ca_5(PO_4)_3OH$ twins of this type (i.e., with (100) the twin plane) have been reported (Palache, Berman and Frondel, 1951). One may speculate that a twinning mechanism of this type (which would also produce optical twins) may have some biological significance/phases in the body. For example, /electron micrographs of the apatitic crystals of dental enamel frequently show a plane of demarkation parallel to (100) which could be the composition plane of a twin.

in that $Ca_5(PO_4)_3OH$ is an idealization of the major inorganic

Relationship of $Ca_4(PO_4)_2O$ to other structures

As was outlined by Dickens and Brown (1972), calcium phosphates typically crystallize in five structural types: (i) structures related to $Ca_5(PO_4)_3(OH,F)$, hydroxyapatite, (ii) structures containing $CaPO_4$ chains and sheets, (iii) structures related to $K_3Na(SO_4)_2$, glaserite, (iv) structures

related to $Ba_3(PO_4)_2$, and (v) structures related to $MgNH_4PO_4 \cdot 6H_2O$, struvite.

Only types (i) and (iii) contain both cation-cation and cation-anion columns. The Ca:P ratio of 2:1 in the formula of $Ca_4(PO_4)_2O$ suggests that it may have a structural relationship to glaserite, $K_3Na(SO_4)_2$ (Gossner, 1928). The presence of the oxide ions means, however, that the glaserite-type structure must be modified to accommodate extra, but small, anions. In other structures in which the cation:anion ratio is not 2:1, e.g., $Ca_5(PO_4)_2SiO_4$ (Dickens and Brown, 1971c) and $Ca_7Mg_9(Ca,Mg)_2(PO_4)_{12}$ (Dickens and Brown, 1971d), the semblance of the glaserite structure is retained by resorting to crystallographically systematic cation vacancies in the cation-anion columns. The relationship between the structures of $K_3Na(SO_4)_2$ (glaserite) (Fig. 4) and $Ca_4(PO_4)_2O$ (shown in an a projection in Fig. 5) can be seen most readily in Fig. 6. The latter is derived from Fig. 5 by shifting the layer bounded by the broken lines at A and A' about 2 Å to the left. (Each layer consists of two sheets of [Ca,Ca] and [Ca,PO_4] columns.) It can be seen that the highly distorted diamond-shaped cells of Fig. 5 have become fairly regular in Fig. 6. Each cell has [Ca,Ca] columns at the corners and two [Ca,PO_4] columns on the major diagonal, much as they are in Fig. 4. The unit cell of

$Ca_4(PO_4)_2O$ corresponds to four glaserite cells.

With the idealization of the structure of $Ca_4(PO_4)_2O$, it is now possible to see why the layers in $Ca_4(PO_4)_2O$ are shifted. In the structure of Fig. 6, O(2) would have coordinated to only three calcium atoms Ca(7), Ca(8) and Ca(5) at three apexes of a tetrahedron; Ca(4) is too far away along a to coordinate to O(2). Similarly, O(1) would coordinate to Ca(1), Ca(2) and Ca(4) but not to Ca(5). When the layer A-A' shifts to its actual position, as shown in Fig. 5, Ca(3) comes into coordination with O(2) and Ca(6) with O(1) so that each oxygen can have full tetrahedral coordination.

The idealized structure approximates orthohexagonal symmetry, suggesting that the orthorhombic, high-temperature form postulated above may become orthohexagonal if O(1) and O(2) become mobilized at higher temperatures.

The lanthanide elements form compounds of the type M_2SiO_4O, which for purposes of comparison with $Ca_4(PO_4)_2O$ may be written $M_4(SiO_4)_2O_2$. These compounds contain the same cation-tetrahedral anion ratio as $Ca_4(PO_4)_2O$ and glaserite, but they contain twice as many oxide oxygens as $Ca_4(PO_4)_2O$. The lanthanide oxysilicates actually form two structurally different series with the

demarkation occurring at Tb (Felsche, 1971). In both series of compounds (Smolin and Tkachev, 1969; Smolin, 1970), there are sheets each of which contains two cation-anion columns for every one cation-cation column, and the oxide ions have tetrahedral coordination of cations as they do in $Ca_4(PO_4)_2O$, but the juxtapositions of these sheets differ significantly from those in $Ca_4(PO_4)_2O$ and glaserite. Thus, there is only a somewhat tenuous relationship between the structures of $Ca_4(PO_4)_2O$ and the lanthanide oxysilicates.

The $Ca_4(PO_4)_2O$ structure also bears a surprising resemblance to part of the $Ca_5(PO_4)_3OH$ structure (Kay, Young and Posner, 1964), i.e., to structural type (i)/ described above.

The atoms inside the BB' layer in Fig. 7, which depicts six unit cells of $Ca_5(PO_4)_3OH$, are compared in Fig. 8 with atoms in the "apatitic layer" AA' of Fig. 5. Although there are some significant differences in orientation of PO_4 groups, both structures contain similarly positioned [Ca,Ca] and [Ca,PO_4] columns comprising two sheets in each layer. Thus, in the relationship of these "apatite layers" in $Ca_4(PO_4)_2O$ and $Ca_5(PO_4)_3OH$, the cation-cation columns [Ca(1),Ca(2)] and [Ca(7),Ca(8)] in $Ca_4(PO_4)_2O$ correspond to the calcium columns Ca(I) in $Ca_5(PO_4)_3OH$. Each of the pairs [Ca(3),Ca(4)] and [Ca(5),Ca(6)] in $Ca_4(PO_4)_2O$

corresponds to one side of a Ca(II) "hexagon" in $Ca_5(PO_4)_3OH$. In this relationship, the locations of the oxide ions O(1) and O(2) in $Ca_4(PO_4)_2O$ correspond to the locations of the OH ions in $Ca_5(PO_4)_3OH$. Because they are actually located in the neighboring apatitic layer in the complete $Ca_4(PO_4)_2O$ structure whereas the OH ions are not in an apatitic layer in $Ca_5(PO_4)_3OH$, the oxide ions account for much of the misorientation of the PO_4 groups in $Ca_4(PO_4)_2O$ as compared with $Ca_5(PO_4)_3OH$.

The salt $Ca_8H_2(PO_4)_6 \cdot 5H_2O$ is also known to contain an apatitic layer (Brown, 1962; 1966). In that case, however, the layer is thicker than the one in $Ca_4(PO_4)_2O$ (approximating the shaded area in Fig. 7) and the atomic positions are closer to those of $Ca_5(PO_4)_3OH$.

A more complete relationship between $Ca_4(PO_4)_2O$ and $Ca_5(PO_4)_3OH$ can be derived from the idealized glaserite structures given in Fig. 4 and Fig. 6. If all [Ca(7),Ca(8)] columns in the next layer below (towards the bottom of figure 6) are replaced by [OH,OH] columns and the oxide ions O(1) and O(2) are removed, one obtains the approximation for the $Ca_5(PO_4)_3OH$ structure first derived from glaserite by Wondratschek (1963). The unit cell for $Ca_5(PO_4)_3OH$, defined by lines of open squares in Fig. 6, is hexagonal and in this projection consists of three glaserite unit cells. Since, as noted above, the $Ca_4(PO_4)_2O$ unit cell

contains four glaserite units, the $Ca_4(PO_4)_2O/Ca_5(PO_4)_3OH$ unit-cell relationship is 4/3, in contrast with the ratio of the volumes of the two cells which is very close to 3/2. The difference is consistent with the fact that each glaserite-like unit cell contains $[Ca_4(PO_4)_2O]$ in $Ca_4(PO_4)_2O$ and only $[Ca_{3.33}(PO_4)_2(OH)_{0.67}]$ on the average in $Ca_5(PO_4)_3OH$.

The coordination of the Ca(II) ion in $Ca_5(PO_4)_3OH$ is to nine oxygens comprising three PO_4 apexes and three PO_4 edges. In $Ca_4(PO_4)_2O$ the coordinations of the corresponding Ca(1), Ca(2), Ca(7), Ca(8) ions are all seven, including at the most [for Ca(2) and Ca(7)] two PO_4 edges. Each of these cations is also coordinated to an oxide ion.) Seven-fold coordination of Ca in calcium phosphates is far more common than 9-fold, the only clear example of which in calcium phosphates is the Ca ion on the 3-fold axis in $Ca_5(PO_4)_3OH$. Note that the 9-fold coordination of Ca in the aragonite phase of $CaCO_3$ is a consequence of (i) the overall packing giving a higher density for aragonite (the high pressure phase) over that of calcite, and (ii) the smaller O...O separation in the edge of the CO_3 group compared to that in the PO_4 group allowing more oxygens to enter a given size of coordination polyhedron. Since apatites are among

the most stable calcium phosphates, the 9-fold coordination of Ca(II) in $Ca_5(PO_4)_3OH$ may be a concomitant of efficient packing of the other ions. This probably accounts for the observation that Ca is on the borderline of apatite stability in terms of its radius.

The sequence Ca(II)...O(3)-P-O(3)...Ca(II) in $Ca_5(PO_4)_3OH$ is reproduced quite well in $Ca_4(PO_4)_2O$ in the sequences Ca(3)...O(22)-P(2)-O(23)...Ca(3); Ca(4)...O(12)-P(1)-O(13)...Ca(4); Ca(5)...O(33)-P(3)-O(32)...Ca(5); Ca(6)...O(41)-P(4)-O(44)...Ca(6). The O...Ca...O columns involving Ca(4), Ca(5) and Ca(6) are fairly straight, but the one involving Ca(3) and the oxygens of the $P(2)O_4$ group is more distorted than the others.

Epitaxy, the ordered growth of one substance on another, is often thought of as being governed chiefly by the metric fits of networks based on the unit cell translations. While epitaxy is certainly not rare, especially if the conditions under which the second phase is forced to grow on the first are sufficiently drastic, in practice only a few orientations are found. Under the mild conditions found *in vivo*, good chemical fits are obviously required. The combination of good metric and chemical fits between $Ca_5(PO_4)_3OH$ and $Ca_8H_2(PO_4)_6 \cdot 5H_2O$ makes epitaxy between these two compounds very important (Brown *et al.*, 1962; Brown, 1966). The unit cells of $Ca_5(PO_4)_3OH$ and $Ca_4(PO_4)_2O$ (Table 4) suggest that there will be many good metric fits of networks between these

two compounds. Because of the structural similarities between $Ca_5(PO_4)_3OH$ and $Ca_4(PO_4)_2O$, epitaxy between them may have considerable importance. Undetected epitaxy between $Ca_5(PO_4)_3OH$ and $Ca_4(PO_4)_2O$ would increase the Ca:P ratio of an apparent apatite above 1.667 and on a fine scale would resemble solid solution. It would also result in an increase in the apparent *c* unit cell dimension and probably a reduction in the apparent *a* dimension relative to the values for pure $Ca_5(PO_4)_3OH$, (because 3/2 (d_{100}) of $Ca_5(PO_4)_3OH$ is less than *b* of $Ca_4(PO_4)_2O$, while the two *a* dimensions are approximately equal). $Ca_5(PO_4)_3OH$ is therefore an unusual salt in that it has two related salts with which it may enter epitactical relationships. One salt, $Ca_8H_2(PO_4)_6 \cdot 5H_2O$, is more acidic, and the other, $Ca_4(PO_4)_2O$, is more basic.

Although production of $Ca_4(PO_4)_2O$ itself in an aqueous environment would be difficult because of the oxide ion, a carbonate-containing product may form more easily. $Ca_4(PO_4)_2O$ is known to react with CO_2 at elevated temperatures, although the reaction products have not yet been identified. Epitaxy between carbonation products of $Ca_4(PO_4)_2O$ and apatites may be important in the problem of carbonate apatites.

Acknowledgement

J. S. Bowen and P. B. Kingsbury provided technical help. This investigation was supported in part by research grant DE-00572 to the American Dental Association and by contract to the National Bureau of Standards from the National Institute of Dental Research. Much of the computer time was obtained through the facilities of the Computer Science Center, University of Maryland, College Park, Maryland 20742.

References

Alexander, L. E. and Smith, G. (1962). Acta Cryst., 15, 983-1004.

Alexander, L. E. and Smith. G. (1964). Acta Cryst., 17, 1195-1201.

Baur, W. H. (1970). Transactions of American Crystallographic Association, 6, 129-155.

Baur, W. H. and Khan, A. A. (1970). Acta Cryst., B26, 1584-1596.

Brown, W. E. (1962). Nature, 196, 1048-1050.

Brown, W. E. and Epstein, E. F. (1965). J. Res. NBS, 69A, 547-551.

Brown, W. E. (1966). Clinical Orthopedics, 44, 205-220.

Brown, W. E., Smith, J. P., Lehr, J. R. and Frazier, A. W. (1962). Nature, 196, 1050-1055.

Bücking, H. and Linck, G. (1887). Stahl und Eisen. 7, 245-249.

Cruickshank, D. W. J. (1961). J. Chem. Soc., 5486-5504.

Dickens, B. and Bowen, J. S. (1971a). Acta Cryst., B27, 2247-2255.

Dickens, B, Bowen, J. S. and Brown, W. E. (1971b). Abstract G3, American Crystallographic Association Winter Meeting, Columbia, S. C.

Dickens, B. and Brown, W. E. (1971c). Tschermaks Mineralogische und Petrographische, 16, 1-27.

Dickens, B. and Brown, W. E. (1971d). Tschermaks Mineralogische und Petrographische, 16, 79-104.

Dickens, B. and Brown, W. E. (1972). Acta Cryst., in press.

Dickinson, C., Stewart, J. M. and Holden, J. R. (1966). Acta Cryst., 21, 663-670.

Felsche, J. (1971). Naturwissen, 58, 565-566.

Gossner, B. (1928). N. Jb. Min. Geol. 57A, 89-116.

International Tables for X-ray Crystallography, (1962). The Kynock Press: Birmingham, England, Vol. III, p.202.

Kay, M. I., Young, R. A. and Posner, A. S. (1964). Nature, 204, 1050-1052.

Larson, A. C. (1970). In:"Crystallographic Computing", F. R. Ahmed, Editor, Munksgaard: Copenhagen, Denmark.

Oftedahl, I. (1927). Zeitsch. F. Phy. Chem. 128, 154-158.

Palache, C., Berman, H. and Frondel, C. (1951). The System of Mineralogy of J. D. Dana and E. S. Dana, 7th Edition, 2, J. Wiley and Sons, New York.

Pauling, L. (1960). The Nature of the Chemical Bond, 3rd Edition, p.559. Ithaca: Cornell University Press.

Reimann, C. W., Mighell, A. D. and Mauer, F. A. (1967). Acta Cryst. 23, 135-141.

Smolin, Y. I. and Tkachev, S. P. (1969). Soviet Physics - cryst. 14, 14-16.

Smolin, Y. I. (1970). Soviet Physics - cryst. 14, 854-858.

Stewart, J. M., Kruger, G. J., Ammon, H. L., Dickinson, C. and Hall, S. R. (1972). X-ray system of crystallographic programs, version of June, 1972.

Technical Report TR-192, The Computer Science Center, University of Maryland, College Park, Maryland 20742.

Termier, M. P. and Richard, M. (1895). Bull. Soc. France Min. 18. 391-395.

Trömel, G. and Fix, W. (1961). Arch. Eisenhüttenw. 32, 209-212.

Trömel, G. and Zaminer, C. (1959). Arch. Eisenhüttenw. 30, 205-209.

Wondratschek, H. (1963). N. Jb. Miner. Abh. 99, 113-160.

Zachariasen, W. H. (1963). Acta Cryst. 16, 1139-1144.

Zachariasen, W. H. (1967). Acta Cryst. 23, 558-564.

Figure legends

Figure 1. - A stereoscopic view of the $Ca_4(PO_4)_2O$ structure viewed along [100]. The origin of the crystallographic coordinate system is at the lower right front corner of the unit cell. Only a unique set of atoms is labelled.

Figure 2. - The environments of the Ca(1),Ca(2),Ca(3),Ca(4), $P(1)O_4$ and $P(2)O_4$ ions in $Ca_4(PO_4)_2O$. These ions lie in/ the same sheet parallel to (010).

Figure 3. - The environments of the Ca(5),Ca(6),Ca(7),Ca(8), $P(3)O_4$ and $P(4)O_4$ ions in $Ca_4(PO_4)_2O$. These ions lie in / the same sheet parallel to (010).

Figure 4. - A schematic drawing of the structure of $K_3Na(SO_4)_2$, glaserite (Gossner, 1928). One S,O,K column in the unit cell points "up" and the other points "down".

Figure 5. - The relationship of $Ca_4(PO_4)_2O$ to $K_3Na(SO_4)_2$ (glaserite) and $Ca_5(PO_4)_3OH$ (hydroxyapatite). The glaserite-type pseudo-cell in $Ca_4(PO_4)_2O$ is shown by ····· type lines. The actual cell of $Ca_4(PO_4)_2O$ is shown by light lines. The layer AA' is the "apatitic" layer in $Ca_4(PO_4)_2O$ and encompasses two sheets of [Ca,Ca] and [Ca,PO_4] columns (see text). The dotted lines show the vestiges in $Ca_4(PO_4)_2O$ of the Ca "hexagons" in $Ca_5(PO_4)_3OH$.

Figure 6. - An idealization of the $Ca_4(PO_4)_2O$ structure. The diagram in Figure 5 has been cut along the lines A and A', and the AA' layer moved to the left by ~2 Å. In this idealization the structure is hexagonal if the oxide ions O(1) and O(2) are either ignored or placed on the nearest [Ca,Ca] column. The $K_3Na(SO_4)_2$-type cell is represented

by -·····. A hexagonal-type cell is shown by dotted lines. A $Ca_5(PO_4)_3OH$-type cell is shown by lines of open squares.

Figure 7. - The structure of $Ca_5(PO_4)_3OH$ (Kay, Young and Posner, 1964). The OH site may be seen in the center of the Ca hexagon in the center of each unit cell. The shaded region is common to the structures of $Ca_5(PO_4)_3OH$ and $Ca_8H_2(PO_4)_6 \cdot 5H_2O$ (Brown, 1962). The layer BB' is common to the structures of $Ca_5(PO_4)_3OH$ and $Ca_4(PO_4)_2O$.

Figure 8. - A comparison of the apatitic layers in $Ca_4(PO_4)_2O$ (AA') and $Ca_5(PO_4)_3OH$ (BB').

Table 1. Atomic parameters in $Ca_4(PO_4)_2O$

Atom	x	y	z	10^4U_{11}*	10^4U_{22}	10^4U_{33}	10^4U_{12}	10^4U_{13}	10^4U_{23}
Ca(1)	0.0311(1)	0.3444	0.89441(9)	0.59(4)	0.59(4)	0.82(4)	0.01(3)	-0.12(3)	0.03(3)
Ca(2)	0.5320(1)	0.3000(1)	0.89733(9)	0.66(4)	0.82(4)	0.77(4)	-0.14(4)	-0.08(3)	-0.02(4)
Ca(3)	0.7654(1)	0.3040(1)	0.5299(1)	2.07(5)	0.45(5)	1.29(4)	0.00(4)	-0.20(4)	-0.07(4)
Ca(4)	0.2685(1)	0.3000(1)	0.25229(9)	0.70(4)	0.54(4)	0.64(3)	0.05(4)	-0.06(3)	-0.04(4)
Ca(5)	0.7409(1)	0.1068(1)	0.25600(9)	0.66(4)	0.81(5)	0.71(4)	-0.04(4)	-0.11(3)	0.00(3)
Ca(6)	0.2501(1)	0.0798(1)	0.01201(9)	0.96(4)	0.58(4)	0.70(4)	-0.08(3)	0.02(3)	-0.06(3)
Ca(7)	-0.0099(1)	0.0700(1)	0.63310(9)	0.72(4)	1.01(5)	0.89(4)	0.27(4)	-0.07(3)	0.23(4)
Ca(8)	0.5146(1)	0.0520(1)	0.59216(9)	0.60(4)	0.71(5)	1.09(4)	-0.04(3)	-0.04(3)	-0.17(3)
P(1)	0.7665(2)	0.3921(1)	0.2140(1)	0.64(5)	0.57(6)	0.57(5)	-0.02(4)	-0.07(4)	-0.02(4)
P(2)	0.2893(2)	0.3247(1)	0.6240(1)	0.80($)	0.55(6)	0.61(5)	-0.06(4)	0.00(4)	0.00(4)
P(3)	0.2376(2)	0.0400(1)	0.3181(1)	0.59(5)	0.59(6)	0.51(4)	-0.04(4)	-0.08(4)	0.00(4)
P(4)	0.7641(2)	0.0773(1)	0.9104(1)	0.54(5)	0.56(6)	0.62(4)	-0.04(4)	-0.10(4)	-0.07(4)
O(11)	0.7319(5)	0.5180(3)	0.2667(3)	1.2(2)	0.5(2)	0.8(1)	0.3(1)	-0.3(1)	-0.1(1)
O(12)	0.6113(4)	0.3244(3)	0.2860(3)	1.0(1)	2.2(2)	1.3(1)	-0.6(1)	-0.1(1)	0.9(1)
O(13)	0.9541(5)	0.3663(3)	0.2936(3)	1.1(2)	1.2(2)	1.5(2)	0.2(1)	-0.5(1)	-0.3(1)
O(14)	0.7702(5)	0.3650(3)	0.0556(3)	1.6(2)	1.6(2)	0.6(1)	-0.5(1)	0.0(1)	-0.2(1)
O(21)	0.2867(5)	0.4090(3)	0.7480(3)	1.3(2)	0.9(2)	0.8(1)	0.1(1)	0.1(1)	-0.1(1)
O(22)	0.0960(5)	0.2645(3)	0.6226(4)	1.0(2)	1.1(2)	2.4(2)	-0.1(1)	-0.5(1)	-0.1(1)
O(23)	0.4557(5)	0.2434(3)	0.6594(3)	1.2(2)	1.0(2)	1.5(2)	0.5(1)	-0.1(1)	-0.4(1)
O(24)	0.3309(6)	0.3802(3)	0.4843(3)	4.1(2)	1.1(2)	0.6(1)	-0.8(2)	0.7(2)	-0.2(1)
O(31)	0.2165(5)	0.0041(3)	0.4737(3)	1.7(2)	1.0(2)	0.7(1)	0.3(1)	0.0(1)	0.2(1)
O(32)	0.0766(5)	0.1137(3)	0.2626(3)	1.7(2)	1.0(2)	0.7(1)	0.3(1)	0.0(1)	0.2(1)
O(33)	0.4194(5)	0.1082(3)	0.3023(4)	0.9(2)	0.9(2)	3.5(2)	0.0(1)	0.2(1)	0.4(2)
O(34)	0.2444(5)	-0.0682(3)	0.2282(3)	1.4(2)	1.6(2)	1.3(2)	0.5(1)	-0.1(1)	-0.8(1)
O(41)	0.5890(5)	0.1053(3)	0.9992(3)	1.0(1)	1.7(2)	1.0(1)	0.1(1)	0.1(1)	-0.5(1)
O(42)	0.8384(5)	0.1855(3)	0.8407(3)	2.0(2)	0.3(2)	1.4(2)	-0.2(1)	-0.1(1)	0.1(1)
O(43)	0.7164(5)	-0.0028(3)	0.7862(3)	1.5(2)	0.6(2)	0.8(1)	0.1(1)	-0.3(1)	-0.3(1)
O(44)	0.9190(5)	0.0290(3)	1.0085(3)	1.2(2)	1.3(2)	1.4(2)	0.0(1)	-0.8(1)	0.1(1)
O(1)	0.2642(5)	0.2629(3)	0.0163(3)	1.0(1)	0.7(2)	0.8(1)	0.0(1)	0.0(1)	-0.1(1)
O(2)	0.7656(5)	0.1282(3)	0.4905(3)	1.1(2)	0.6(2)	0.6(1)	0.1(1)	-0.2(1)	-0.1(1)

* Thermal parameters have the form $\exp[-2\pi^2(U_{11}h^2a^{*2} + U_{22}k^2b^{*2} + U_{33}l^2c^{*2} + 2U_{12}hka^*b^* + 2U_{13}hla^*c^* + 2U_{23}klb^*c^*)]$

Figures in parentheses are standard deviations in last significant digit.

Table 2. Calculated and observed structure factors for $Ca_4(PO_4)_2O$. Columns are ℓ, 10 F_o, 10 F_c and 10 $\sigma(F_o)$. Unobserved reflections are those with intensity less than 2 $\sigma(I)$ and are marked by *.

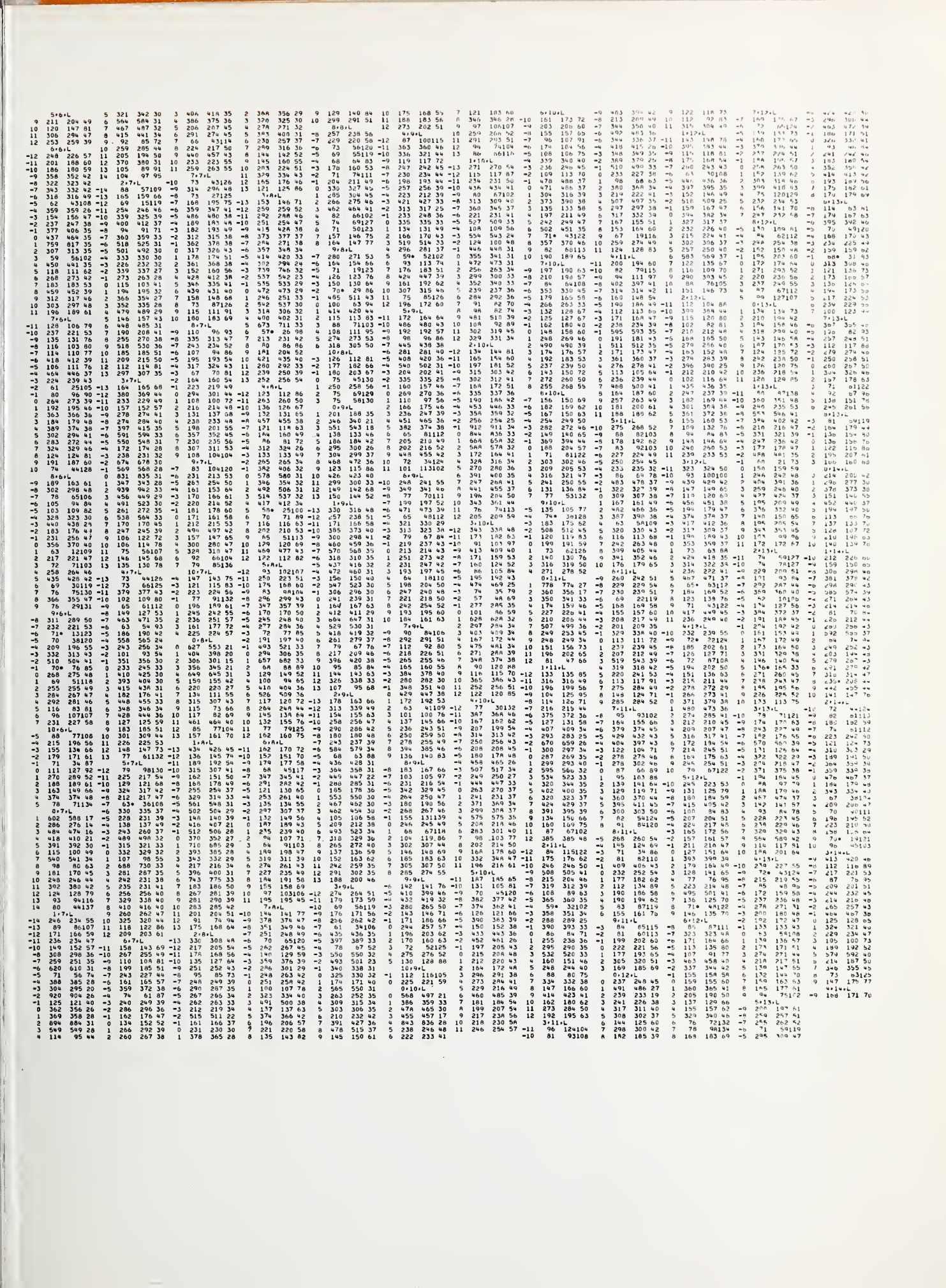

Table 3. Distances and angles in the $Ca_4(PO_4)_2O$ structure

atoms	distance, Å or angle, deg.
Cation environments	
Ca(1), O(1)	2.214(3)
Ca(1), O(42)	2.384(3)
Ca(1), O(21)	2.412(3)
Ca(1), O(14)	2.415(3)
Ca(1), O(44)	2.416(4)
Ca(1), O(34)	2.474(4)
Ca(1), O(22)	2.788(4)
Ca(2), O(1)	2.251(3)
Ca(2), O(14)	2.360(3)
Ca(2), O(23)	2.403(3)
Ca(2), O(34)	2.534(4)
Ca(2), O(41)	2.550(4)
Ca(2), O(21)	2.567(3)
Ca(2), O(42)	2.613(4)
Ca(3), O(2)	2.136(4)
Ca(3), O(31)	2.399(4)
Ca(3), O(22)	2.515(4)
Ca(3), O(12)	2.546(3)
Ca(3), O(23)	2.615(4)
Ca(3), O(13)	2.721(3)
Ca(3), O(34)	2.755(4)
Ca(4), O(1)	2.277(3)
Ca(4), O(13)	2.383(4)
Ca(4), O(43)	2.389(4)
Ca(4), O(24)	2.429(3)
Ca(4), O(12)	2.441(3)
Ca(4), O(33)	2.570(4)
Ca(4), O(32)	2.608(4)
Ca(5), O(2)	2.238(3)
Ca(5), O(33)	2.307(4)
Ca(5), O(32)	2.359(3)
Ca(5), O(21)	2.376(4)
Ca(5), O(41)	2.639(3)
Ca(5), O(12)	2.774(4)
Ca(5), O(44)	2.829(3)
Ca(6), O(1)	2.193(4)
Ca(6), O(11)	2.381(3)
Ca(6), O(44)	2.404(3)
Ca(6), O(41)	2.404(3)
Ca(6), O(14)	2.652(4)
Ca(6), O(34)	2.706(4)
Ca(6), O(32)	2.713(3)
Ca(6), O(33)	2.996(4)
Ca(7), O(2)	2.174(3)
Ca(7), O(31)	2.345(3)
Ca(7), O(11)	2.425(3)
Ca(7), O(22)	2.446(4)
Ca(7), O(13)	2.563(4)
Ca(7), O(43)	2.576(3)
Ca(7), O(42)	2.639(4)
Ca(8), O(2)	2.217(3)
Ca(8), O(43)	2.394(3)
Ca(8), O(23)	2.414(4)
Ca(8), O(31)	2.428(3)
Ca(8), O(24)	2.440(4)
Ca(8), O(11)	2.488(3)
Ca(8), O(33)	2.892(4)
Ca(8), O(12)	3.092(4)
PO_4 groups	
P(1), O(11)	1.531(4)
P(1), O(12)	1.527(4)
P(1), O(13)	1.539(4)
P(1), O(14)	1.534(3)
O(11), O(12)	2.533(5)
O(11), O(13)	2.471(5)
O(11), O(14)	2.461(5)
O(12), O(13)	2.459(5)
O(12), O(14)	2.512(5)
O(13), O(14)	2.579(5)
O(11), P(1), O(12)	111.8(2)°
O(11), P(1), O(13)	107.2(2)
O(11), P(1), O(14)	106.8(2)
O(12), P(1), O(13)	106.6(2)
O(12), P(1), O(14)	110.3(2)
O(13), P(1), O(14)	114.1(2)
P(2), O(21)	1.547(4) Å
P(2), O(22)	1.537(4)
P(2), O(23)	1.553(4)
P(2), O(24)	1.511(4)
O(21), O(22)	2.478(5)
O(21), O(23)	2.462(5)
O(21), O(24)	2.542(4)
O(22), O(23)	2.557(5)
O(22), O(24)	2.533(5)
O(23), O(24)	2.479(5)
O(21), P(2), O(22)	107.0(2)°
O(21), P(2), O(23)	105.2(2)
O(21), P(2), O(24)	112.5(2)
O(22), P(2), O(23)	111.7(2)
O(22), P(2), O(24)	112.4(2)
O(23), P(2), O(24)	108.0(2)
P(3), O(31)	1.543(3) Å
P(3), O(32)	1.521(4)
P(3), O(33)	1.524(4)
P(3), O(34)	1.550(4)
O(31), O(32)	2.572(5)
O(31), O(33)	2.506(5)
O(31), O(34)	2.489(5)
O(32), O(33)	2.431(5)
O(32), O(34)	2.498(5)
O(33), O(34)	2.535(5)
O(31), P(3), O(32)	114.1(2)°
O(31), P(3), O(33)	109.6(2)
O(31), P(3), O(34)	107.2(2)
O(32), P(3), O(33)	106.0(2)
O(32), P(3), O(34)	108.9(2)
O(33), P(3), O(34)	111.1(2)
P(4), O(41)	1.537(3) Å
P(4), O(42)	1.547(4)
P(4), O(43)	1.549(3)
P(4), O(44)	1.532(4)
O(41), O(42)	2.513(5)
O(41), O(43)	2.567(5)
O(41), O(44)	2.491(5)
O(42), O(43)	2.462(5)
O(42), O(44)	2.515(5)
O(43), O(44)	2.550(5)
O(41), P(4), O(42)	109.1(2)°
O(41), P(4), O(43)	112.6(2)
O(41), P(4), O(44)	108.5(2)
O(42), P(4), O(43)	105.3(2)
O(42), P(4), O(44)	109.5(2)
O(43), P(4), O(44)	111.7(2)
Oxygen atom environments	
(i) oxide ions	
O(1), Ca(6)	2.173(4) Å
O(1), Ca(1)	2.214(3)
O(1), Ca(2)	2.251(3)
O(1), Ca(4)	2.277(3)
O(2), Ca(3)	2.136(4)
O(2), Ca(7)	2.174(3)
O(2), Ca(8)	2.217(3)
O(2), Ca(5)	2.238(3)
Ca(6), O(1), Ca(1)	113.4(1)°
Ca(6), O(1), Ca(2)	103.0(1)
Ca(6), O(1), Ca(4)	102.3(1)
Ca(1), O(1), Ca(2)	105.6(1)
Ca(1), O(1), Ca(4)	115.1(1)
Ca(2), O(1), Ca(4)	117.0(1)
Ca(3), O(2), Ca(7)	102.1(1)
Ca(3), O(2), Ca(8)	109.0(1)
Ca(3), O(2), Ca(5)	106.6(1)
Ca(7), O(2), Ca(8)	100.0(1)
Ca(7), O(2), Ca(5)	128.6(2)
Ca(8), O(2), Ca(5)	109.5(1)
(ii) PO_4 oxygens	
O(11), Ca(6)	2.381(3) Å
O(11), Ca(7)	2.425(3)
O(11), Ca(8)	2.488(3)
O(12), Ca(4)	2.441(3)
O(12), Ca(3)	2.546(3)
O(12), Ca(5)	2.774(4)
O(13), Ca(4)	2.383(4)
O(13), Ca(7)	2.563(4)
O(13), Ca(3)	2.721(3)
O(14), Ca(2)	2.360(3)
O(14), Ca(1)	2.415(3)
O(14), Ca(6)	2.652(4)
O(21), Ca(5)	2.376(4)
O(21), Ca(1)	2.412(3)
O(21), Ca(2)	2.567(3)
O(22), Ca(7)	2.446(4)
O(22), Ca(3)	2.515(4)
O(22), Ca(1)	2.788(4)
O(23), Ca(2)	2.403(3)
O(23), Ca(8)	2.414(4)
O(23), Ca(3)	2.615(4)
O(24), Ca(4)	2.429(3)
O(24), Ca(8)	2.440(4)
O(31), Ca(7)	2.345(3)
O(31), Ca(3)	2.399(4)
O(31), Ca(8)	2.428(3)
O(32), Ca(5)	2.359(3)
O(32), Ca(4)	2.608(4)
O(32), Ca(6)	2.713(3)
O(33), Ca(5)	2.307(4)
O(33), Ca(4)	2.570(4)
O(33), Ca(8)	2.892(4)
O(33), Ca(6)	2.996(4)
O(34), Ca(1)	2.474(4)
O(34), Ca(2)	2.534(4)
O(34), Ca(6)	2.706(4)
O(34), Ca(3)	2.755(4)
O(41), Ca(6)	2.404(3)
O(41), Ca(2)	2.550(4)
O(41), Ca(5)	2.639(3)
O(42), Ca(1)	2.384(3)
O(42), Ca(2)	2.613(4)
O(42), Ca(7)	2.639(4)
O(43), Ca(4)	2.389(4)
O(43), Ca(8)	2.394(3)
O(43), Ca(7)	2.576(3)
O(44), Ca(6)	2.404(3)
O(44), Ca(1)	2.416(4)
O(44), Ca(5)	2.829(3)

The figures in parentheses are the standard deviations in the last significant digit.

Table 4

A Comparison of the Unit Cells of

$Ca_5(PO_4)_3OH$(I) and $Ca_4(PO_4)_2O$(II)

	I	II
a	9.432 Å	9.462 Å
b	9.432	11.965
c	6.881	7.023
γ	120°	90.8°
vol.	530 $Å^3$	795 $Å^3$
space group	$P6_3/m$	$P2_1$

d_{100}(I) x 1.5 = 12.27 Å

530 $Å^3$ x 1.5 = 795 $Å^3$

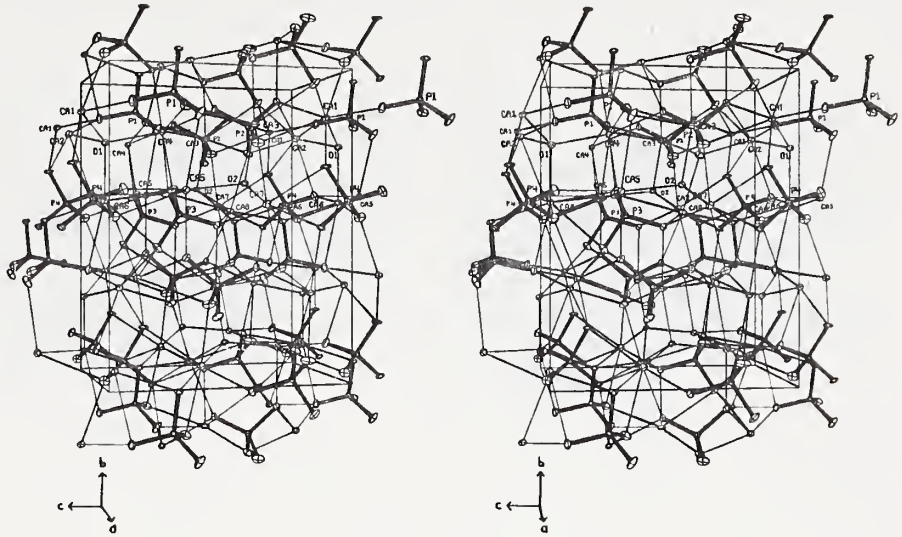

Figure 1 - A stereoscopic view of the $Ca_4(PO_4)_2O$ structure viewed along [100]. The origin of the crystallographic coordinate system is at the lower right front corner of the unit cell. Only a unique set of atoms is labelled.

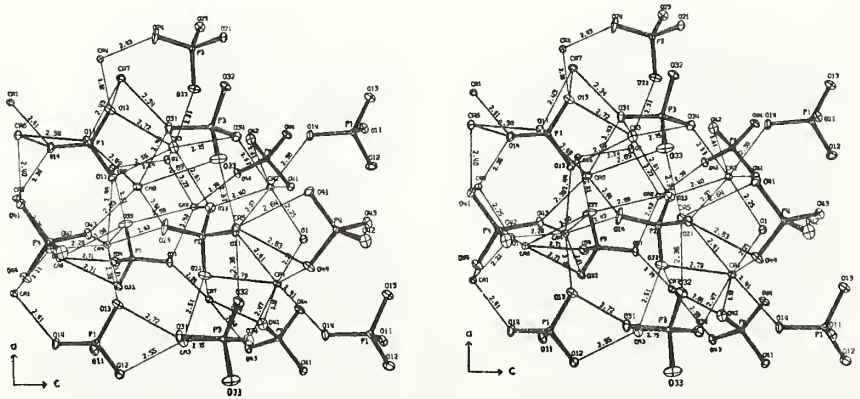

Figure 2 - The environments of the Ca(1),Ca(2),Ca(3),Ca(4), $P(1)O_4$ and $P(2)O_4$ ions in $Ca_4(PO_4)_2O$. These ions lie in the same sheet parallel to (010).

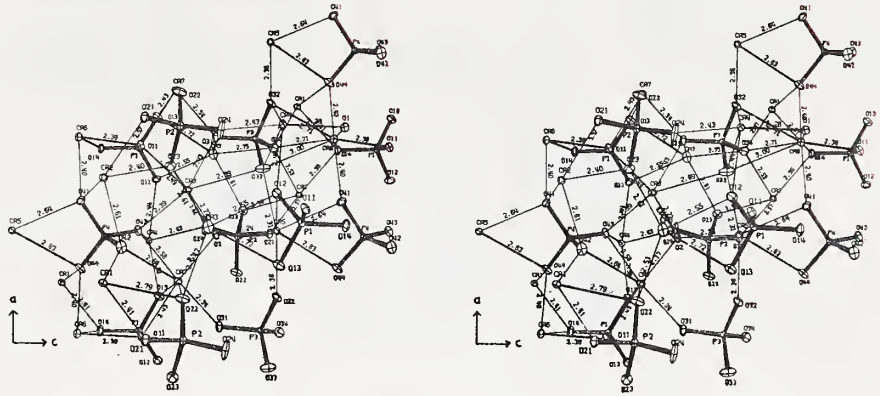

Figure 3 - The environments of the Ca(5),Ca(6),Ca(7),Ca(8), $P(3)O_4$ and $P(4)O_4$ ions in $Ca_4(PO_4)_2O$. These ions lie in the same sheet parallel to (010).

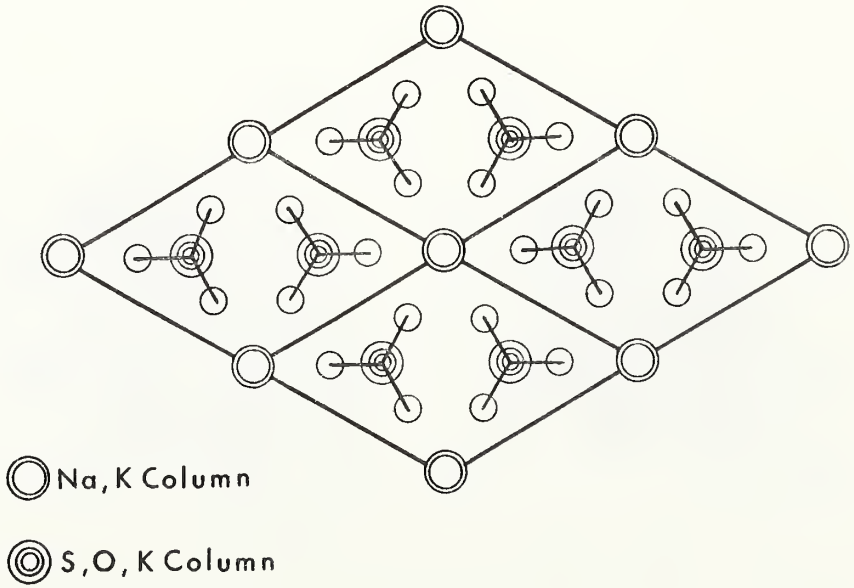

Figure 4 - A schematic drawing of the structure of $K_3Na(SO_4)_2$, glaserite (Gossner, 1928). One S,O,K column in the unit cell points "up" and the other points "down".

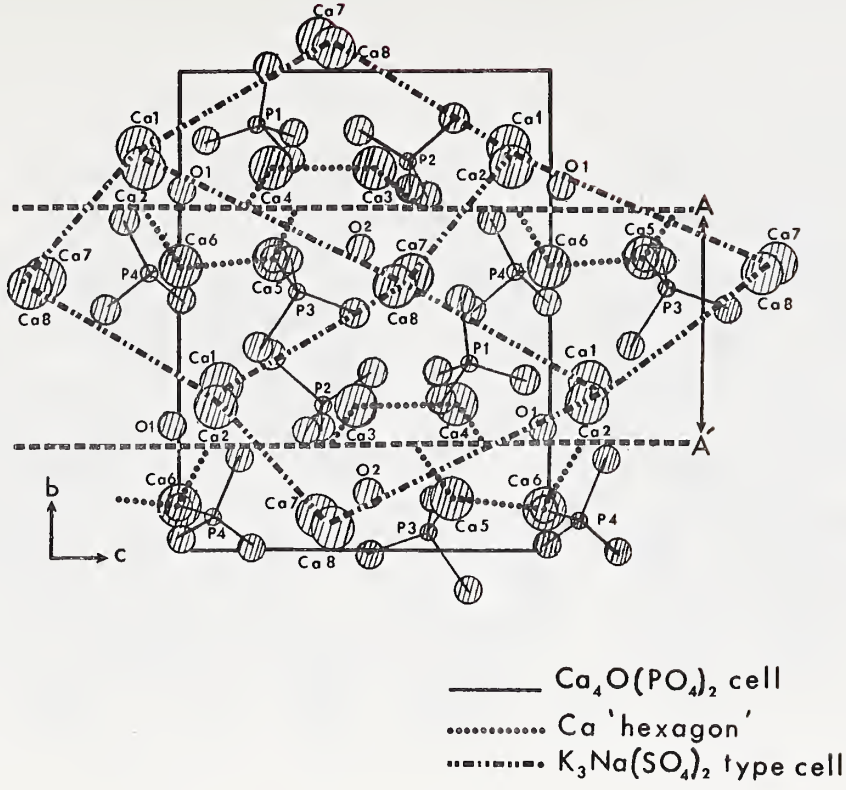

Figure 5 - The relationship of $Ca_4(PO_4)_2O$ to $K_3Na(SO_4)_2$ (glaserite) and $Ca_5(PO_4)_3OH$ (hydroxyapatite). The glaserite-type pseudo-cell in $Ca_4(PO_4)_2O$ is shown by ··-·· type lines. The actual cell of $Ca_4(PO_4)_2O$ is shown by light lines. The layer AA' is the "apatitic" layer in $Ca_4(PO_4)_2O$ and encompasses two sheets of [Ca,Ca] and [Ca,PO_4] columns (see text). The dotted lines show the vestiges in $Ca_4(PO_4)_2O$ of the Ca "hexagons" in $Ca_5(PO_4)_3OH$.

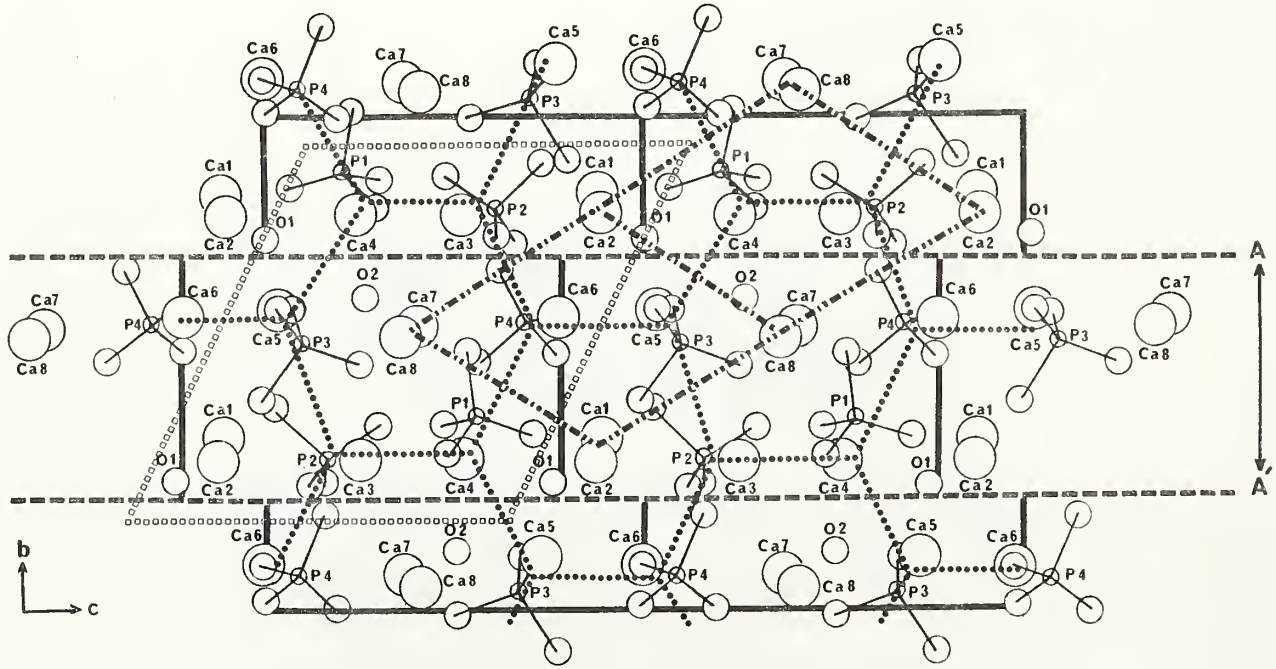

Figure 6 - An idealization of the $Ca_4(PO_4)_2O$ structure. The diagram in Figure 5 has been cut along the lines A and A', and the AA' layer moved to the left by ~2 Å. In this idealization the structure is hexagonal if the oxide ions O(1) and O(2) are either ignored or placed on the nearest [Ca,Ca] column. The $K_3Na(SO_4)_2$-type cell is represented by -·-·-·. A hexagonal-type cell is shown by dotted lines. A $Ca_5(PO_4)_3OH$-type cell is shown by lines of open squares.

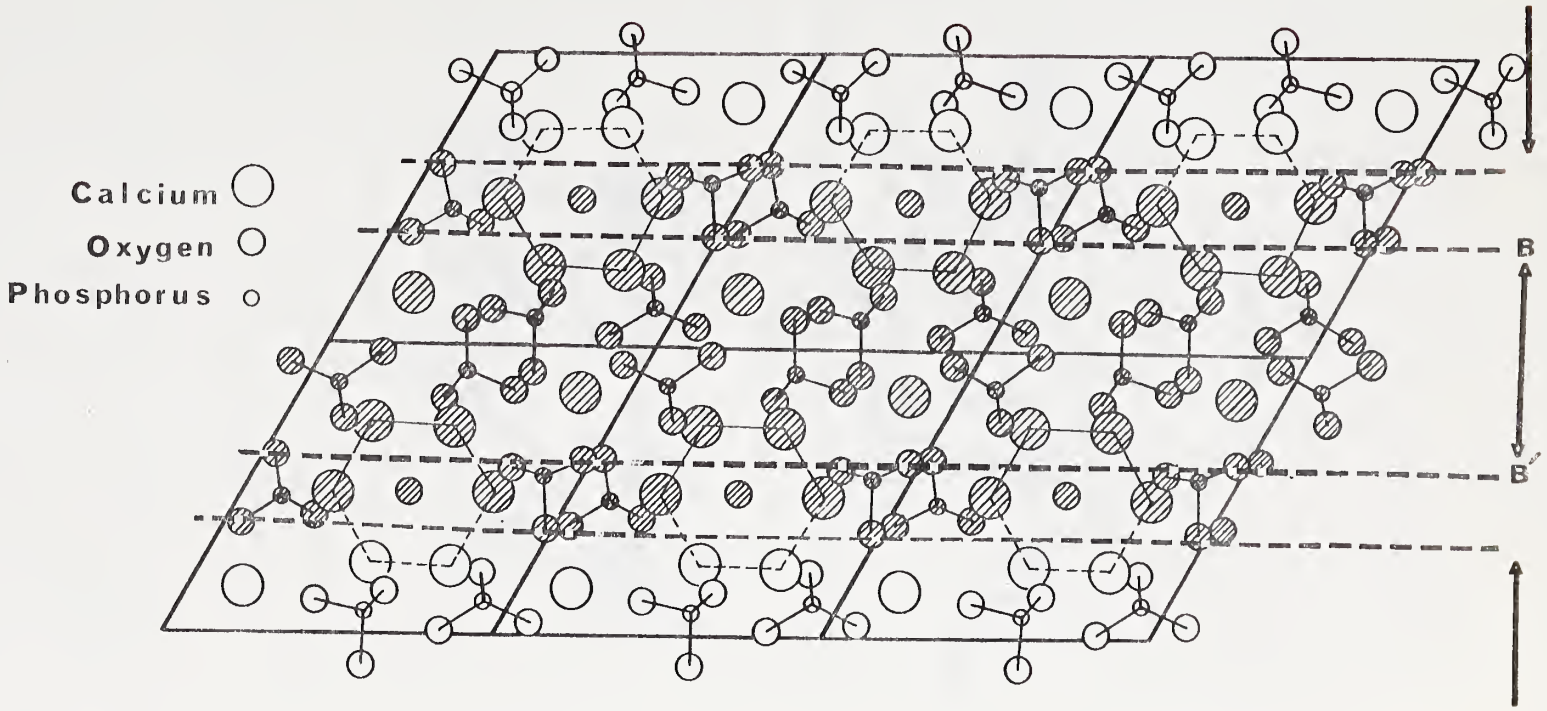

Figure 7 - The structure of $Ca_5(PO_4)_3OH$ (Kay, Young and Posner, 1964). The OH site may be seen in the center of the Ca hexagon in the center of each unit cell. The shaded region is common to the structures of $Ca_5(PO_4)_3OH$ and $Ca_8H_2(PO_4)_6 \cdot 5H_2O$ (Brown, 1962). The layer BB' is common to the structures of $Ca_5(PO_4)_3OH$ and $Ca_4(PO_4)_2O$.

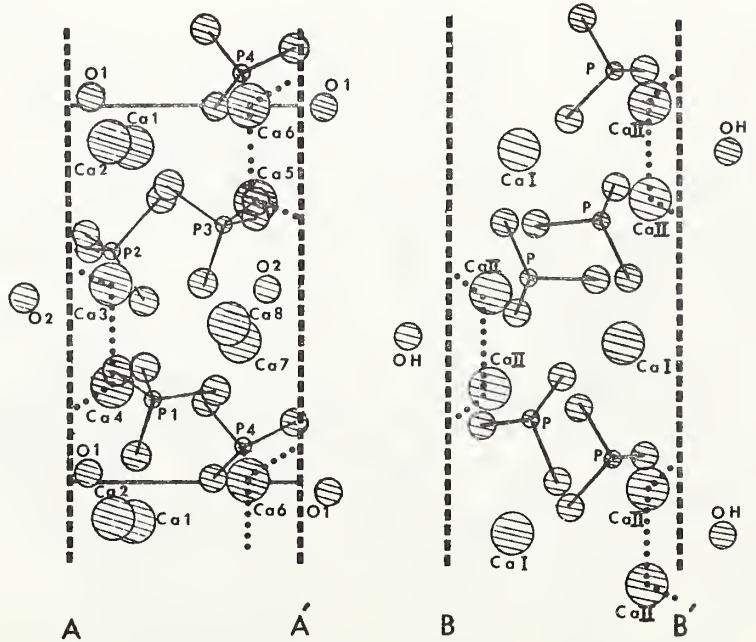

Figure 8 - A comparison of the apatitic layers in $Ca_4(PO_4)_2O$ (AA') and $Ca_5(PO_4)_3OH$ (BB').

THE REACTION OF DICALCIUM PHOSPHATE DIHYDRATE WITH FLUORIDE

By

L. C. Chow and W. E. Brown

INTRODUCTION

The reaction of hydroxyapatite (OHAp), $Ca_5(PO_4)_3OH$, with a fluoride solution to form fluorapatite (FAp), $Ca_5(PO_4)_3F$, is used extensively to reduce dental caries, but it proceeds slowly with poor yields. As a result, the amount of fluoride permanently taken up by enamel after a topical treatment is low; furthermore, the depth of fluoride penetration into enamel is small. Recent work[1] has shown that tooth enamel acquired larger amounts of fluoride when pretreated with dilute phosphoric acid before being exposed to the fluoride-containing solution; the deposited fluoride in this process seemed to be retained more permanently. The mechanism behind this effect has not been reported. As described below, it is believed that the intermediate formation of an acid calcium phosphate and its subsequent conversion to FAp and/or CaF_2 may be a major factor in this improvement.

One would expect from the phase diagram for the system $Ca(OH)_2$-H_3PO_4-H_2O[2,3] that dicalcium phosphate dihydrate (DCPD), $CaHPO_4 \cdot 2H_2O$, or dicalcium phosphate anhydrous (DCPA), $CaHPO_4$, would form when tooth enamel is treated with saturated DCPD solutions or with phosphoric

acid more concentrated than approximately 3.4×10^{-3}M and less concentrated than about 3 M. Of these two dicalcium phosphates, DCPA is the more stable and would be the final equilibrium product in the acid range of concentrations. However, DCPD is known to be capable of forming more rapidly than DCPA and to persist for relatively long periods at ambient temperatures. Thus, DCPD is expected to form on tooth enamel when the acidic solution is applied topically. In support of this, a number of studies have shown that DCPD is produced by treating OHAp or tooth enamel with acids. Gray and Francis[4] reported the existence of DCPD on the surface of enamel samples equilibrated with weak acid buffers; McCann and Brudevold[5] showed that DCPD is formed by shaking OHAp in a 0.5 M phosphoric acid solution. More recently, Patel and Brown[6] found DCPD crystals when powdered tooth enamel was equilibrated with 0.02 M phosphoric acid; LeGeros and Klein[7] reported the growth of DCPD crystals on teeth immersed in phosphate solutions at pH range of 3 to 7. In view of these findings, it appears that DCPD is likely to form when tooth enamel receives the presently used 0.05 M phosphoric acid pretreatment during the topical application.

The reaction of OHAp with fluoride to form FAp takes place with virtually no change in crystal volume because the two compounds are isostructural. As a result, the OHAp crystal may become covered with a thin layer of FAp coating. Further reaction would thus require the diffusion of F^- and OH^- ions through the solid. This would properly be described as a solid-state reaction and one would expect it to take place much more slowly than diffusion in a liquid. For this reason the conversion of the interior of OHAp crystals into FAp seems far too slow to occur to the desired extent in a clinical situation. In contrast to OHAp, the reaction of fluoride with DCPD proceeds quite rapidly because the loss of water and phosphate ions inherent to the reaction results in a shrinkage in the volume of the crystal. The F^- ions may, therefore, penetrate into the crystal through the openings produced by the shrinkage.

Since DCPD can easily be formed in enamel and it reacts rapidly with fluoride, we propose that FAp may be formed more efficiently from OHAp in tooth enamel through the path,

$$\text{OHAp} \xrightarrow[\text{pretreatment}]{\text{acid}} \text{DCPD} \xrightarrow{F^-} \text{FAp} \ .$$

Accordingly, OHAp would first be partially converted to DCPD by an acidic pretreatment which then reacts with fluoride to form FAp.

In preliminary experiments[8] designed to study the feasibility of this proposed path, extracted human tooth enamel was pretreated with saturated DCPD solutions (to produce some DCPD on enamel) before being exposed to the fluoride solution. The F deposition in this process was found to be consistently greater than that from sodium fluoride or acidulated phosphate-fluoride treatments alone. A quantitative study on the formation of DCPD from enamel will be reported in a subsequent paper. The present work deals with the second step in the proposed path, i.e., the reaction of DCPD with fluoride.

Although the reaction of DCPD with fluoride is known to proceed rapidly, there is uncertainty as to the products formed. McCann and Brudevold[5] reported that OHAp was formed when DCPD was equilibrated for ten weeks at 34°C in 0.02 M iminazol buffers (pH = 6.2) containing 0.01 to 0.5 mM of F^- ions. Iizuka and Ohashi[9], on the other hand, concluded that DCPD appeared to be unchanged under similar conditions when F^- concentrations were below 10 ppm (0.526 mM). Duff[10], in a more recent work, calculated the free energies of formation of FAp, OHAp and DCPD at

25°C assuming that complete conversion of DCPD to FAp was attainable by equilibrating DCPD with 0.1 M KF solution. In addition to apatite, CaF_2 is also likely to be a product of this reaction particularly under high F^- concentrations.

In order to obtain quantitative information concerning the products, the reactions of DCPD with solutions containing systematically varied amounts of F^- and PO_4^{3-} ions were studied. In view of the activity products of the two most probable products, i.e., $Ca_5(PO_4)_3F$ and CaF_2, the activities of the F^- and PO_4^{3-} ions are thought to be the major factors governing the choice between the possible reaction paths. If the effectiveness of a topical agent is proportional to its ability to incorporate fluoride as fluorapatite in enamel[11], the results obtained in this study may provide information needed in searching for the most appropriate fluoride treatment when some DCPD has been produced by a prior treatment in the topical application.

EXPERIMENTAL

DCPD was prepared by the method described by Moreno, Brown and Osborn[13]. Chemical analysis of this salt yielded (vs. theoretical) Ca, 23.1% (23.3) and P, 18.0% (18.0). Petrographically the material appeared as pure, homogeneous DCPD. The sodium fluoride and trisodium phosphate reagents were prepared from high purity commercial products; they were used without further purification. Solutions containing various concentrations of NaF and Na_3PO_4 were prepared by either adding appropriate amounts of the solid materials to or diluting the stock solutions of NaF and Na_3PO_4 with CO_2-free distilled water. Figure 1 shows the compositions of the solutions prepared.

50 ml aliquots of the solutions were transferred to 125 ml polypropylene Erlenmyer flasks; the flasks were capped with ----------

polyethylene stoppers and then placed in a water bath kept at 25 ± 0.1°C. After the solutions reached bath temperature, 0.5 g portions of DCPD were added to each flask. The samples were agitated continuously by a shaking mechanism. The pH of each solution was measured twice daily and the equilibration process was continued until the change was less than 0.02 pH units per day. The solid and liquid portions of the samples were then separated by filtration. The filtrates were subjected to final pH measurement and chemical analyses for P and F. Ca analysis was not done because many of the solutions were extremely low in Ca (less than 10^{-6} M) and were highly concentrated with respect to P and F which interfere with the Ca determination. The solid portions of the samples were washed briefly in distilled water and in acetone and were then air dried. They were then characterized by powder X-ray diffractometry and petrographic examination and analyzed for Ca, P and F.

It was observed, in several cases, that there is an appreciable change in the solution pH between the initial and final states of the reaction. For these cases, a duplicate reaction was carried out in which the pH was monitored continuously. A representative recording of pH versus time (for sample No. 24) is shown in Figure 3. An interpretation of the pH change as related to the progress of reaction is given in the discussion section.

The pH measurements were made to within 0.01 pH unit with a combination electrode and a pH meter with a readability of 0.001 pH unit. Ca was determined by atomic absorption[13] with an estimated relative error of 0.02 . P analyses (relative error 0.015) were carried out using the vanado-molybdate reagent of Brabson, et al.[14]. F was determined (relative error 0.02) by the method of McCann[15]. Petrographic examinations were made with a standard polarizing microscope. X-ray diffraction was carried out on a diffractometer with CuK_α radiation filtered through Ni foil.

RESULTS

Table I shows the initial and final conditions of the liquids. These include the pH, P and F concentrations. The Ca, P and F contents of the solids are listed in Table II; also shown in this table are the Ca/P and Ca/F molar ratios and the major solid phases of the samples as identified by X-ray diffraction and/or petrographic examination. Solids precipitated from solutions that were high in sodium concentration and, as a result, highly alkaline (e.g., Nos. 13 and 19) were found to contain small amounts of sodium (less than 3 wt.%). Infrared spectra of these samples also showed detectable carbonate peaks at 1440 and 670 cm^{-1}. It appears that CO_2 still entered the system under highly alkaline conditions

despite the use of CO_2-free distilled water and closed reaction vessels. (The plastic used in these vessels is not totally impervious to CO_2.) The manner of incorporation of sodium and carbonate in the solids is not known, and their presence is neglected in the subsequent discussion.

It is seen from Table II that fluoride was incorporated into the solids in all cases. Within each group of constant initial F^- concentration (e.g., Nos. 2, 3, 4, 5 and 6), the amount of fluoride in the solids increased with decreasing initial Na_3PO_4 concentration in the solution. The phosphate content of the solids, on the other hand, decreased under the same circumstances. Within each group of samples with a given initial Na_3PO_4 concentration (e.g., Nos. 2, 8, 14 and 20), the amount of fluoride incorporated decreased with decreasing F^- concentration in the solution; the phosphate content again showed a trend opposite to that of fluoride.

DISCUSSION

Since none of the samples was found to possess Ca/P and Ca/F molar ratios close to those of CaF_2, FAp or OHAp, they appeared to be mixtures of compounds rather than pure substances. While the major phases of the samples were qualitatively identified as shown in Table II, the amounts present were estimated quantitatively from the Ca/P and Ca/F values. Ca/P and Ca/F ratios, representing two independent

pieces of information on sample composition, permitted the construction of two simultaneous mass balance equations. Therefore, it was necessary to make an assumption that no more than three solid phases were present in any given sample.

DCPD is a possible phase in all cases because complete conversion of DCPD is not expected. ----------
For the remaining two phases the following combinations are possible: (i) FAp and CaF_2 and (ii) FAp and OHAp. The solubility behaviors of OHAp and CaF_2 are such that they are not likely to precipitate from the same solution either simultaneously or subsequently. Therefore, the possibility of having both OHAp and CaF_2 present can be eliminated. In the first case where the solids are assumed to consist of FAp, CaF_2 and DCPD the mass balance of Ca, P and F can be expressed by the following two equations:

$$\frac{Ca}{P} = \frac{\frac{X}{F.W._{CaF_2}} + \frac{5Y}{F.W._{FAp}} + \frac{1-X-Y}{F.W._{DCPD}}}{\frac{3Y}{F.W._{FAp}} + \frac{1-X-Y}{F.W._{DCPD}}} \qquad (1)$$

$$\frac{Ca}{F} = \frac{\frac{X}{F.W._{CaF_2}} + \frac{5Y}{F.W._{FAp}} + \frac{1-X-Y}{F.W._{DCPD}}}{\frac{2X}{F.W._{CaF_2}} + \frac{Y}{F.W._{FAp}}} \qquad (2)$$

where X, Y and 1-X-Y, respectively, are the numbers of grams

of CaF_2, FAp and DCPD present in one gram of sample; $F.W._{CaF_2} = 78.08$, $F.W._{FAp} = 504.4$ and $F.W._{DCPD} = 136.06$ are the formular weights of the respective compounds.

In the case where OHAp, FAp and DCPD are present, the following two equations can be set up using previously defined symbols except that X and $F.W._{OHAp} = 502.4$ now denote the corresponding quantities for OHAp:

$$\frac{Ca}{P} = \frac{\frac{5X}{F.W._{OHAp}} + \frac{5Y}{F.W._{FAp}} + \frac{1-X-Y}{F.W._{DCPD}}}{\frac{3X}{F.W._{OHAp}} + \frac{3Y}{F.W._{FAp}} + \frac{1-X-Y}{F.W._{DCPD}}} \qquad (3)$$

$$\frac{Ca}{F} \equiv \frac{\frac{5X}{F.W._{OHAp}} + \frac{5Y}{F.W._{FAp}} + \frac{1-X-Y}{F.W._{DCPD}}}{\frac{Y}{F.W._{FAp}}} \quad . \qquad (4)$$

The Ca/P and Ca/F values of the samples were substituted into both sets of the two simultaneous equations to solve for X and Y. As expected, only one of the two sets of equations was found to be applicable to any given sample, i.e., to yield positive values for the quantities X, Y and 1-X-Y. The computed percentage compositions of the samples are shown in the last four columns in Table II. A graphical presentation showing these estimated sample compositions and the initial experimental condition, as listed in Table I, is given in Figure 2.

The principal conclusions of this study are made evident by inspection of Figure 2. When PO_4^{3-} ions are not added to the system, the formation of FAp over CaF_2 is favored only at low F^- concentrations (10^3 ppm or less). CaF_2 is the predominant product at higher F^- concentrations; this observation is in harmony with the findings of several investigations[16,17] that CaF_2 was the major product formed from the reaction of tooth enamel or dentin with APF* or 2% NaF solutions. The introduction of PO_4^{3-} ions stabilizes the formation of apatite and thus suppresses CaF_2 precipitation. As a result, in the presence of Na_3PO_4 (at the concentration of 0.05 M or higher), FAp can be produced from more concentrated (10^4 ppm) F^- solutions. Under similar Na_3PO_4 concentrations, partially fluoridated hydroxyapatite is formed from solutions with lower F^- concentrations. The apatite materials formed in the more concentrated PO_4^{3-} and F^- solutions are generally in poorer crystalline form than are the materials formed from dilute solutions. This is probably because the former were precipitated under more alkaline conditions.

---

* 1.23% fluoride from NaF and HF in a 0.1 M phosphoric acid solution (Acidulated Phosphate Fluoride).

The calculations based on the chemical analyses suggest that small amounts of DCPD are present in most of the samples. The residual DCPD could be due to the incompleteness of conversion, but the possible substitution of sodium for calcium in the solids, producing lower Ca/P values, may account for a portion of the calculated DCPD presence. The presence of DCPD in the samples does not seem to mask the clear trends of FAp and CaF_2 formation discussed in the preceeding section.

In some cases (as shown in Table I) there is an appreciable change in the solution pH between the initial and final states of the reaction. In these cases, the change in pH may therefore provide some information on the progress of reaction. Shown in Figure 3 (curve a) is the pH change versus time for sample No. 24. The product formed in this reaction was predominantly FAp as indicated in Table II and Figure 2. Since FAp is a more basic salt than DCPD, the drop of pH (from 7 to 4.3) is expected. There is an initial surge of pH from 7 to 7.5 which then falls back to 7.3. This is believed to be due to the rapid dissolution of DCPD before the precipitation of FAp begins. Following this initial change the pH remained at 7.3 for more than 1.5 hours before going down steadily toward the final reading of 4.3. In a separate run of a similar experiment (0.5 g of DCPD was placed in 500 ml

of solution containing 500 ppm F^-) the solid portion was separated from the solution at the time when pH was at the plateau. Petrographic examination of the solid indicated that CaF_2 was present in the form of small granuals deposited on essentially unaltered DCPD crystals. The x-ray diffraction pattern showed that this material was predominantly DCPD with detectable CaF_2 peaks at 28.3° and 47° 2θ. No FAp appeared to have formed at this stage. These observations suggest that there is a rather long induction period during which nuclei of FAp are formed with CaF_2 precipitating at the same time.

Duff[10] carried out a similar experiment in which DCPD was added to a 0.1 M KF solution. It can be seen in Table I of Reference 10 that a pattern of pH changes similar to the one reported here was observed; the pH increased initially to 7.30 and remained at this value for one hour followed by a steady decrease to the final value of 3.14. An examination of the data given in this table suggested that calcium fluoride may have formed initially as indicated by the relative amounts of fluoride and calcium ions removed from the solution. The ratio of F/Ca removed from the solution is 1.89 during the first stage (when pH was kept constant at 7.3) of the reaction suggesting the predominance of CaF_2 formation. The ratio decreased with decreasing pH and finally reached 0.251.

(It may be adjusted to 0.248 if one assumes that all the potassium ions lost from the solution went on to the calcium sites in apatite.) Since the formation of pure FAp would result in a ratio of 0.200, the final product appears (as estimated from the analytical data for the liquid) to be a mixture of predominantly FAp with some CaF_2. The first order fluoride uptake and the second order phosphate release reported in Reference 10 may possibly result from the initial formation of CaF_2.

After the induction period (Fig. 3), FAp seemed to precipitate out rapidly (as indicated by the steady falling of pH). In a separate run of a similar experiment, a small quantity of OHAp was mixed with DCPD before the addition of the solid into the solution. The pH change of this reaction (Fig. 3, curve b) showed no apparent induction period suggesting that OHAp acts as a template for the growth of FAp crystals.

FAp is very possibly a more desirable reservoir of fluoride than CaF_2 in the oral environment because the latter is thought to be more soluble in saliva and too quickly lost by dissolution to provide lasting benefits. Although this view remains unproven, it appears reasonable and seems to be widely accepted. The findings reported here suggest that the formation of CaF_2 in topical treatments can be reduced sub-

stantially if a solution containing appropriate amounts of F^- and PO_4^{3-} ions, as indicated in Figure 2, is used. When some DCPD has been formed by a pretreatment, a dilute (10^3 ppm or less) fluoride solution should produce FAp on tooth enamel without forming appreciable amounts of CaF_2. However, it appears advantageous to use more concentrated fluoride-phosphate solutions, which still produce FAp instead of CaF_2, because they may additionally provide greater fluoride penetration. In some cases, CaF_2 may form initially partly because at that time the F^- concentration is high. FAp, which is the more stable product under the equilibrium situation, would precipitate after the induction period is over; this causes the redissolution of CaF_2. The initial precipitation of CaF_2 is reduced by the presence of apatite crystals which seem to shorten the induction period and to act as templates for the formation of FAp. This effect parallels that of excess PO_4^{3-} ions in solution which stabilize the formation of apatite over CaF_2.

References

1. Aasenden, R., Brudevold, F. and McCann, H. G.: The Response of Intact and Experimentally Altered Human Enamel to Topical Fluoride, Arch Oral Biol 13:543-552, 1968.

2. Moreno, E. C., Gregory, T. M. and Brown, W. E.: Preparation and Solubility of Hydroxyapatite, J Res NBS, 72A:773-782, 1968.

3. Farr, T. D., Tarbutton, G. and Lewis, Jr., H. T.: System $CaO-P_2O_5-HF-H_2O$: Equilibrium at 25 and 50°, J Phys Chem 66:318-321, 1962.

4. Gray, J. A. and Francis, M. D.: Physical Chemistry of Enamel Dissolution, in Sognnaes, R. F. (ed.): Mechanisms of Hard Tissue Destruction, Washington, D. C.: American Association for the Advancement of Science, 1963, pp. 253-257.

5. McCann, H. G. and Brudevold, F.: The Mechanism of the Caries-Inhibiting Effect of Fluoride, in Kreshover, S. J. and McClure, F. J. (eds.): Environmental Variables in Oral Disease, Washington, D. C.: American Association for the Advancement of Science, 1966, pp. 121-123.

6. Patel, P. R. and Brown, W. E.: Solubility Behavior of Powdered Human Tooth Enamel at 25°C, abstracted, IADR Program and Abstracts of Papers, No. 801, 1971.

7. LeGeros, R. Z. and Klein, E.: Brushite Crystals Grown by Diffusion, abstracted, IADR Program and Abstracts of Papers, No. 466, 1972.

8. Chow, L. C. and Brown, W. E.: Incorporation of Fluoride into Tooth Enamel, abstracted, IADR Program and Abstracts of Papers, No. 65, 1971.

9. Iizuka, Y. and Ohashi, K.: Experiment with Apatites and the Effect of Fluoride - II, Bull Tokyo Dent Coll., 11: 1-9, 1970.

10. Duff, E. J.: Orthophosphates, Part II. The Transformations Brushite → Fluorapatite and Monotite → Fluorapatite in Aqueous Potassium Fluoride Solution, J Chem Soc (A), 33-38, 1971.

11. Brudevold, F., McCann, H. G., Nilsson, R., Richardson, B. and Coklica, V.: The Chemistry of Caries Inhibition Problems and Challenges in Topical Treatments, J Dent Res, 46:37-45, 1967.

12. Moreno, E. C., Brown, W. E. and Osborn, G.: Solubility of Dicalcium Phosphate Dihydrate in Aqueous Systems, Soil Sci Soc Am Proc, 24:94-98, 1960.

13. Willis, J. B.: The Determinations of Metals in Blood Serum by Atomic Absorption Spectroscopy-I Calcium, Spectrochim Acta, 16:259-262, 1960.

14. Brabson, J. A., Dunn, R. L., Epps, E.A., Hoffman, W.M. and Jacob, K. D.: Report on Phosphorus in Fertilizers: Photometric Determination of Total Phosphorus, JAOAC, 41:517-524, 1958.

15. McCann, H. G.: Determination of Fluoride in Mineralized Tissue Using the Fluoride Ion Electrode, Arch Oral Biol, 13:475-477, 1968.

16. Wei, S. H. Y. and Forbes, W. C.: X-ray Diffraction Analyses of the Reactions Between Intact and Powdered Enamel and Several Fluoride Solutions, J Dent Res, 47: 471-477, 1968.

17. Wei, S. H. Y. and Forbes, W. C.: Reactions of Powdered Sound Dentin with Several Fluoride Solutions, J Dent Res, 48:149-152, 1969.

Figure 1

F^- / PO_4^{3-}	0.526M	0.263	0.0526	0.0263
	10^4 ppm	5×10^3	10^3	5×10^2
0.5M	*	*	#13	#19
0.1	#2	#8	#14	#20
0.05	#3	#9	#15	#21
0.01	#4	#10	#16	#22
0.001	#5	#11	#17	#23
0.	#6	#12	#18	#24

F^- source is NaF; PO_4^{3-} source is Na_3PO_4

* Not prepared due to solubility limitations.

Fig. 1 - Compositions of the Reactant Fluoride-Phosphate Solutions (sample numbers are shown in the chart).

USCOMM-NBS-DC

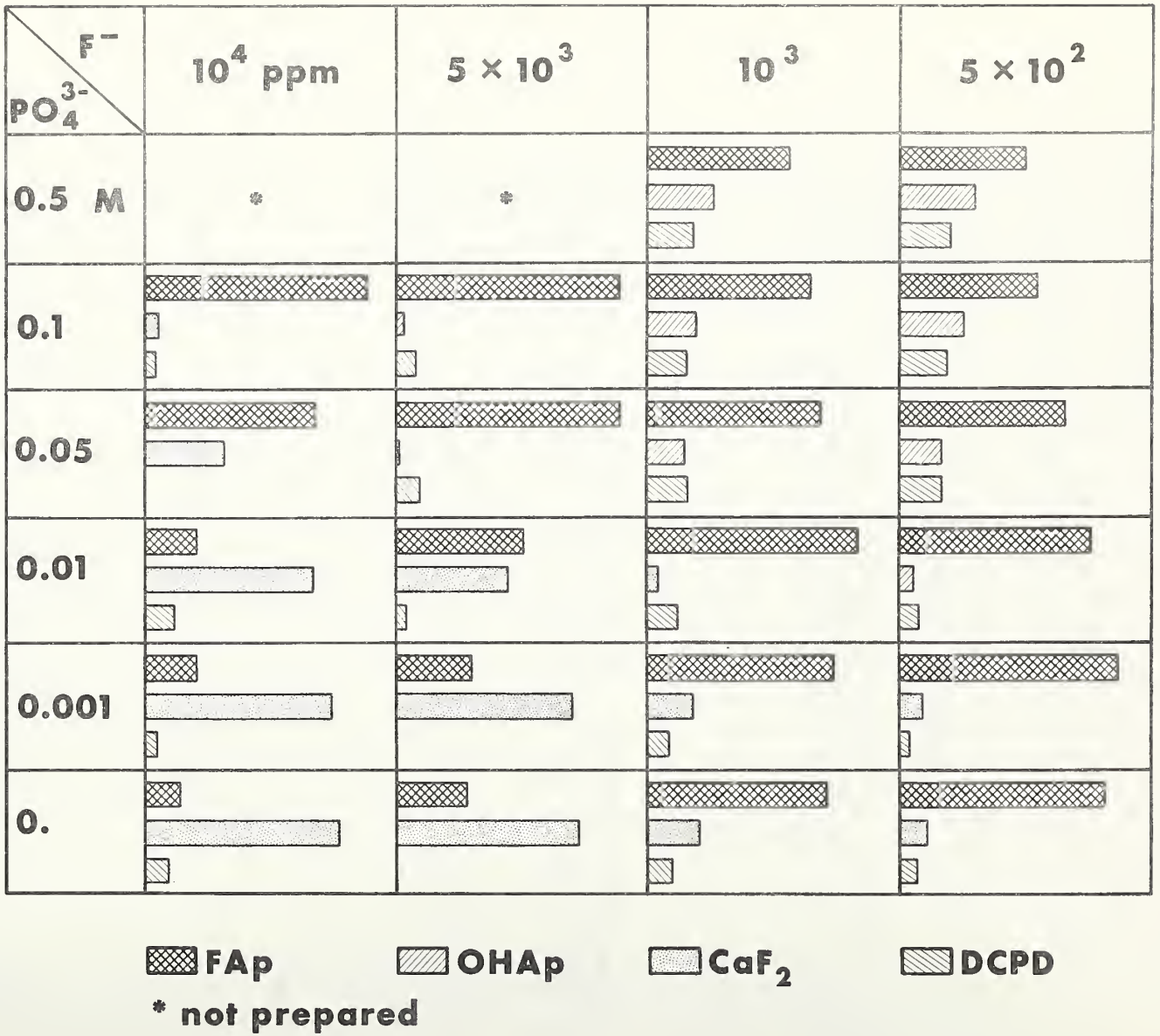

Fig. 2 - Percentage Compositions of the Solid Products (the distance between two vertical lines corresponds to 100 wt. %).

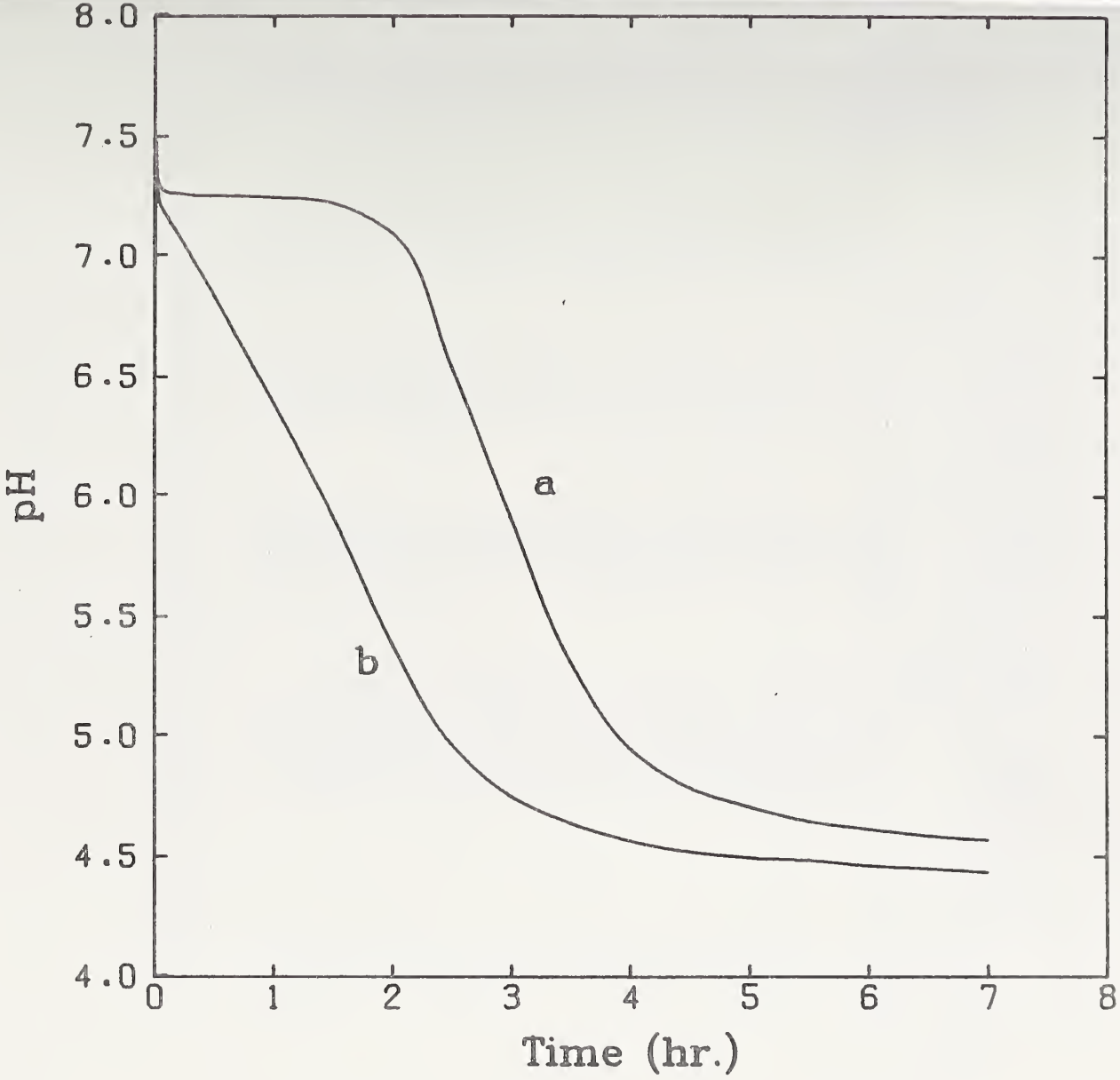

Fig. 3 - pH Change vs. Time for Reaction No. 24.
Curve a: 0.5 g DCPD in 50 ml F^- (500 ppm) solution.
Curve b: 0.5 g DCPD + 0.05 g OHAp in 50 ml F^- (500 ppm) solution.

Table I - Analytical Data for the Liquids Before and After the Reaction with $CaHPO_4 \cdot 2H_2O$

Sample Number	pH		F^- (ppm)		Total Phosphate (M)	
	Initial	Final	Initial	Final	Initial	Final
2	11.96	11.18	10^4	9.50×10^3	0.1	0.120
3	11.80	10.90	10^4	8.85×10^3	0.05	0.0936
4	11.45	9.27	10^4	8.49×10^3	0.01	0.0554
5	10.47	7.95	10^4	7.77×10^3	0.001	0.0494
6	9.20	7.82	10^4	7.34×10^3	0.	0.0488
8	12.01	11.24	5×10^3	4.91×10^3	0.1	0.116
9	11.86	10.65	5×10^3	4.83×10^3	0.05	0.0697
10	11.55	8.74	5×10^3	3.27×10^3	0.01	0.0541
11	10.69	7.83	5×10^3	3.00×10^3	0.001	0.0491
12	7.69	7.80	5×10^3	2.92×10^3	0.	0.0500
13	12.37	11.92	10^3	8.71×10^2	0.5	0.487*
14	12.02	11.32	10^3	8.57×10^2	0.1	0.116
15	11.89	10.80	10^3	8.28×10^2	0.05	0.0679
16	11.66	6.65	10^3	7.24×10^2	0.01	0.0320
17	10.65	6.32	10^3	3.22×10^2	0.001	0.0301
18	7.08	6.30	10^3	2.92×10^2	0.	0.0294
19	12.38	11.92	5×10^2	3.88×10^2	0.5	0.495*
20	12.05	11.32	5×10^2	3.62×10^2	0.1	0.112
21	11.93	10.90	5×10^2	3.53×10^2	0.05	0.0671
22	11.66	6.54	5×10^2	2.74×10^2	0.01	0.0312
23	10.75	4.75	5×10^2	33.5	0.001	0.0268
24	6.96	4.26	5×10^2	19.8	0.	0.0263

* Some phosphate has precipitated at the time of analysis.

Table II Composition of the Solid Products

Sample Number	Elemental Analysis: Weight percentage Ca	P	F	Molar ratio Ca/P	Ca/F	Solid* Phase	Calculated Percentage Composition: $Ca_5(PO_4)_3F$	$Ca_5(PO_4)_3OH$	CaF_2	$CaHPO_4-2H_2O$
2	34.9	15.4	5.42	1.75	3.06	Ap	88.7		5.8	5.5
3	36.1	10.4	15.1	2.69	1.13	Ap+CaF_2	67.8		32.1	0.1
4	37.8	5.47	27.2	5.34	0.658	CaF_2+Ap	20.8		66.7	12.5
5	39.6	4.11	30.5	7.44	0.605	CaF_2	21.4		74.1	4.5
6	42.5	4.10	33.9	8.01	0.593	CaF_2	13.6		77.2	9.2
8	32.2	15.5	2.77	1.60	5.50	Ap	89.1	3.0		7.9
9	34.6	16.7	3.33	1.60	4.93	Ap	89.1		0.8	10.1
10	37.6	8.75	20.4	3.32	0.889	Ap+CaF_2	51.1		44.8	4.1
11	42.2	4.56	31.3	7.15	0.640	CaF_2	31.9		71.0	-2.9
12	41.9	4.09	31.9	7.92	0.662	CaF_2	28.4		73.8	-2.2
13	31.5	16.0	1.74	1.52	8.58	Ap	55.6	26.1		18.4
14	31.7	15.9	2.03	1.54	7.43	Ap	64.8	19.3		15.9
15	34.0	17.1	2.31	1.54	6.98	Ap	68.7	14.9		16.4
16	35.7	16.8	4.55	1.64	3.72	Ap	83.7		3.7	12.6
17	38.8	14.5	11.1	2.07	1.66	Ap	74.0		18.4	7.6
18	38.4	14.2	11.5	2.09	1.58	Ap+CaF_2	70.9		19.8	9.3
19	31.2	16.0	1.55	1.51	9.56	Ap	49.7	30.0		20.3
20	33.6	17.1	1.85	1.52	8.63	Ap	55.3	25.9		18.8
21	34.1	17.2	2.22	1.53	7.26	Ap	65.7	17.3		17.0
22	36.8	17.8	2.70	1.60	6.46	Ap	75.7	15.8		8.5
23	38.1	15.9	7.39	1.86	2.44	Ap	86.9		9.4	3.7
24	36.4	15.2	7.50	1.85	2.30	Ap	81.7		10.7	7.6

* Identified by x-ray diffractometry and/or petrographic examination; first symbol represents major phase:
Ap = Apatite

NATIONAL BUREAU OF STANDARDS REPORT

NBS PROJECT
311.05-3110561

December 29, 1972

NBS REPORT
10 983

Progress Report

on

EXPERIMENTAL STUDY OF THE SURFACE AND LATTICE EFFECTS ON THE SOLUBILITY OF HYDROXYAPATITE

Robert Chuong*

* Summer Student of the American Dental Association Research Unit at the National Bureau of Standards, Washington, D. C. 20234.

This investigation was supported in part by research grants DE00572 and T 1 DE 162-08 to the American Dental Association from the National Institute for Dental Research and is part of the dental research program conducted by the National Bureau of Standards in cooperation with the American Dental Association; the United States Army Medical Research and Development Command; the Dental Sciences Division of the School of Aerospace Medicine, USAF; the National Institute of Dental Research; and the Veterans Administration.

U.S. DEPARTMENT OF COMMERCE

NATIONAL BUREAU OF STANDARDS

Experimental Study of Surface and Lattice Effects on the Solubility of Hydroxyapatite

R. Chuong

Introduction

The solubility of hydroxyapatite (OHAp), $Ca_5(PO_4)_3OH$, has been the subject of many investigations. It has been an area of sustained interest because the solution behavior of OHAp is fundamental to processes of physiological adaptation in bone and teeth. However, experimental studies on the solubility of OHAp have often culminated in confusing results. The responsibility for much of this confusion lies with the use of variable and nonrigorous definitions of "solubility" in the framework of a particular study and with the failure to consider the effect of surface on the dissolution process. Other factors[1] that may have caused difficulties include (i) the sensitivity of the apparent solubility of OHAp to impurities; (ii) the difficulty involved in the preparation of pure OHAp, and (iii) the slow growth of OHAp crystals in solution, often resulting in the failure to achieve equilibrium with the lattice.

Many of these difficulties can be avoided if an internally consistent thermodynamic treatment for the solubility of OHAp is formulated. This has been done by Brown, Moreno and Gregory.[1] Their treatment reveals the importance of separating "lattice" and "surface" reactions in the study of the solubility of sparingly soluble salts. It is perhaps useful to briefly explain this distinction.

"Lattice reaction" refers to the process where in a local region of a crystal the stoichiometry of the dissolution reaction is fixed by the composition of that portion of the crystal lattice being dissolved or reformed. "Surface reaction" refers to the reaction of liquid with the interfacial region (solid-liquid interface) which need have no fixed stoichiometry. The distinction between these reactions is most readily seen in terms of the number of degrees of freedom, $\underline{f}$, for their equilibria: in the ternary system $Ca(OH)_2$-H_3PO_4-H_2O at constant temperature and pressure, the equilibrium between the lattice and liquid has $\underline{f} = 1$, and for the equilibrium between interface and liquid, $\underline{f} = 2$.[1] The consequence of two degrees of freedom for the equilibrium with the interfacial region is that the composition of the liquid is not confined to an isotherm. When the two equilibria are considered simultaneously the system is confined by the equilibrium with the fewest degrees of freedom so that $\underline{f} = 1$; therefore, the solution compositions are restricted to the isotherm for the lattice-solution equilibrium. Thus, the surface of the solid substrate should not affect the <u>thermodynamic</u> solubility, a quantity expressed by the solubility product and the phase diagram. The surface should, however, affect the stoichiometry of the overall reaction and the composition of the equilibrium solution; that is, the <u>apparent</u> solubility of the substrate depends in part on the surface.

Brown, et al[1] have also indicated that the constancy of the solubility product is a measure of a stoichiometric reaction for the lattice, and that surface characteristics such as charge should not affect the solubility product even though they may affect apparent solubility.

Avnimelech et al[2] have shown that the separation of the lattice and surface effects is valid for the $Ca(OH)_2$-H_3PO_4-H_2O system by showing that although the overall dissolution of OHAp may be nonstoichiometric (as measured by the molar calcium-to-phosphorus ratio), the OHAp behaves as a compound with definite thermodynamic properties as indicated by the constancy of the solubility product, $K_S = (Ca^{2+})^5(PO_4^{3-})^3(OH^-)$ and by the excellent agreement between the Ca/P ratio of the equilibrating solid (determined from the potential diagram) and the theoretical ratio. The present study concerns the investigation of the solubility of OHAp in the quaternary system of $Ca(OH)_2$-H_3PO_4-H_2O-HCl. The purpose of this study is to show that the effect of the solid-to-solution ratio on the calcium-to-phosphorus ratio in solutions of OHAp can be explained by a consideration of both lattice and surface reactions.

Methods and Results

Different solid-to-solution ratios (grams/100 ml) of OHAp in 7×10^{-4} M, 1×10^{-3} M, or 1×10^{-2} M HCl were prepared by placing 0.2, 0.4, 0.5, 0.8, 1.0 and 2.0 grams of solid into

Erlenmeyer flasks with 100 ml of solution. In total, 18 solutions were prepared, as summarized in Table I. The flasks were sealed with parafilm paper and placed for five days in a constant temperature shaker bath at 25°C. The rate of oscillation of the shaker was maintained at a level sufficient to keep the solid in suspension continuously. At the end of the five-day period all flasks contained residual solid and the solutions were filtered through millipore filters of 0.22 μ pore diameter. Their pH's were determined at 25°C using the Radiometer digital pH meter, PHM 52* standardized with the NBS standard buffer of pH 4.008. Calcium was determined with an atomic absorption spectrophotometer. Strontium chloride was used to suppress phosphorus interference. Phosphorus was determined using the colorimetric method of Brabson et al.[3] The ion activity products and the electroneutrality unbalances were calculated as described by Gregory et al[4] for each solution.

Discussion

From Table I, the following generalizations can be made:

(i) Marked deviations from the theoretical Ca/P ratio of 1.67 occur in the dissolved calcium and phosphorus.

---

* Certain commerical equipment, instruments, or materials are identified in this paper in order adequately to specify the experimental procedure. In no case does such identification imply recommendation or endorsement by the National Bureau of Standards, nor does it imply that the material or equipment identified is necessarily the best available for the purpose.

(ii) The deviations are greater, the higher the solid-to-solution ratio.

(iii) The deviations are greater, the lower the initial HCl concentration; the series with the highest initial HCl concentration shows no significant change in the Ca/P ratio of the dissolved material, and this ratio was somewhat higher than theoretical.

(iv) Ion activity products are consistently on the order of the solubility product of hydroxyapatite ($K_{S,OHAp} \cong 3 \times 10^{-59}$) within experimental error.

The variation of Ca/P with solid-to-solution ratio indicates that surface effects contribute to the stoichiometry of the overall reaction, but the constancy of the solubility product indicates a stoichiometric lattice equilibrium. The observation that as the concentration of HCl is higher, i.e., series B relative to A, the Ca/P ratio is closer to the theoretical value of 1.67, indicates that the effect of the surface is reduced as the concentration of HCl is greater. This is expected since the lattice equilibrium is described by an isotherm and as the acidity of the solution is greater (lower value of pU(-), where U(-) is the electroneutrality balance[1,4,6]) the relative contribution to the concentrations of calcium and phosphorus from the lattice will be greater.

The values of Ca/P for series C vary only slightly with changes in the solid-to-solution ratio. This fact also shows that as the acid concentration increases, the contribution of the surface to the overall dissolution is diminished relative to that of the lattice. The reason for the greater-than-theoretical values of Ca/P for the solutions of series C is not immediately apparent. One possibility is the presence of a calcium-containing impurity that is held in the OHAp crystal structure but is released at the higher HCl concentrations. This is not an attractive explanation since it introduces new variables into the system, but is consistent with the observation that the apparent Ca/P ratio of the initial solid, 1.69, was slightly greater than theoretical. An alternative is to attribute the Ca/P values to the formation of $CaHPO_4$. The pH's of the equilibrated solutions in series C are all fairly close to the pH of the expected singular point for $CaHPO_4$ and OHAp. However, the calculated solubility products for $CaHPO_4$ of these solutions, $(6.0 \pm 0.2) \times 10^{-8}$ are only about one-half the value, 1.26×10^{-7}, reported by McDowell *et al*,[6] thereby detracting from this explanation for the high values of the Ca/P ratio of the dissolved material. A third explanation--that the surface became more enriched in phosphorus in the solutions with the lowest pH's--is consistent with the observations of Avnimelech *et al*,[2] but there should

have been some observable effect due to changes in solid-to-solution ratio. Thus, there appears to be no entirely consistent single explanation for the slightly high Ca/P ratios in series C.

Otherwise, the results of this study are adequately explained by the theory of Brown et al.[1] The results are an example of the fact that although the overall dissolution of hydroxyapatite may be nonstoichiometric, the free energy of the dissolution-precipitation reaction at equilibrium is governed by the stoichiometric reaction for the lattice.

Earlier investigations into the solubility of OHAp encountered difficulties because of the failure to explicitly account for contributions from the surface to the reaction in a manner that would not relegate the lattice to a subordinate role, and also to the failure of workers to achieve equilibrium with the lattice due to insufficient allotments of time for the complete precipitation of OHAp in the approach to equilibrium. Earlier workers have also invoked the possibility of complexes on the solid surface which control the solubility, but inherent in this approach is the dubious assumption that the chemical potential of the complex is independent of its concentration on the surface.[1] Confusion has also arisen from the use of solvents of insufficient acidity in preparing solutions for equilibration with OHAp, thus allowing relatively large contributions of the surface to their compositions.

The difficulties and confusions in the past concerning the solubility of OHAp arose in general, from a failure to explicitly consider the distinction between lattice and surface phenomena. Once this distinction is realized and observed consistently, the applicability of standard solubility product principles to OHAp and other sparingly soluble salts which show apparently aberrant behavior is seen to be valid and that there is no need to invoke new forms for the ion activity product of OHAp to describe its solution behavior.

Acknowledgment

The guidance and encouragement of W. E. Brown and P. R. Patel are gratefully acknowledged. Financial support for carrying out this research was received under Grants DE-00572 and T 1 DE 162-08.

References

1. Brown, W. E.; Moreno, E. C.; and Gregory, T. M. Thermodynamics of Hydroxyapatite Solubility. (In press.)

2. Avnimelech, Y.; Moreno, E. C.; and Brown, W. E. Solubility and Surface Properties of Finely Divided Hydroxyapatite. (In press.)

3. Brabson, J. A.; Dunn, R. L.; Epps, Jr., E. A.; Hoffman, W. M.; and Jacob, K. D. J.A.O.A.C. 41:517, 1958.

4. Gregory, T. M.; Moreno, E. C.; and Brown, W. E. J. Res NBS 74A:461, 1970.

5. Brown, W. E.; and Wallace, B. M. Ann NY Acad Sci 131:690, 1965.

6. McDowell, H. M.; Brown, W. E.; and Sutter, J. R. Inorg chem 10:1638, 1971.

TABLE I

The Effect of the Solid-to-Solution Ratio on the Calcium-to-Phosphorus Ratio in Saturated Solutions of Hydroxyapatite

Solution	Solid / Soln. (g/100ml)	HCl (mmoles/l)	pH 25°C	Ca (mmoles/l)	P (mmoles/l)	Ca/P	a_{OHAp} x 10^{59}	U(±) x 10^{3}
A1	0.2	0.70	5.97	0.518	0.315	1.64	4.97	+0.000473
A2	0.4	0.70	5.98	0.528	0.336	1.57	7.66	-0.00255
A3	0.5	0.70	5.96	0.532	0.347	1.53	6.38	-0.00527
A4	0.8	0.70	5.92	0.547	0.379	1.44	5.08	-0.00788
A5	1.0	0.70	5.92	0.557	0.394	1.41	6.13	-0.00326
A6	2.0	0.70	5.88	0.590	0.470	1.26	7.15	-0.00156
B1	0.2	1.00	5.82	0.713	0.431	1.65	5.02	+0.0257
B2	0.4	1.00	5.80	0.731	0.452	1.62	4.72	+0.0108
B3	0.5	1.00	5.79	0.732	0.458	1.60	4.22	+0.0146
B4	0.8	1.00	5.80	0.742	0.482	1.54	6.10	+0.0204
B5	1.0	1.00	5.79	0.762	0.508	1.50	6.87	+0.00715
B6	2.0	1.00	5.74	0.794	0.567	1.40	5.20	+0.00208
C1	0.2	10.0	4.80	7.16	4.16	1.72	4.93	-0.146
C2	0.4	10.0	4.81	7.10	4.13	1.72	5.48	-0.0548
C3	0.5	10.0	4.80	7.06	4.13	1.71	4.56	-0.0236
C4	0.8	10.0	4.80	7.07	4.13	1.71	4.59	+0.00363
C5	1.0	10.0	4.80	7.11	4.09	1.74	4.57	-0.117
C6	2.0	10.0	4.82	7.00	4.02	1.74	5.62	-0.035

a_{OHAp} = ion activity product for OHAp, $(Ca^{2+})^5(PO_4^{3-})^3(OH^-)$.

U(±) = electroneutrality unbalance (allowing for the presence of the added (Cl).

U.S. DEPT. OF COMM. BIBLIOGRAPHIC DATA SHEET	1. PUBLICATION OR REPORT NO. NBSIR 73-130	2. Gov't Accession No.	3. Recipient's Accession No.

4. TITLE AND SUBTITLE

Report on Dental Research at the National Bureau of Standards
July 1 - December 31, 1972

5. Publication Date

6. Performing Organization Code

7. AUTHOR(S)
Dr. James M. Cassel, et al

8. Performing Organization
NBSIR 73-130

9. PERFORMING ORGANIZATION NAME AND ADDRESS

NATIONAL BUREAU OF STANDARDS
DEPARTMENT OF COMMERCE
WASHINGTON, D.C. 20234

10. Project/Task/Work Unit No.
3110561

11. Contract/Grant No.

12. Sponsoring Organization Name and Address
American Dental Association, Chicago, Illinois
National Institute of Dental Research, Bethesda, Md.
Veterans Administration, Washington, DC
U.S. Army Medical Research & Development Command, Washington

13. Type of Report & Period Covered
Semi-annual
July 1 - Dec. 31, 1972

14. Sponsoring Agency Code

15. SUPPLEMENTARY NOTES

A copy of this report is also kept at the ADA Headquarters Library, Chicago, but it is not publicized in any manner.

16. ABSTRACT (A 200-word or less factual summary of most significant information. If document includes a significant bibliography or literature survey, mention it here.)

Semi-annual Progress Report
July 1 - December 31, 1972

17. KEY WORDS (Alphabetical order, separated by semicolons)

18. AVAILABILITY STATEMENT

[ ] UNLIMITED.

[X] FOR OFFICIAL DISTRIBUTION. DO NOT RELEASE TO NTIS.

19. SECURITY CLASS (THIS REPORT)	21. NO. OF PAGES
UNCLASSIFIED	
20. SECURITY CLASS (THIS PAGE)	22. Price
UNCLASSIFIED	

USCOMM-DC 66244-P71